

**BED-MATERIAL TRANSPORT RATE DERIVED FROM  
DELTA PROGRADATION IN A SMALL ALPINE BASIN,  
FITZSIMMONS CREEK, COAST MOUNTAINS,  
BRITISH COLUMBIA**

By

**Channa P. Pelpola**

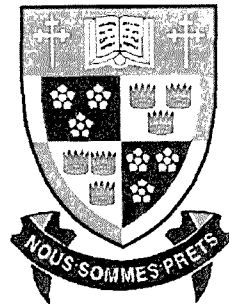
Bachelor of Science (Honours), Carleton University, Ottawa, 1996

THESIS SUBMITTED IN PARTIAL FULFILLMENT OF

THE REQUIREMENTS FOR THE DEGREE OF

MASTER OF SCIENCE

in the Department of Geography



© Channa P. Pelpola 2001

SIMON FRASER UNIVERSITY

APRIL 2001

All rights reserved. This work may not be reproduced in whole or in part, by photocopy or other means, without permission of the author.

## APPROVAL

Name: Channa Patrick Pelpola  
Degree: Master of Science  
Title of Thesis: Bed-Material Transport Rate Derived From Delta  
Progradation In A Small Alpine Basin, Fitzsimmons  
Creek, Coast Mountains, British Columbia  
  
Examining Committee:  
Chair: M.V. Hayes, Associate Professor

---

E.J. Hickin, Professor  
Senior Supervisor

---

M.C. Roberts, Professor  
Committee Member

---

Robert F. Gerath, P. Geo  
Senior Geoscientist and Associate  
Thurber Engineering Ltd.  
External Examiner

Date Approved: April 3, 2001

## ABSTRACT

A sediment budget was determined for Fitzsimmons Creek in order to assess the long-term bed-material efflux from a high-energy, debris-flow dominated alpine stream in the Coast Mountains of British Columbia. The primary component of the thesis (Part 1) examines the long-term bed-material transport rate from morphologic data, sonar bathymetry, and ground-penetrating radar surveys of the fan-delta built by Fitzsimmons Creek and recorded on sequential aerial photography for the period 1947-1999. The average annual bed-material transport rate is  $1.60 \pm 0.28 \times 10^4 \text{ Mg yr}^{-1}$  for the 52-year period, with a range of  $2.20 \times 10^4 \text{ Mg yr}^{-1}$  for decadal estimates. Considerable temporal variability of the average bed-material efflux is evident over the 52-year record. The length of time required to measure a stable average annual bed-material transport rate in this particular system appears to be not less than 50 years.

A secondary component of the thesis (Part 2) examines the total sediment budget based on direct measurements of bed-material accumulated in the fan-delta and estimates of suspended-sediment over the 52-year period. The long-term minimum specific sediment yield is  $0.57 \pm 0.14 \text{ Mg km}^{-2} \text{ day}^{-1}$  based on direct measurements and the estimate of the specific sediment yield for this system is  $0.90 \pm 0.48 \text{ Mg km}^{-2} \text{ day}^{-1}$ . A significant proportion of the total sediment load (averaging 49% over the 52-years) is deposited as bed-material in Fitzsimmons Creek's fan-delta.

## ACKNOWLEDGEMENTS

Thanks to Dr. E.J. Hickin, who allowed me the freedom to research topics of personal interest in relation to fluvial geomorphology. He has earned my utmost respect as an academic, professional, mentor, and friend. I always smile when recalling the day I first asked for research funds. He looked at me with a furrowed brow and screamed "GET OUT!" I leaned back in my chair only to see "Little Bear" in his doorway. Dr. M.C. Roberts provided guidance as part of my Supervisory Committee from the preliminary stages of this study, to the final preparation of this thesis. His recommendations proved invaluable. Many thanks go out to Mr. Robert Gerath, P.Geo., who offered constructive feedback and improvements to the final copy of the thesis.

I was fortunate enough to work with an enthusiastic and entertaining field assistant, Simon Broughton, despite the dawn wake up calls. Lucas Curran and Marie-Claude Bourgie provided additional field assistance and humour. I am indebted to Kevin Dunk at the Water Survey of Canada for field assistance, hydrologic data, and good advice, Rob Knight, Ministry of Environment, Lands and Parks for the recent aerial photographs and Arthur DeJong of Whistler/Blackcomb who generously took slides of the watershed. Thanks to Brian Samson of Sigma Engineering who consulted on background knowledge of Fitzsimmons Creek. A big thanks to my summer employer, Heather Beresford, Resort Municipality of Whistler offered flexibility and encouragement of my research project.

A big thank you goes out to Claire Beaney, Colin Wooldridge, and Chris Simpson who managed to digest first drafts of the research and provide feedback, laughter, and good conversation. Additional thanks to: Craig Coburn, Lorraine Gibson, Adrienne Burk, Kevin Tabata, and Tammie Tupechka. Preparation of my studies and thesis was made easier with the assistance of the Geography Department Staff, thank you. To my close friends and family, thank-you for your support and for maintaining my sanity.

Funding was provided in part by a NSERC Research Grant to Dr. E. J. Hickin, and a Graduate Fellowship from the Geography Department at SFU.

*I was not made for academic writings,  
Action is my domain.*

**MOHANDAS GHANDI**

# TABLE OF CONTENTS

APPROVAL.....	ii
ABSTRACT.....	iii
ACKNOWLEDGEMENTS.....	iv
QUOTATION.....	v
TABLE OF CONTENTS.....	vi
LIST OF TABLES.....	ix
LIST OF FIGURES.....	x
<b>CHAPTER 1: OVERVIEW .....</b>	<b>1</b>
1.1    GENERAL INTRODUCTION .....	1
1.2    THE RESEARCH PROBLEM .....	4
1.3    RESEARCH OBJECTIVES .....	7
1.4    LITERATURE REVIEW .....	8
1.4.1 <i>Geomorphic Setting</i> .....	8
1.4.2 <i>Bed load and Sediment Yield in British Columbia: A Review</i> .....	12
1.4.3 <i>Ground Penetrating Radar</i> .....	14
1.5    STUDY AREA .....	16
1.5.1 <i>Local and Regional Setting</i> .....	16
1.5.2 <i>Human and Other Impacts on Sediment Delivery to the Fan-delta</i> .....	24
<b>CHAPTER 2: METHODOLOGY .....</b>	<b>28</b>
2.1    GENERAL METHODOLOGY .....	28
2.2    DATA ANALYSIS .....	29
2.2.1 <i>Aerial Photograph Interpretation</i> .....	29
2.3    FIELD METHODOLOGY AND METHODS.....	31
2.3.1 <i>Contemporary Bathymetric Survey</i> .....	31
2.3.2 <i>Ground Penetrating Radar: Theory and Techniques</i> .....	33
2.3.2.1 <i>Electrical Properties of Materials</i> .....	34
2.3.2.2 <i>GPR Instrumentation</i> .....	35

2.3.2.3	<i>GPR Survey Design</i> .....	38
2.3.2.4	<i>Interpretation of Depth from GPR Profiles</i> .....	38
2.3.2.5	<i>Accuracy of Interpretations</i> .....	41
2.4	BULK DENSITY SAMPLING .....	42
2.4.1	<i>Survey Design</i> .....	42
2.4.2	<i>Sampling Procedure</i> .....	42
2.4.3	<i>Lab Analysis of Bulk Samples</i> .....	44
2.5	APPLICATION OF GEOGRAPHICAL INFORMATION SYSTEMS (GIS).....	45
2.5.1	<i>Measurement of Planimetric Growth</i> .....	45
2.5.2	<i>Error Estimation of Planimetric Growth</i> .....	45
2.5.3	<i>Estimation of Volume</i> .....	46
2.6	SEDIMENT BUDGET .....	46
2.6.1	<i>Sampling Suspended-Sediment</i> .....	47
2.6.2	<i>Suspended-Sediment Analysis</i> .....	47
2.6.3	<i>Discharge Data</i> .....	47
2.6.4	<i>Sediment-Rating Curve</i> .....	48
2.6.5	<i>Lacustrine Sedimentation</i> .....	48
<b>CHAPTER 3: RESULTS</b> .....		<b>50</b>
3.1	DETERMINATION OF BED-MATERIAL EFFLUX.....	50
3.1.1	<i>Planform development: Photo Differencing</i> .....	50
3.1.2	<i>Vertical Development: Bathymetry of the Receiving Basin</i> .....	55
3.1.3	<i>Vertical Development: Ground Penetrating Radar of the Fan-Delta</i> .....	57
3.1.4	<i>Bulk Density</i> .....	63
3.1.5	<i>Estimates of Bed-Material Efflux</i> .....	66
3.2	SEDIMENT BUDGET .....	73
3.2.1	<i>Suspended-Sediment Settling in the Receiving Basin</i> .....	73
3.2.2	<i>Suspended-Sediment Modeling (DH<sub>48</sub>)</i> .....	74
3.2.3	<i>Sediment Transported as Bed-load</i> .....	81
<b>CHAPTER 4: DISCUSSION</b> .....		<b>83</b>
4.1	PHOTO DIFFERENCING .....	83
4.2	VERTICAL DIMENSION OF THE FAN-DELTA: SURVEY RESULTS.....	85
4.2.1	<i>Bathymetric Surveys</i> .....	85
4.2.2	<i>Ground Penetrating Radar(GPR) Surveys</i> .....	85
4.3	VARIABILITY AND ESTIMATE OF BED-MATERIAL EFFLUX.....	90
4.3.1	<i>Long-Term Estimate of Bed-Material Efflux</i> .....	90
4.3.2	<i>Variability of Bed-Material Efflux</i> .....	90



4.4	SEDIMENT BUDGET.....	94
4.4.1	<i>Overview</i> .....	94
4.4.2	<i>Resolving the Sediment Budget</i> .....	94
4.5	ENGINEERING APPLICATIONS.....	101
<b>CHAPTER 5: CONCLUSIONS .....</b>		<b>104</b>
5.1	THE BED-MATERIAL EFFLUX.....	104
5.2	SEDIMENT YIELD AND THE PROPORTION OF BED LOAD.....	105
5.3	SUGGESTIONS FOR FUTURE RESEARCH .....	108
<b>APPENDIX A CALCULATIONS.....</b>		<b>110</b>
<b>APPENDIX B SUPPLEMENTARY DATA.....</b>		<b>124</b>
<b>LIST OF REFERENCES .....</b>		<b>148</b>

## LIST OF TABLES

Table 2.1	Calculated scales of aerial photo enlargements.....	30
Table 2.2	Typical permittivity, electrical conductivity, and attenuation in geologic materials.....	35
Table 2.3	Velocity, wavelength, and theoretical maximum resolution of three frequencies in geologic materials.....	41
Table 3.1	Summary of surface sediment samples.....	65
Table 3.2a	Bed-material efflux and total volume with time.....	68
Table 3.2b	Bed-material efflux and total yield (mass) over time.....	70
Table 3.3	Lacustrine sedimentation rates.....	73
Table 3.4	Suspended-sediment samples (DH <sub>48</sub> ).....	75
Table 3.5	Minimum and total sediment yield over sequential periods.....	80
Table 3.6	Maximum contribution of bed load and estimate of bed load proportion of the total sediment yield in Fitzsimmons Creek.....	82

## LIST OF FIGURES

Figure 1.1	Correlation of specific sediment yield and drainage basin area.....	6
Figure 1.2a	Illustration of the prograding fan-delta complex and feeder system.....	10
Figure 1.2b	Sedimentological characteristics and architecture of a fan-delta and schematic lithostratigraphic log.....	11
Figure 1.3	GPR principle and reflection profiling.....	15
Figure 1.4	The fan-delta of Fitzsimmons Creek; general location.....	17
Figure 1.5	Upstream view of the fan-delta illustrating multiple distributary channels and general topography of the study site.....	19
Figure 1.6	Overview photo of upstream natural and anthropogenic influences on sediment delivery to the receiving basin.....	20
Figure 1.7a	Annual hydrograph for 1994.....	22
Figure 1.7b	Annual hydrograph for 1995.....	22
Figure 1.8	Longitudinal profile of Fitzsimmons Creek illustrating the change in slope as the river becomes unconfined.....	23
Figure 1.9	Bathymetry map of Green Lake and relative location of the fan-delta to the receiving basin.....	25
Figure 2.1	Bathymetric profile locations with respect to the fan-delta.....	32
Figure 2.2	Ground penetrating radar setup on a gravel bar in Fitzsimmons Creek.....	37
Figure 2.3	Common mid-point (CMP1) ground penetrating radar profile.....	39
Figure 2.4	Location of ground penetrating radar and CMP profiles on the fan-delta.....	40
Figure 2.5	Location of surface sediment core samples on the fan-delta.....	43
Figure 2.6	Location of lacustrine sediment core samples in Green Lake.....	49
Figure 3.1a	Time sequential aerial photographs of the study site (1947-1973).....	51
Figure 3.1b	Time sequential aerial photographs of the study site (1982-1999).....	52

Figure 3.2 Planform evolution base map revealing the location of time sequential fan-delta margins over the 52-year record.....	54
Figure 3.3 Bathymetry profile illustrating the steep delta front and gently sloping pro-delta grading into the receiving basin.....	56
Figure 3.4a Radar profile FC2 in the direction of dip.....	59
Figure 3.4b Radar profile FC4 opposite the direction of dip.....	60
Figure 3.4c Radar profile FC5 in the direction of dip.....	61
Figure 3.4d Radar profile FC8 in the direction of dip.....	62
Figure 3.5 Paleo-lake contour model.....	64
Figure 3.6 Base map created in GIS to calculate areas and volumes for photo-differencing.....	67
Figure 3.7 Average annual bed-material efflux illustrating variability over the 52-year record.....	69
Figure 3.8 Average bed-material efflux with increasing length of record.....	72
Figure 3.9 Sediment rating curve showing the relationship between suspended-sediment concentration and mean daily discharges.....	76
Figure 3.10 Scattergram plot illustrating correlation between measured daily discharges of the Lillooet River and Fitzsimmons Creek.....	78
Figure 3.11 Synthesized and measured daily discharges of Fitzsimmons Creek, British Columbia from August 02, 1947 to August 30, 1999.....	79
Figure 4.1 Comparison of the sub-surface architecture of deltaic systems.....	88
Figure 4.2 Correlation of specific sediment yield and drainage basin area and the corresponding estimates of specific sediment yield of Fitzsimmons Creek...	97
Figure 4.3 Flooding hazard associated with bed-material accumulating on the up-stream side of the B.C. Rail bridge in Fitzsimmons Creek.....	102

# CHAPTER 1: OVERVIEW

## 1.1 General Introduction

The evolution of the earth's physical landscape implies a redistribution of sediment from one location to another. Transport by water is generally the primary mode for sediment movement and therefore it is an important control on sediment yield from river basins. Sediment yield is defined as the total sediment discharge from a drainage basin measured at some point of reference over a defined period of time (Slaymaker, 1972; Patric *et al.*, 1984; Schumm, 1995).

Fitzsimmons Creek is the main-stem from a small alpine watershed draining into Green Lake in the Coast Mountains of British Columbia. The delta deposited at the shore of the lake is a repository of information on the quantity and nature of sediment transported within the watershed. Sediment transport can be separated into three components: dissolved load - material transported in solution; wash load - particles finer than those usually found in the bed and moving readily in suspension ( $< 0.062$  mm); and bed-material load - all material found in appreciable quantities in the bed (generally  $> 0.062$  mm) (Knighton, 1998). Although the dissolved and wash loads are significant components of the sediment yield, determining the quantity of material transported as bed-material load is important because of its influence on the adjustment of river channel form (Knighton, 1998). This becomes more imperative in streams draining alpine environments where the proportion of the total sediment yield transported as bed load,

that part of the sediment load that moves in contact with the bed in a rolling or saltating mode (Gomez and Church, 1989), may be much higher than associated with less energetic streams found on gentler slopes.

Estimation of sediment transport rates in rivers, especially those draining alpine environments is difficult because of the variable nature of the environmental factors governing sediment delivery to a river system. Four major environmental factors control sediment delivery: geology, relief, climate, and land use (Meade *et al.*, 1990). Geology may be taken to include factors such as the glacial history of a drainage basin, which may be a dominating influence in British Columbia (Church and Slaymaker, 1989). Variability in sediment transport is evident over a wide range of timescale, from hours to years, and includes discrete events such as debris flows, seasonal hydrologic regimes, and inter-annual fluctuations driven by climatic cycles and intermittency.

Sediment yields during periods when there are debris flows, for example, may be an order of magnitude greater than those unaffected by such events. Clearly, the sediment transported during such debris-flow events must be included in sediment transport estimates if such measurements are to be meaningful. Yet it is very likely that even the most intense in-stream sediment-sampling program will miss such infrequent catastrophic sediment pulses.

Furthermore, the fact that almost all sediment surveys on BC rivers are of short duration (less than 10 years) exacerbates the problem of non-representative sampling by failing to integrate sediment yield variability occurring at a decadal timescale. Since the transport of bed load is a function of the transport capacity of the flow (Knighton, 1998), a long-term representative sampling procedure is fundamental, and essential because the

bed load is thought to comprise greater than 10% of the total sediment yield in alpine drainage systems (Gurnell, 1987).

Examining changes in geomorphology may provide a solution to sediment sampling problems. Long-term measurements of sediment transport using survey differencing of features such as deltas can provide well-averaged estimates of bed-material that capture the effects of catastrophic events as well as long-term variability (Hickin, 1989). When combined with estimates of the material transported in suspension this method provides an estimate of the total sediment yield for the system. Very little long-term information has been obtained on sediment transport rates in British Columbia rivers. That which is available is for just two basins (Lillooet River and Squamish River) of similar size, about 3600 km<sup>2</sup> (Gilbert, 1975; Hickin, 1989). Further research is needed on steep alpine rivers with small drainage basins, which are influenced by debris flow events.

Identification of controlling factors and the quantification of bed-material are of particular interest to river engineers, geomorphologists, and hydrologists because bed-material load is involved in the process-form linkage controlling channel morphology. The volume of sediment in a river system is determined both by erosion and deposition, and reflects the interaction of discharge fluctuations with the availability of sediment (Lane and Richards, 1997). Deposition or erosion of sediment within a channel results in changes to the morphology of the river expressed through adjustments in flow depth, velocity and channel width.

Distinguishing mechanisms of sediment transport in alpine environments is problematic due to the dynamic nature of these systems. Therefore little research has

been conducted in these environments. Most research has been conducted on rivers not characteristic of Fitzsimmons Creek, which find that less than five percent of total sediment load transported by a river is bed load with the remainder comprising suspended load (Knighton, 1998). Bed-load transport is a mechanism in which sediment moves in contact with the bed of the river (Leopold *et al.*, 1964). Suspended load transport involves particles temporally maintained in the water column by turbulent mixing processes (Leopold *et al.*, 1964). It is likely however as Gurnell (1987) states, that more than five percent of the sediment transported in rivers draining high alpine environments is moved as bed load. Smaller mountain rivers are prone to infrequent debris-flow events and because of their steep gradients and proximity to source material, likely have greater than average contributions of bed-load material (Milliman and Syvitski, 1992).

## **1.2 The Research Problem**

A literature review of sediment yield reveals a gap in the general understanding of sediment transport in British Columbian rivers. There is a scarcity of long-term data for small (less than 100 km<sup>2</sup>) high-energy alpine basins (Church *et al.*, 1985). Studies have focused on rivers with average to large (1000 km<sup>2</sup> to 10 000 km<sup>2</sup>) drainage basin areas. These short-term studies (1-10 years) suggest that sediment transport may be underestimated in small drainage basins in alpine environments. Most sediment is mobilized during infrequent events and may escape representative sampling (Church and Kellerhals, 1979). Indeed, sediment transport in mountain environments is highly variable, even at the same discharges (Troendle *et al.*, 1996). The lack of long-term



studies highlights the need for further research on sediment transport within alpine environments over long periods (greater than 10 years).

The Water Survey of Canada (WSC) collects sediment and discharge data for a number of rivers in British Columbia. Church *et al.*, (1989) used the available data to examine the dependency of specific sediment yield, the sediment yield per unit area, on drainage-basin size. Figure 1.1 correlates specific sediment yield with drainage area, categorizing drainage basins into disturbed, undisturbed, glacially influenced, and lacustrine domains. Disturbed glacially influenced basins produced the greatest specific sediment yields.

Another method for determining sediment yield is based on differencing of aerial photographic and bathymetric surveys of delta morphology to estimate progradation rates, and therefore long-term sediment yield. Gilbert (1975) and Hickin (1989) have shown that long-term data for sediment yield from two drainage basins of similar size (~3600 km<sup>2</sup>) are consistent with those for the short term based on in-stream sampling.

One limitation of these successive photographic surveys of delta progradation is the assumption that the morphology of the surface on which the sediment is accumulating (the receiving basin floor) is known, when in fact this is rarely the case. Typically, calculations are made by translating in space the form of the contemporary delta front along an upper bounding surface corresponding to the water level in the receiving basin. The geomorphic assumptions implicit in this survey-differencing method have never been tested.

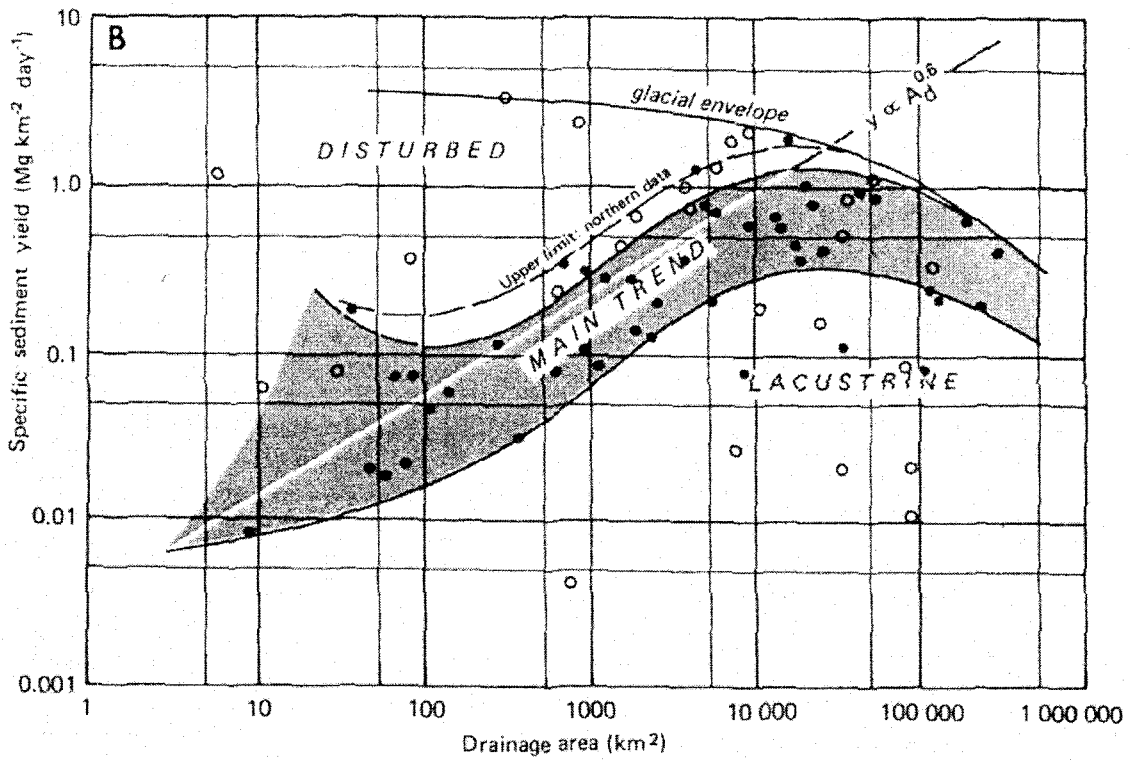


**FIGURE 1.1** Correlation of specific sediment yield and drainage basin area.  
(Reproduced from Church, *et al.*, 1989)

### 1.3 Research Objectives

The main objective of this study is to characterize the bed-material efflux regime of Fitzsimmons Creek, Whistler, British Columbia; a gravel-bed stream characterized by a small drainage basin (approximately 100 km<sup>2</sup>), debris-flow events, and a steep alpine environment. This is the high-energy fluvial environment notably absent in the data sets of previous studies.

This study will apply the “reservoir approach” to indirectly measure the bed-material transport rate for the study channel. Back calculation of bed-material efflux from changes in morphology leads to an estimate of the transport rate (Ashmore and Church, 1998), which will be measured by examining the progradation rate of the Fitzsimmons Creek fan-delta into Green Lake. The fan-delta provides information on the sediment yield and composition of material transported primarily as bed load (Ryan and Troendle, 1997). The morphological approach to determine sediment efflux does not distinguish between transport mechanisms, therefore, it is a measure of the bed-material transport rate.

Survey differencing at a decade time scale will also allow an examination of the variability of bed-material transport over a long period. The study will also attempt to determine the proportion of the total sediment yield transported as bed load and as suspended-sediment load. In determining the proportion of sediment transported by as bed load and as suspended load an estimate of the total sediment budget for the watershed must be established.

The following primary research questions are investigated:

1. What is the annual bed-material efflux from Fitzsimmons Creek?
2. How variable is the bed-material efflux from Fitzsimmons Creek?
3. What is the minimum sampling time to estimate reliably the 50-year average bed-material efflux from Fitzsimmons Creek?

The following secondary research questions will also be investigated:

4. What is the specific sediment yield from Fitzsimmons Creek?
5. What is the proportion of material transported as bed load?

## **1.4 Literature Review**

### **1.4.1 Geomorphic Setting**

Herodotus first used the term “delta” in 440 BC to describe the sedimentary feature located at the mouth of the Nile River where it emptied into the Mediterranean Sea (Nemec and Steel, 1988). Since that first observation, many examinations of deltaic environments have been carried out and reported in the literature. Specific studies of deltas formed in mountain environments are of direct interest to this study since Fitzsimmons Creek is in an alpine environment. Alluvial fans and fan deltas are two sedimentary features common in mountain settings.

An alluvial fan is a triangular shaped (in plan view) accumulation of sediment deposited where a river exits a confined valley (Nemec and Steel, 1988; De Chant *et al.*, 1999). Fan-deltas straddle the transition zone between the sub-aerial alluvial fan and the domain of the sub-aqueous processes of the receiving basin (Wescott and Ethridge,

1990). As Figure 1.2a illustrates, emphasis in this classification is placed on the sediment supply from either the adjacent highlands or from the alluvial fan. Holmes (1965) defined a fan-delta as an alluvial fan that has prograded from an adjacent highland into a standing body of water. Figure 1.2a illustrates the geomorphology and nature of the environment typical of fan-deltas. While McPherson *et al.* (1987) favour the Holmes' definition, Nemec and Steel (1988) recommend using the terms alluvial-fan delta or river delta as descriptive geomorphic terms because of the confusion between fan-deltas and fan-shaped deltas.

Deltas formed in lacustrine environments are also classified on the basis of depositional processes inferred from sedimentary structures and lithofacies architecture. As the vertical facies in Figure 1.2b illustrate, fan-deltas contain horizontal top set facies, thick foreset facies dipping at 25°, and sub-horizontal bottom set facies (Smith, 1991). The internal architecture of the three principal facies, first identified through Gilbert's (Gilbert, 1890) examination of deltas in Lake Bonneville, has been an important area of research (Wood and Ethridge, 1988; Flores, 1990; Smith and Jol, 1997). Facies models from these studies illustrate the sedimentological characteristics and composition of a fan-delta as defined by Holmes (1965). In this study, the original definition of a "fan-delta" (Holmes, 1965) will be used to describe the feature formed by Fitzsimmons Creek as it drains into Green Lake. This is because the fan shaped delta is in close proximity to the adjacent highland, and has an alluvial fan as the primary sediment supply (Nemec and Steel, 1988; Wescott and Ethridge, 1990).

Gilbert-type deltas are common in a glaciolacustrine environment where coarse-grained sediment supply is high, basin water depth is not excessive, and where wave and

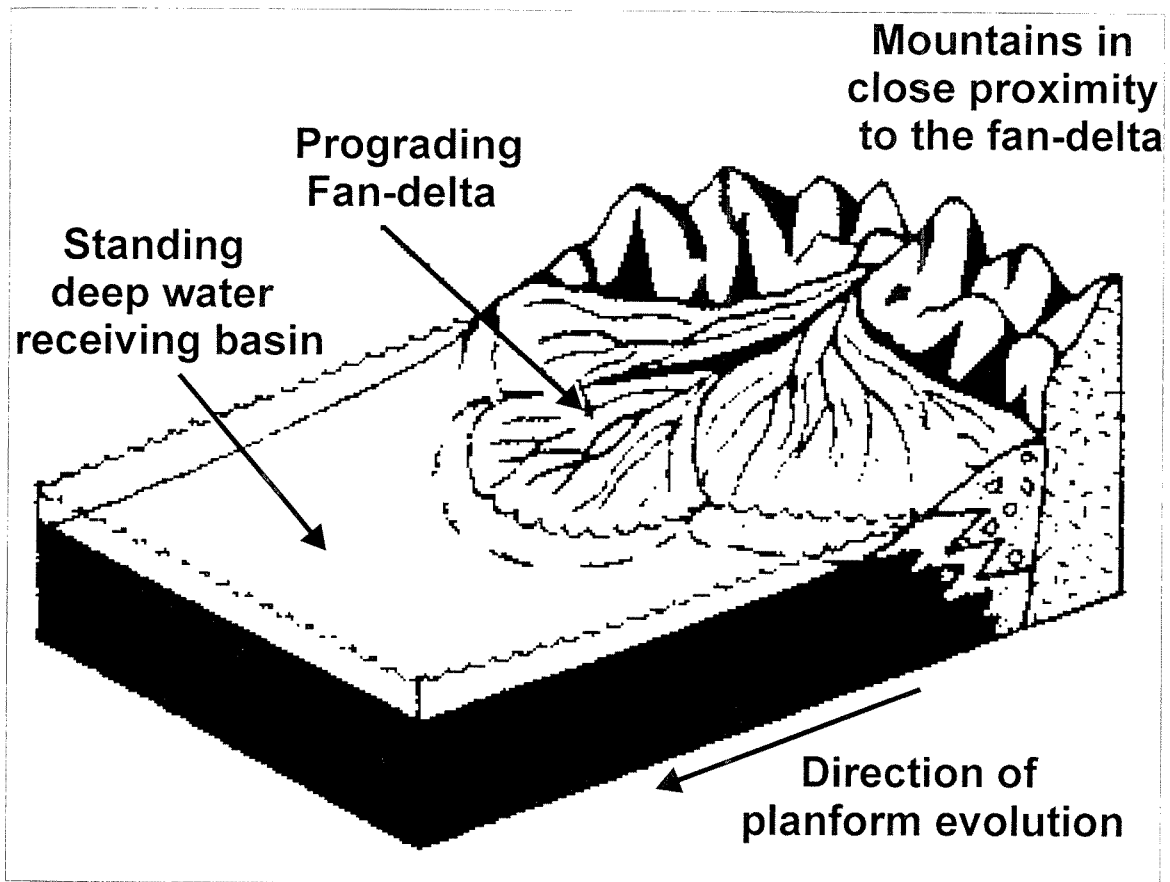


**Figure 1.2a** Illustration of a prograding fan-delta complex and the feeder system.  
(modified from Nemec and Steel, 1988)

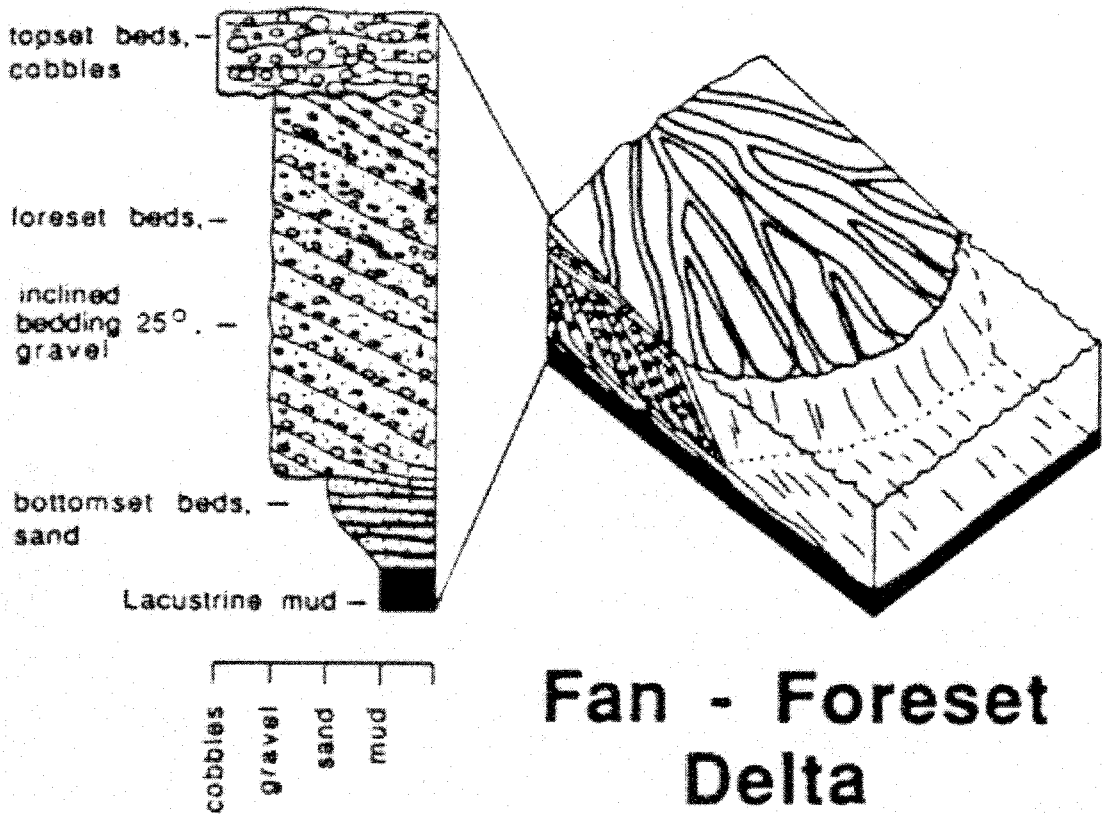


**Figure 1.2b** Sedimentologic characteristics and architecture of a fan-delta and schematic lithostratigraphic log. (Reproduced from Smith, 1991)

tidal influences are negligible (McPherson *et al.*, 1988). All of these conditions characterize this project. In a more recent study, Postma (1990) argues that the primary recognition of a fan-delta should be based on the physiography and facies of the delta plain, delta front, and prodelta. The evidence from this study will show that the classification of the delta formed by Fitzsimmons Creek as a Gilbert-type fan-delta is appropriately based on both the internal stratigraphy and the overall planform related to the geomorphic environment.

#### **1.4.2 Bed load and Sediment Yield in British Columbia: A Review**

Most current research on bed-load transport has shown the inadequacy of standard transport equations to provide rational predictions of sediment transfer (Gomez and Church, 1989; Martin and Church, 2000). Standard bed load formulae were largely based on data from non-alpine environments. The problem of predicting bed-load transport from these formulas becomes more apparent in mountain channels for which the formulae were not developed (Parker *et al.*, 1982). The problem lies in the inability of some measurement techniques and formulae to accurately characterize a system, which is both spatially and temporally variable. Comparisons of most theoretical models with measured stream bed-load transport rates have revealed only limited success in modeling which may be attributable to common assumptions: grains are assumed to be cohesionless, water temperature and its effect on viscosity is often neglected, and a single grain diameter is used in models, while natural streams carry a wide range of particle sizes (Graf, 1971).

Recently, geomorphologists have estimated bed-material efflux from channel morphodynamics (Martin and Church, 1995; Ashmore and Church, 1998; Ham and



Church, 2000). This technique relies on multiple channel cross-sections or sequential aerial photography, and knowledge of the bed-load transport rate at one of the cross sections. The benefit of such an approach is the ability to measure average bed-material transport rates over longer periods of time, thereby incorporating temporal and spatial variability.

Studies have shown that specific sediment yield decreases downstream as drainage area increases and opportunities for sediment storage in river bars and floodplains increase (Knighton, 1998). Some researchers have recently challenged this assertion because it is based largely on data from United States agricultural regions not necessarily representative of Western Canada. Their results demonstrate that declining specific sediment yield does not apply in all regions (Church and Slaymaker, 1989; Church *et al.*, 1989; Trimble, 1997; Church *et al.*, 1999). In British Columbia, specific sediment yield increases downstream at all spatial scales up to  $3 \times 10^4 \text{ km}^2$  as a result of glacial modification of river valleys that has led to large amounts of sediment being stored along the river rather than being uniformly distributed across the basin (Church *et al.*, 1989). Increasing sediment storage along the channel provides additional sediment available to be mobilized during high discharge events.

Short-term average annual sediment-transport measurements fail to take into account the variability of sediment transport. In mountain environments mass movement events may contribute a large proportion of the short-term sediment yield, so that estimates over periods of 1-10 years could provide misleading results (Church *et al.*, 1985). Ideally, sediment yield should be assessed over a long record by measuring for example, the volume of sediment impounded behind a dam or deposited in a lake.

It is not yet clear how short-term (1-10 years) sediment transport rates relate to decade-scale measurements because very little long-term data exist. It is encouraging, however, that sediment yield estimates from two long-term studies of the Lillooet and Squamish rivers based on respective periods of 57 and 54 years (Gilbert, 1975; Hickin, 1989), appear consistent with the short-term data for rivers in British Columbia (Church *et al.*, 1989). Nevertheless these two studies of similar sized drainage basins provide a weak test at best of the relationship because it may vary with drainage basin size. Long-term data must be greatly expanded in order to make a reliable assessment of this correspondence. This study will use photo differencing to provide an indirect method of determining the average bed-material transport rate over a 52-year record.

#### **1.4.3 Ground Penetrating Radar**

Generally, paleo-lake depth estimates under an advancing delta are based on the contemporary depth of the receiving basin immediately proximal to the delta (Gilbert, 1975; Hickin, 1989). While this assumption is commonly used to interpret the vertical thickness of sediment accumulated in the delta, ground-penetrating radar provides a means to test this technique in determining the depth of sediment in coarse-grained river deltas (Smith and Jol, 1997).

Ground-penetrating radar (GPR) is a shallow geophysical technique based on the propagation of electromagnetic waves at varying frequencies (10 - 1000 MHz). Images of subsurface features are produced from electromagnetic energy reflections, as some of the energy is reflected back to the surface because of changes in the dielectric properties of the subsurface material (Figure 1.3). Such differences reflect changes in sediment grain

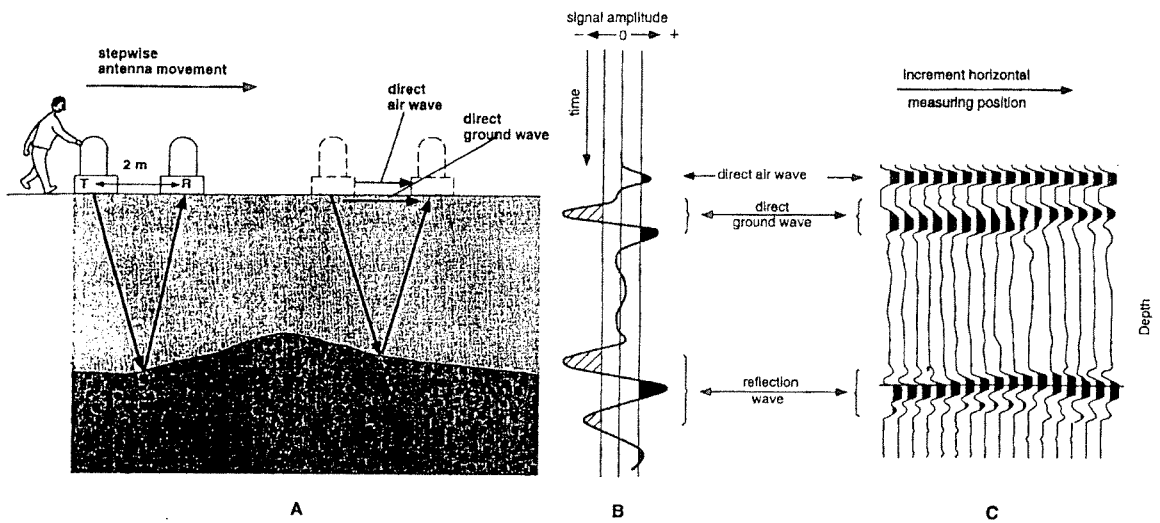


**Figure 1.3** GPR principle and reflection profiling  
 A: paths of main electromagnetic waves  
 B: sample of a single corresponding radar signal  
 C: resulting radar profile  
 (Modified from Naegeli *et al.*, 1996)

size, water content, location of the ground-water table, density, bedrock contacts, or facies changes (Smith and Jol, 1997).


Suitability of GPR at a specific site depends on whether the target feature can be distinguished. Because geomorphologists are largely concerned with depositional environments, the sediment deposited should have a contrasting composition with the underlying strata and be at a depth to which the GPR can detect the boundary (less than 50 m). Boundary layers arise from electronically conductive environments such as lacustrine sediments of silt and clay. In the case of a coarse-grained delta prograding into a lake, the boundary between the deltaic and lacustrine sediment should be easily identifiable. Coarse sediment is highly suited for GPR profiling while resistive environments such as lacustrine sediments attenuate (absorb and reflect) GPR waves. Depth of the sediment accumulated in the delta is calculated from the two-way travel time of GPR waves in the sediment. GPR can be used to better understand deltaic sedimentation processes and thus reconstruct the environment of deposition (Jol and Smith, 1991). In this respect, GPR is a valuable geophysical tool in the context of this study.

## **1.5 Study Area**

### ***1.5.1 Local and Regional Setting***

Fitzsimmons Creek (Figure 1.4) is located in Whistler, British Columbia, approximately 120 kilometers north of Vancouver within the Pacific Range of the Western System of the Canadian Cordillera, known as the Coast Mountains. The study

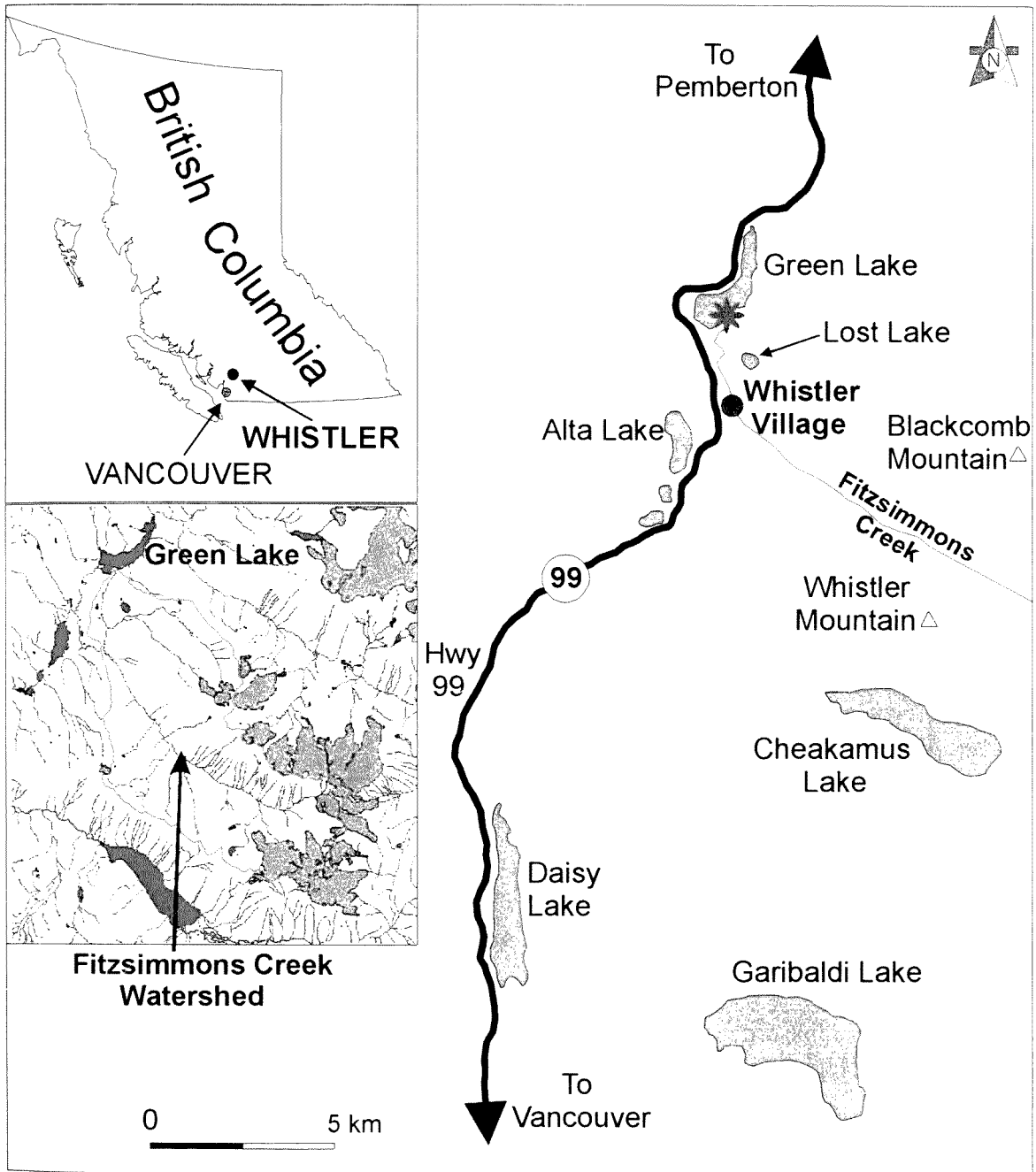


**Figure 1.4** The fan-delta of Fitzsimmons Creek; general location indicated by 

Inset map of watershed is indicated by the boundary line at a scale of 1:146 000 approximately.

area encompasses the lower reaches of Fitzsimmons Creek where it enters the receiving basin, Green Lake. Fitzsimmons Creek forms a fan-delta largely composed of sand and gravel at the southern end of Green Lake. The surface of the fan-delta has little relief (Figure 1.5) and is characterized by multiple distributary channels.

Fitzsimmons Creek drains approximately 100 km<sup>2</sup> within a well-defined valley basin (Woods, 1993). The distance from the headwaters (2634 masl) to Green Lake (690 masl), is approximately 18 kilometres. Along the alluvial fan, the creek channel becomes a wandering gravel-bed river (Figure 1.6) and varies between 10 – 20 metres in width during average discharges with a depth of one to two metres (Woods, 1993).

Glaciers, lateral moraines, and steep valley walls characterize the headwater region of Fitzsimmons Creek in the glacier-snowfields of Overlord Mountain, Fissile Mountain, and Mount Fitzsimmons. Composition of the bedrock geology in the upper reaches of the creek includes metamorphic greenstones and phyllites of the Lower Cretaceous Gambier Group (Geological Survey of Canada, 1977). Thick terraces of unconsolidated sediment were deposited during the Holocene and contain till deposits composed of angular to rounded gravel, cobble, and boulder sized sediment with a high clast content, up to 50% by weight (Mierzejewski, 1992). Undercutting of these deposits has produced several mass movement events as evidenced by various landslide scars. An overview map of the drainage area shown in Figure 1.6 identifies the location of multiple sediment sources and factors (geology, relief, and land use) which may influence sediment yield. The sub-glacial drainage systems of glaciers, which develop during Spring melt events, are presumed to contribute large amounts of sediment with a high percentage of fines to the proglacial streams (Rothlisberger and Lang, 1987).

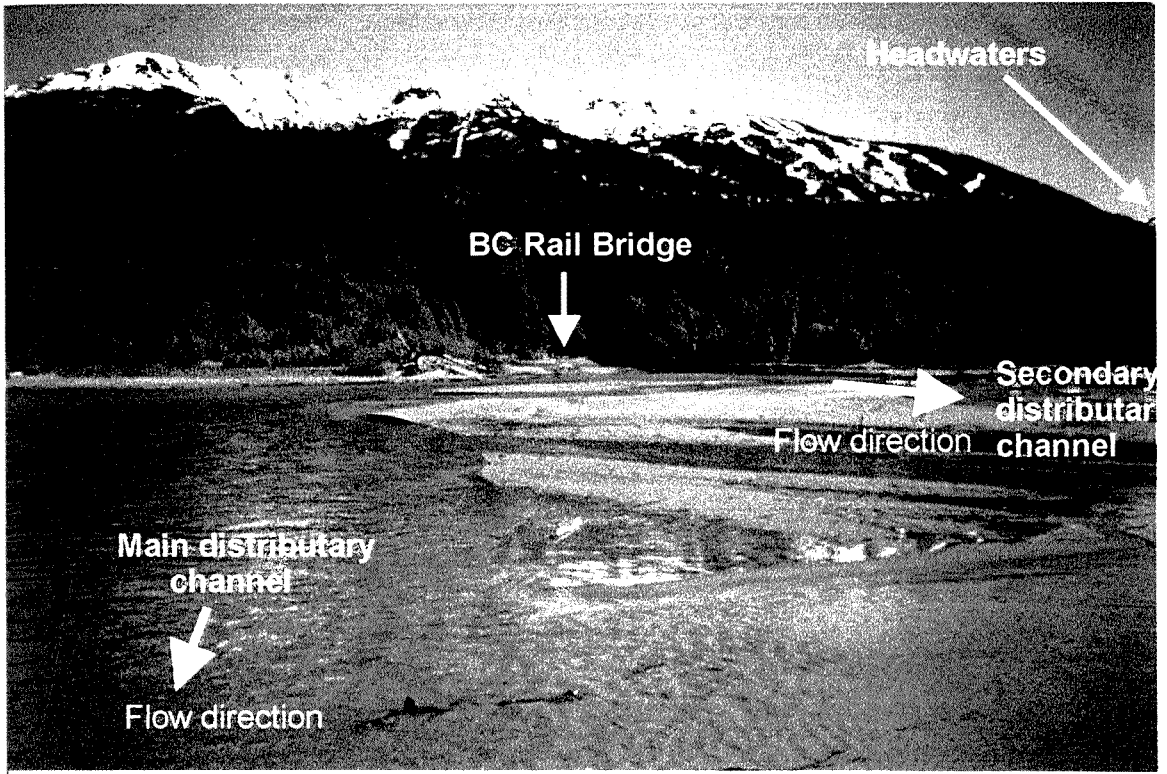


**Figure 1.5** Upstream view of fan-delta illustrating multiple distributary channels and general topography of the study site. Vegetation indicates floodplain areas of the fan-delta.

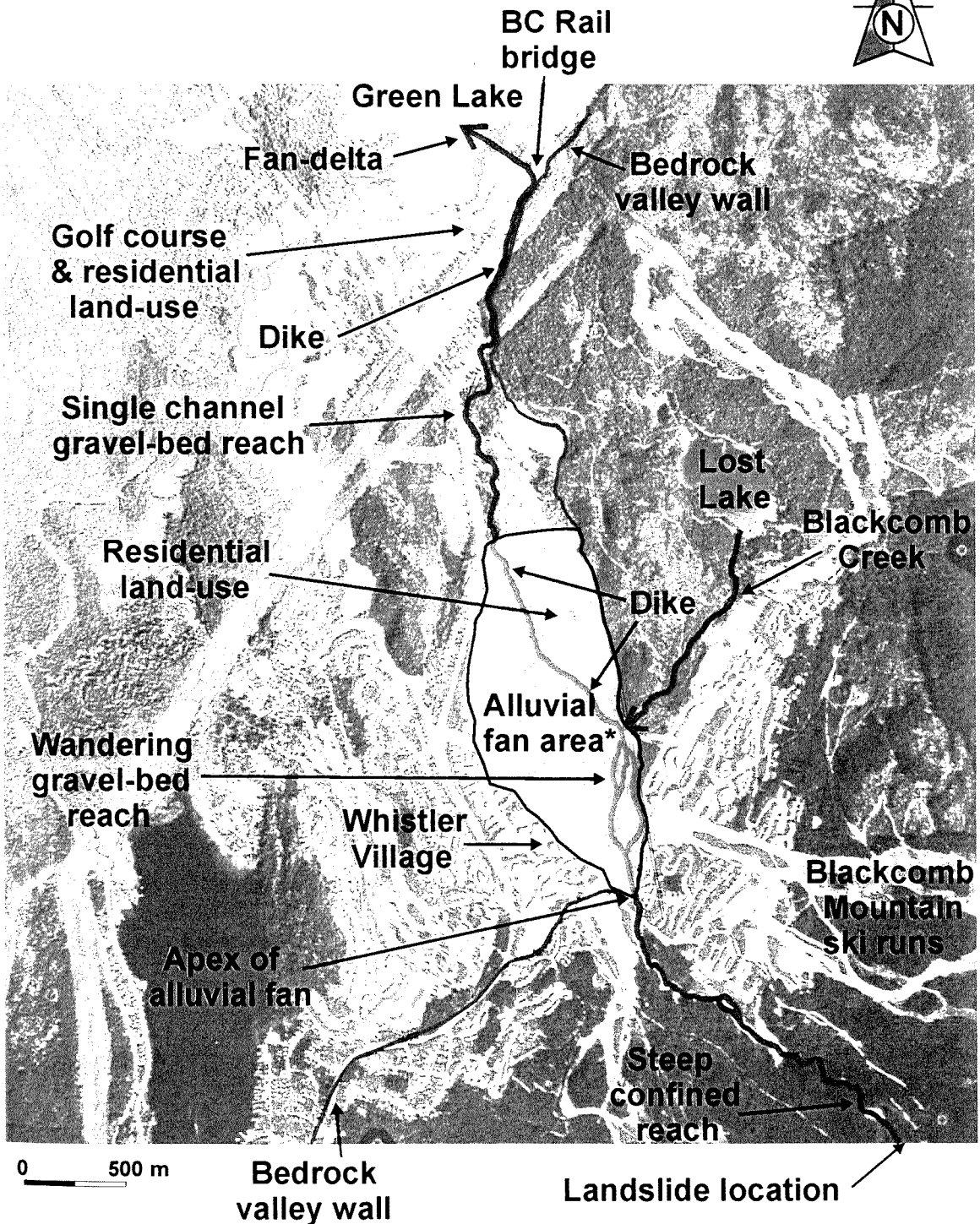


**Figure 1.6** Overview photo of upstream natural and anthropogenic influences on sediment delivery to the receiving basin. Fitzsimmons Creek is confined to the East side of the alluvial fan. Bedrock valley wall indicates interpreted alluvial fan. \*Fan area shown is approximate.



Fitzsimmons Creek drains a steep alpine environment of the Coast Mountain Range, which is influenced by both intense rainfall events, and extensive snowfall. Average annual rainfall at an elevation equivalent to the mouth of Fitzsimmons Creek is 801 mm and average annual snowfall is 6574 mm (Environment Canada, 1981). Discharge of Fitzsimmons Creek is derived from a variety of events. The flow regime of the creek is driven by two peak events, spring snowmelt and fall rainstorms. The average daily discharge of Fitzsimmons Creek calculated from existing Water Survey of Canada records is  $4.45 \text{ m}^3\text{s}^{-1}$ . Extreme flood events are known to have occurred with the most recent event in August 1991. During this intense rain event, portions of the valley side located two kilometres upstream of Whistler Village failed and slid into the creek, producing a temporary dam. Over-topping and failure of the dam produced an instantaneous peak-flood discharge estimated to be as high as  $130 \text{ m}^3\text{s}^{-1}$  (Brown, 1993). Typical annual hydrographs for Fitzsimmons Creek are shown in Figures 1.7a and 1.7b. Discharges greater than  $10 \text{ m}^3\text{s}^{-1}$  are usually associated with spring snowmelt and fall and winter rainstorm events. The spring snowmelt discharges are longer in duration (2 - 3 months) in comparison to the fall precipitation events, which are high intensity and short duration, lasting only a few days to weeks.

Where Fitzsimmons Creek becomes unconfined by the valley walls it has produced an alluvial fan with an area of  $3.4 \text{ km}^2$  (Woods, 1993). The alluvial fan has a triangular plan-form and conical surface form typical of other alluvial fans with a slope between  $2^\circ$  and  $12^\circ$  (Blair and McPherson, 1994). A longitudinal profile shown in Figure 1.8 indicates the various slope changes from the confined reaches to the fan-delta. Slopes vary from 1% to 10% from the mouth upstream along the alluvial fan to the confined

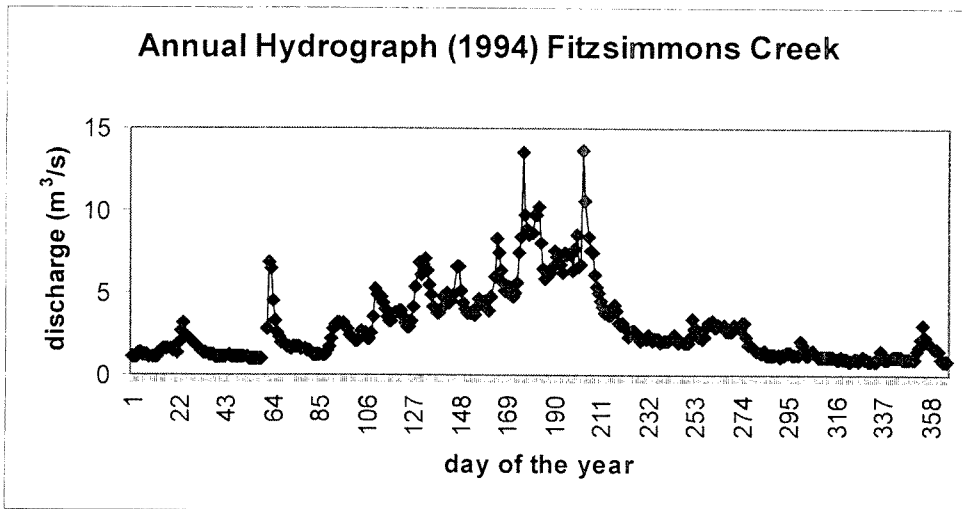


**Figure 1.7a** Annual hydrograph for 1994. Peak discharges are associated with spring snow melt.  
(Data from the Water Survey of Canada, 1999)

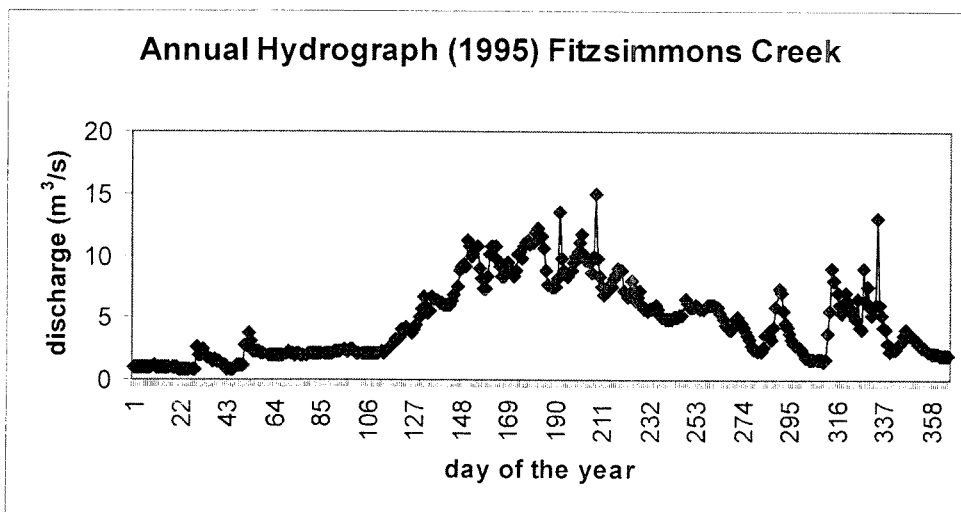


**Figure 1.7b** Annual hydrograph for 1995. Peak discharges are also revealed for fall and winter rainstorm events.  
(Data from the Water Survey of Canada, 1999)

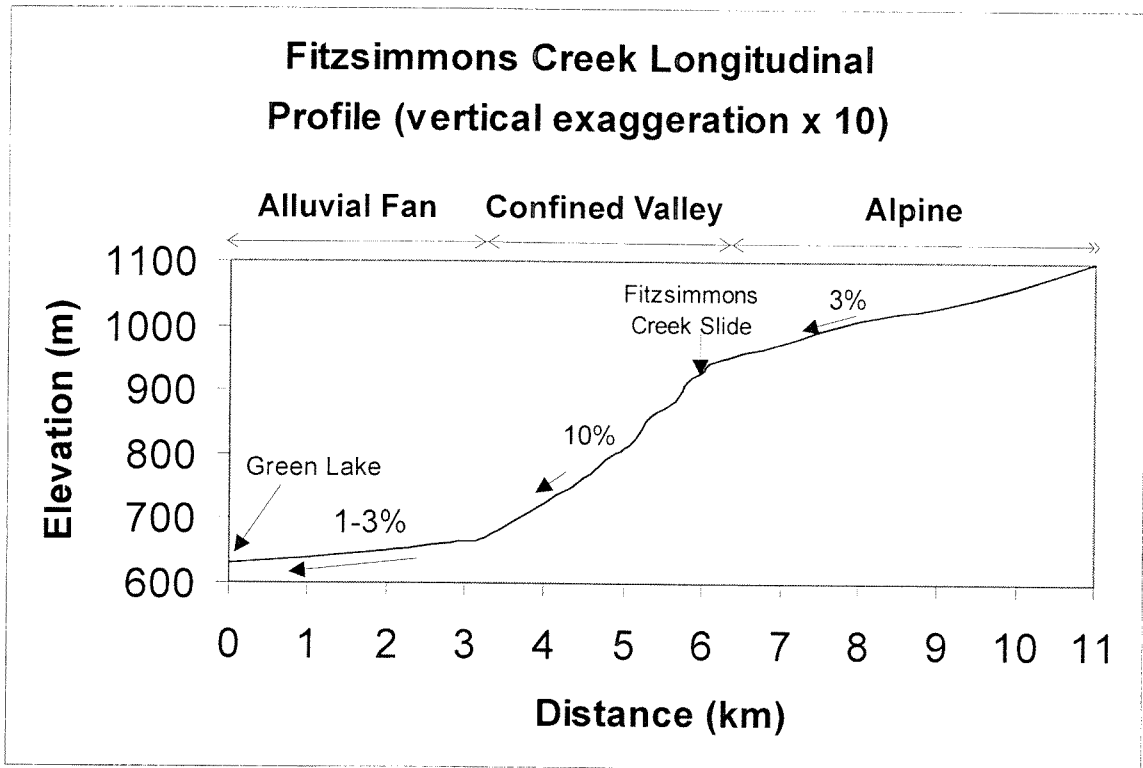


**Figure 1.8** Longitudinal profile of Fitzsimmons Creek illustrating the change in slope as the river becomes unconfined. (Modified from Mierzejewski, 1992)

steep reaches immediately upstream of Whistler Village. Slope of the last reach, located between the British Columbia Rail bridge and Green Lake, is less than 1% (0.005). Sediment in the alluvial fan consists of grain sizes ranging from boulders to silt and clay, with the largest clasts located at the apex of the alluvial fan.

The receiving basin for Fitzsimmons Creek, Green Lake, is shown in Figure 1.9. The lake is irregular in planform, narrow and long with an approximate area of 2.05 km<sup>2</sup>. Depths are illustrated in 5-metre contour intervals up to the maximum depth of 44 metres. Green Lake has two additional tributaries, 19 Mile Creek and Alta Creek. Both are presumed to contribute insignificant quantities of sediment relative to the total sediment load of Green Lake (Brian Menounos, U.B.C., personal communication, 2000). The outflow of Green Lake is the Green River, located at the northern end of the lake.

The fan-delta formed by Fitzsimmons Creek is located adjacent to a prograding beach on the southwestern end of the lake. The sediment accumulated in the beach is assumed to be redistributed suspended sediment from Fitzsimmons Creek, conveyed by waves generated by the predominantly northeasterly wind. Observations of lake levels over several seasons and local knowledge reveal fluctuations up to 1 metre with spring snowmelt and fall precipitation events.

### ***1.5.2 Human and Other Impacts on Sediment Delivery to the Fan-delta***

The settlement presently known as Whistler was founded in 1918 as a fishing resort following construction of the British Columbia (BC) Rail line from Squamish to Lillooet, British Columbia. Berm construction confined Fitzsimmons Creek in the lower reaches to its present location. Figure 1.6 illustrates the course of the river as it undergoes a ninety-degree bend at the BC Rail bridge and flows into Green Lake.

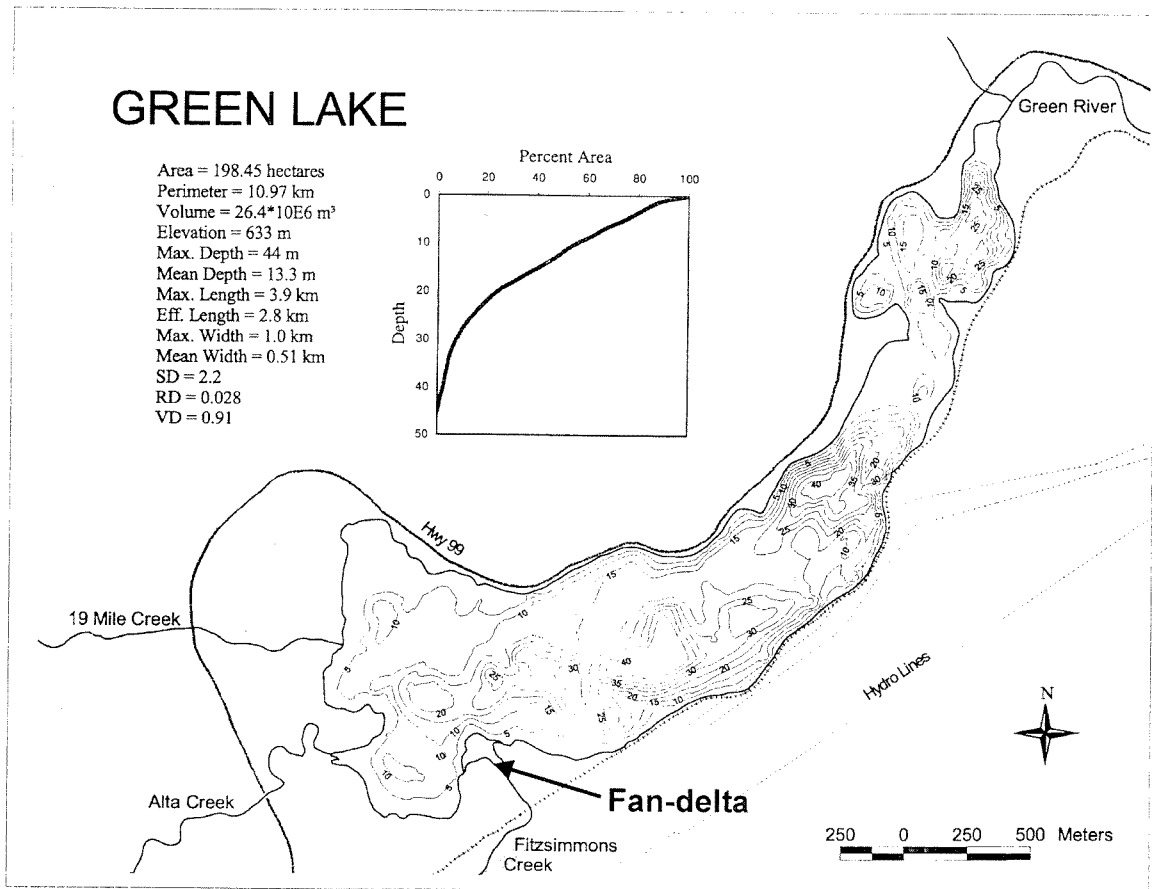


**Figure 1.9** Bathymetry map of Green Lake and relative location of fan-delta with respect to the receiving basin. (Scheifer, 2000)

Until the 1950's, the drainage basin of Fitzsimmons Creek was relatively undisturbed by human influence. During the period 1959 through 1963, extensive clear-cut logging was conducted along terraces in the confined valley section of Fitzsimmons Creek. Development of the Whistler ski resort began in the 1960's and resulted in further logging of the drainage basin. Urbanization of the resort and rapid development since 1980 resulted in decreased riparian area along the alluvial fan, increased impervious surface area, channel constraints at bridge crossings and flood protection structures. Dikes and riprap were constructed along the margins of the creek during the development of the Resort Municipality of Whistler.

Landslide activity results in sediment input to the creek as incompetent valley walls erode. The largest slide, located approximately two kilometres upstream of Whistler Village (Figure 1.6), is estimated to have a volume of one million cubic metres (Mierzejewski, 1992) and is believed to be the primary cause of the August 1991 debris flow event. The slide is located on the steepest reach of the creek (approximately 10%), evident in the longitudinal profile shown in Figure 1.8.

Mitigation followed the debris flow event and involved enlarging training dikes along the margin of the creek and adding riprap. Presently, the river course is restricted along the alluvial fan between a training dike and the edge of the valley walls until it drains into Green Lake. Only during extreme flood events can the river access its confined floodplain.

The accumulation of coarse sediments in the lower reaches of the creek pose engineering hazards to the BC Rail bridge and private residences and businesses along the lower floodplain of the creek. Mitigation of flood related events have involved the

annual excavation of gravel from the creek since 1991. Despite the hazards associated with development on the alluvial fan of Fitzsimmons Creek and detailed environmental investigation, little is known about sediment transport in this system.

# CHAPTER 2:

## METHODOLOGY

### 2.1 General Methodology

Estimates of sediment efflux based on differencing bathymetric surveys and aerial photographs have been recommended as an alternative to conventional sediment transport monitoring (Church *et al.*, 1985; Ashmore and Church, 1998). The technique of survey differencing to provide long-term estimates of bed-material obtained in this study is based on aerial photo differencing, bathymetry data, and subsurface imaging by GPR.

Accuracy of bed-material efflux based on photo differencing depends on the precision of depth and surface-area measurements of delta morphology. Bathymetric profiling of a receiving basin has been assumed to provide a good basis for estimating the basal elevation of sediment accumulated in a prograding delta, although the assumption is rarely tested (Gilbert, 1975; Hickin, 1989). Estimates of sediment thickness and characterization of the internal structure of deltas have been based on exposures, drill cores, and matching surface delta characteristics to established models such as that of Gilbert (1890). Although these methods enable the internal structure to be predicted if the surface and sub-surface morphology conforms to the model, the vertical dimension of sediment accumulated in the delta cannot be predicted accurately if the receiving basin has an irregular basal morphology (Smith and Jol, 1997).

Subsurface profiling methods such as ground penetrating radar (GPR) can reveal the thickness of coarse sedimentary deposits to a high degree of accuracy (Beres *et al.*,



1999). Variations in the thickness of sediment are visible with GPR profiling, eliminating the need to assume uniform sediment thickness. In combination with survey differencing from aerial photographs, GPR can be applied to reconstruct the three-dimensional morphology of a fan-delta over time.

## **2.2 Data Analysis**

### **2.2.1 Aerial Photograph Interpretation**

Determining the progradation rate of an advancing delta requires that a measurable change in the planform area of the delta can be observed. In this study the measurable change must be visible on sequential aerial photographs. Survey differencing is not widely used in geomorphology because most geomorphic surfaces are too extensive and the survey interval short relative to accumulation rates (Hickin, 1989). Preliminary examination of aerial photographs of Fitzsimmons Creek indicated measurable changes at scales greater than 1:5000.

Original aerial photographs (1947, 1958, 1963, 1973, 1982, 1990, 1994) were obtained from MAPS BC, the Ministry of Environment, Lands and Parks Survey and the Resource Mapping Branch. The Ministry of Environment Lands and Parks, Water Resources Branch donated a recent aerial photograph (1999). Sequential aerial photographs from 1958 to 1994 were enlarged from original negative film while the 1947 and 1999 aerial photographs were enlarged using a flatbed scanner (300 dpi) and printed onto photograph quality paper (300 dpi). The scale of enlarged aerial photographs was calculated from the ratio of distances between landmarks on each photo and the true distance between landmarks surveyed in the field. The calculated average scale for each

**Table 2.1** Calculated scales of aerial photo enlargements

<b>Date of Photo</b>	<b>Scale 1:xxxx</b>	<b>Source Aerial Photograph</b>
Aug 2 1947	3866	BC 400:14
Jun 15 1958	3060	BC 2429:25
Jul 2 1963	2946	BC 5077:25
Aug 8 1973	3718	BC 7520:224
Sept 18 1982	4302	BC 82062:270
July 16 1990	3602	BC B90050:149
July 28 1994	2854	BC C94104:050
Aug 30 1999*	3789	16733-0 R352 L6-3

\* from Ministry of Environment, Lands, and Parks

(refer to Appendix A-1 for detailed calculation)

aerial photograph, listed in Table 2.1, was based on the average of three to six ratio calculations (Appendix A-1). Aerial photographs in this study were not ortho-rectified because the study area was relatively small, essentially horizontal, and had little relief. Correction of aerial photographs for tip or tilt displacements is not warranted because any likely correction would be smaller than the limit of measurement precision (Roberts and Church, 1986). That is, any error associated with non-rectification of aerial photograph enlargements in this study is within the measurement error of  $\pm$  one metre. The margin of the fan-delta was taken as the planform boundary since it was clearly visible in aerial photograph enlargements. The margin was measurable within  $\pm$  one metre due to distinct colour changes between the sediment of the delta and the water of the lake. Photo differencing required accurate measurements, scale and a fixed point common to all sequential aerial photographs. The BC Rail bridge crossing at Fitzsimmons Creek provided an ideal primary reference point for baseline measurements on all aerial

photography. Therefore, a simple mapping and measuring procedure was developed based on this clearly visible base point. Distance from the primary base point to the margin of the fan-delta was measured along a radial grid fanned outward at 7.5° intervals. All line-work was drawn on transparent overlay sheets to protect the original aerial photographs. Measured distances from eight successive aerial photographs were transferred to a base map. The base map indicates the planimetric advancement of the fan-delta over the period of analysis (1947-1999) at a scale of 1:2000. Error associated with distances measured from aerial photographs was ± one metre. The margin of the fan-delta was not clearly identified on the high-level aerial photograph from 1946 because a sediment-laden plume obscured the periphery of the fan-delta.

## **2.3 Field Methodology and Methods**

### **2.3.1 Contemporary Bathymetric Survey**

A bathymetric survey of the receiving basin, Green Lake, was measured along a radial grid convergent on a base point on the modern delta front (Figure 2.1) with the objective of estimating the vertical dimension of sediment accumulated in the fan-delta. Survey transects were located with respect to known survey points using a prismatic compass and laser range finder. Bathymetry data were collected with a Lowrance low-frequency echo sounder and plotter from a Zodiac inflatable boat powered by a five horsepower outboard engine.

A primary survey transect was conducted in the direction of river flow and fan-delta progradation. Eight radial transects, centered on the primary transect were fanned

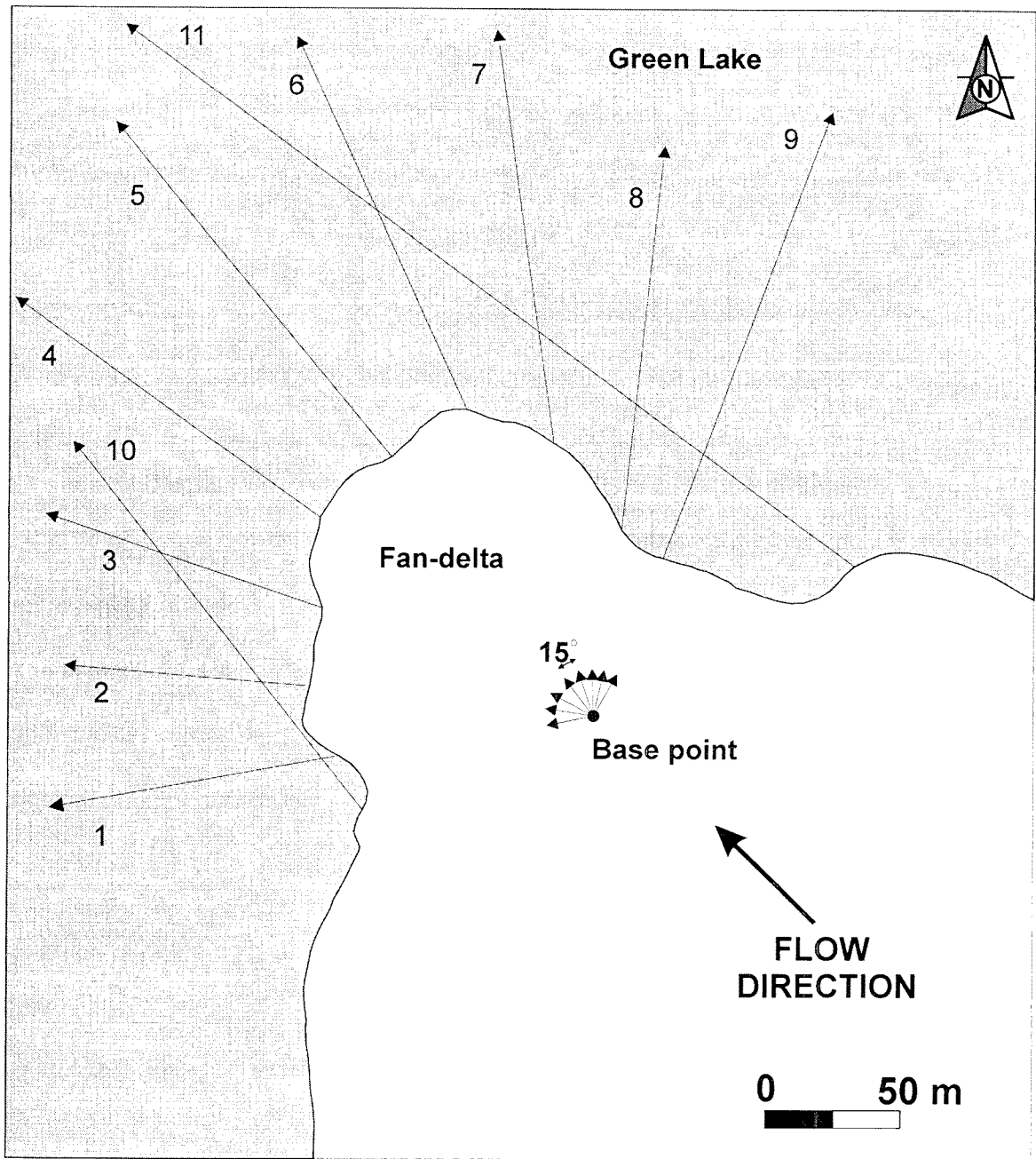


**Figure 2.1** Bathymetric profile locations with respect to the fan-delta. Depths from bathymetry profiles are summarized in Appendix B-1. Base point located 270 m 141° true north from the B.C. Rail bridge.

out at 15° intervals located relative to a base marker. Depth profiles were spatially located with respect to the margin of the fan-delta using a laser range finder and survey markers. Two successive measurements of each transect were conducted to provide additional depth measurements and verify profiles. Additional survey profiles were measured north and south of the fan-delta to provide estimates of depth of the receiving basin in order to reconstruct the paleo-lake bottom. Depths measured along bathymetric transects were generalized as lake-bottom contours plotted on a base map.

### **2.3.2 Ground Penetrating Radar: Theory and Techniques**

GPR is a geophysical apparatus used to map shallow subsurface structure and stratigraphy in sediment of low electrical conductivity (Davis and Annan, 1989). High frequency (10 - 1000 MHz) electromagnetic (EM) waves are transmitted into the ground and are reflected to the surface due to changes in bulk electrical properties of different subsurface lithology (Smith and Jol, 1997). Variations of electrical properties are largely controlled by the grain size composition of the subsurface sediment and the water content (Sensors and Software, 1996). GPR profiles are plotted with reflectors as wiggle traces on an axis of time versus position using the pulseEKKO™ software. Subsurface structure and stratigraphy are directly interpreted from reflector patterns, orientation, thickness and continuity.

The success of a GPR survey largely depends on the ability to penetrate to the intended target depth while ensuring an acceptable level of resolution. Changes in reflector orientation, thickness and pattern are due to changes in the dielectric (permittivity and conductivity) properties of the sediment (Reynolds, 1997). The dielectric constant between the sediment in the fan-delta and the lacustrine sediment is

distinct enough to provide a minimum resolution of  $\pm 0.5$  metres. Depth is calculated from the two-way travel times of electromagnetic waves by applying a velocity experimentally determined from common mid-point surveys.

### **2.3.2.1 Electrical Properties of Materials**

The ability of a GPR survey to detect subsurface stratigraphy is largely dictated by the conductivity of the material (Table 2.2). Resistant sediment such as gravel and sand allow deep GPR profiling, while conductive sediment such as silt and clay attenuate EM waves, preventing deeper penetration. GPR is not suited for environments with a high silt and clay composition (Beres *et al.*, 1999). The fan-delta of Fitzsimmons Creek is assumed to be relatively homogeneous and composed of sand and gravel. Clay and silt are flushed through the delta distributary as washload and settle on the distal lake bottom.

The location of the water table and salinity of water affect the reflection efficiency of GPR to a greater degree than changes from sand to gravel. In their examination of fluvial deposits, LeClerc and Hickin (1997) found that changes from sand to gravel did not necessarily produce distinct radar reflection while the water table produced a pronounced reflection. As electromagnetic waves pass through the water table, a change in the two-way travel time of EM waves occurs. In this study, the survey site is essentially coupled to the water table, which is coincident with Green Lake. These site conditions, combined with the uniformity and coarse sediment composition of the fan-delta, suggested the site was highly suited for GPR surveying.

**Table 2.2** Typical permittivity, electrical conductivity, and attenuation in geologic materials

<b>Material</b>	<b>Dielectric Constant</b> K	<b>Conductivity</b> (mS/m) $\sigma$	<b>Velocity</b> (m/ns) V	<b>Attenuation</b> (dB/m) $\alpha$
air	1	0.00	0.30	0.00
distilled water	80	0.01	0.03	$2 \times 10^{-3}$
fresh water	80	0.50	0.03	0.10
sea water	80	$3 \times 10^3$	0.01	103.00
dry sand	3-5	0.01	0.15	0.01
saturated sand	20-30	0.1-1.0	0.06	0.03-0.3
limestone	4-8	0.5-2.0	0.12	0.4-1
shales	5-15	1-100	0.09	1-100
silts	5-30	1-100	0.07	1-100
clays	5-40	2-1000	0.06	1-300
granite	4-6	0.01-1	0.13	0.01-1
dry salt	5-6	0.01-1	0.13	0.01-1

(modified from Sensors and Software, 1996)

### **2.3.2.2 GPR Instrumentation**

Wave penetration decreases with depth in GPR surveys. This results from associated factors including the reflection of waves due to variations in dielectric constants of subsurface sediment, the ability of sediment to store an electric charge, and sufficient energy propagating into the next horizon so deeper structures can be profiled (Davis and Annan, 1989). GPR instrumentation, involves choosing the appropriate antennae frequency determined by the characteristics of the site and the objectives of the study.

All data were collected with a 400V Sensors and Software pulseEKKO™ IV radar system. Initial testing with 100 MHz antennae revealed good resolution of internal

structures in the deltaic sediment, but the basal boundary was not unequivocally apparent. The 50 MHz antennae were used, trading resolution for penetration since the objective of this study is to determine the depth to the delta-lake bed interface with a theoretical maximum resolution of  $\pm 0.4$  metres in saturated gravel (Davis and Annan, 1989).

The GPR console was connected to a 486 PC laptop computer and powered by a 12 V, 17Ah battery mounted on a golf cart. Radar transceivers and receivers were mounted on the 50 MHz antennae and connected to the console with 25 metre long fibre optic cables (Figure 2.2). Antennas were separated (two-metre spacing) and moved broadside perpendicular at 0.5 metre intervals along transects marked with a fibreglass tape measure. Variables such as the time window, sampling interval, and trace stacking were pre-set at 1000 ns, 1600 ps and stacked 64 times respectively. GPR signal processing consisted of automatic gain control (AGC), which amplified the weaker reflections at depth. AGC increases the amplitude of signals by a factor that is inversely proportional to the signal strength and was universally applied to all GPR profiles since sedimentary structures commonly produce only low-amplitude reflections (Vandenberghe and van Overmeeren, 1999). No migration or trace averaging of GPR data was performed.

Multiple common mid-point (CMP) surveys were conducted to determine the EM wave propagation velocity in the surface sediments. A CMP profile records a plot of a antennae separation versus two-way travel time (Figure 2.3). CMP surveys have a similar set-up as continuous GPR surveys except data collection is conducted in step mode, with antennas initially spaced at two metres and incrementally separated 0.25 m away from the



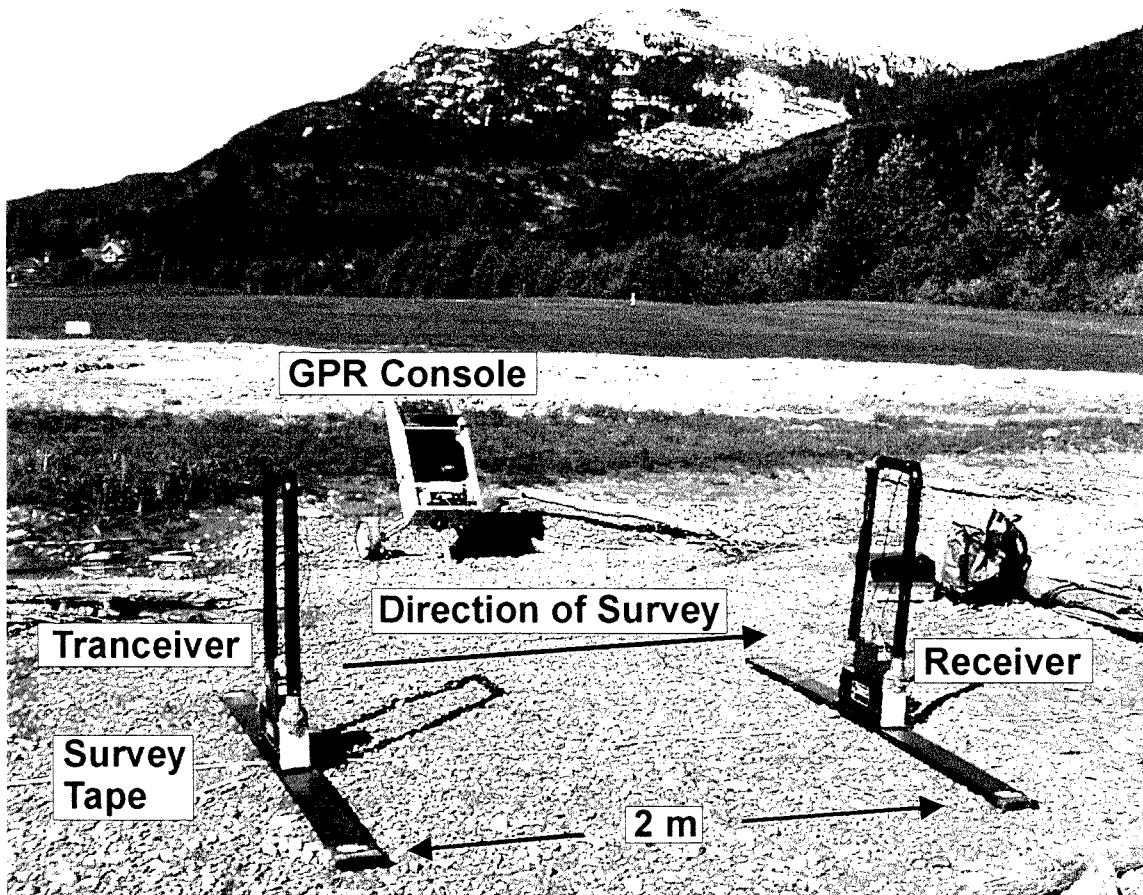


**Figure 2.2** Ground penetrating radar setup on a gravel bar in Fitzsimmons Creek (transect FC5). The computer, console, 12V battery and transformer are transported on a golf cart, connected to the transeiver and receiver by fibre optic cables.

midpoint of the survey line. An average near-surface velocity of the EM waves in the fan-delta was calculated from the inverse of the slope of the ground wave, shown in Figure 2.3. Two-way travel times of EM waves were translated to a vertical depth on each GPR profile with the average calculated velocity derived from three CMP measurements.

### **2.3.2.3 GPR Survey Design**

A grid pattern of profiling was not adopted for this study due to site restrictions resulting from the presence of dense vegetation and multiple distributary channels. Initial transects were surveyed along lines coincident with bathymetry profiles. A total of twelve transects were surveyed in the study site (Figure 2.4).

### **2.3.2.4 Interpretation of Depth from GPR Profiles**

Profiles from GPR surveys were plotted as depth and time versus distance on pulseEKKO™ software and imported into CoreDRAW (version 9.0). Recognition of major radar reflector patterns enabled depositional facies to be identified (Jol and Smith, 1991). Interpretation of reflector patterns is also based on comparison of similar characteristics from GPR profiles of outcrops (Jol and Smith, 1992). Each profile was characterized by an attenuation of electromagnetic waves at depth. Interpretation of the boundary between coarse sediment of the fan-delta and the underlying lacustrine sediment was highlighted with the addition of a boundary line in CoreDRAW. Depth estimates are based on the interpreted location of the boundary line on each GPR profile.

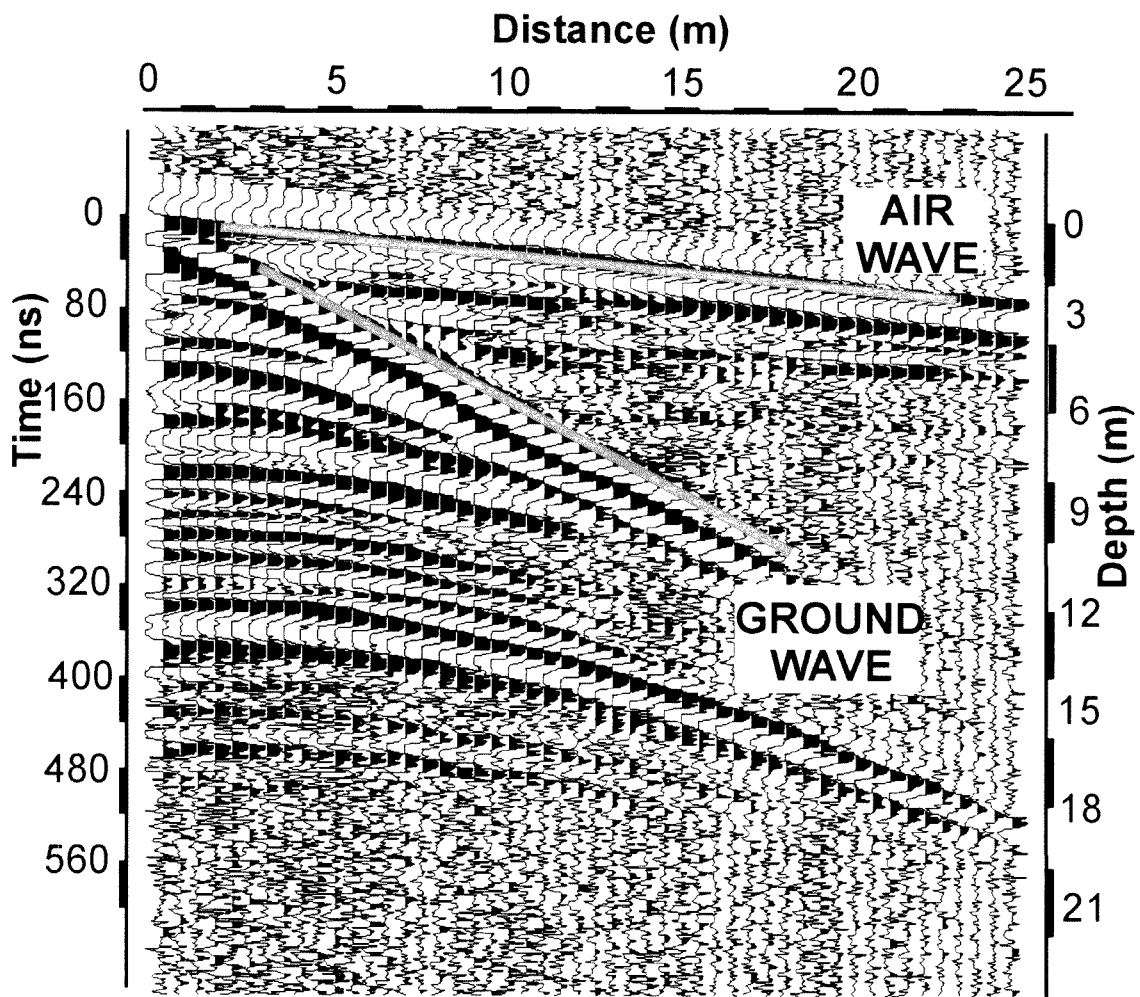


**Figure 2.3** Common mid-point (CMP1) ground penetrating radar profile. The ground wave is highlighted in order to calculate the slope of the line. The inverse slope gives the velocity of the ground wave in m/ns.

Velocity calculation:  $\text{Velocity} = 1 / \text{slope (of ground wave)}$   
 $= \text{depth} / \text{time}$

Example:  $v = (14.60 - 3.15)\text{m} / (225 - 48)\text{ns}$   
 $v = 0.065 \text{ m/ns}$

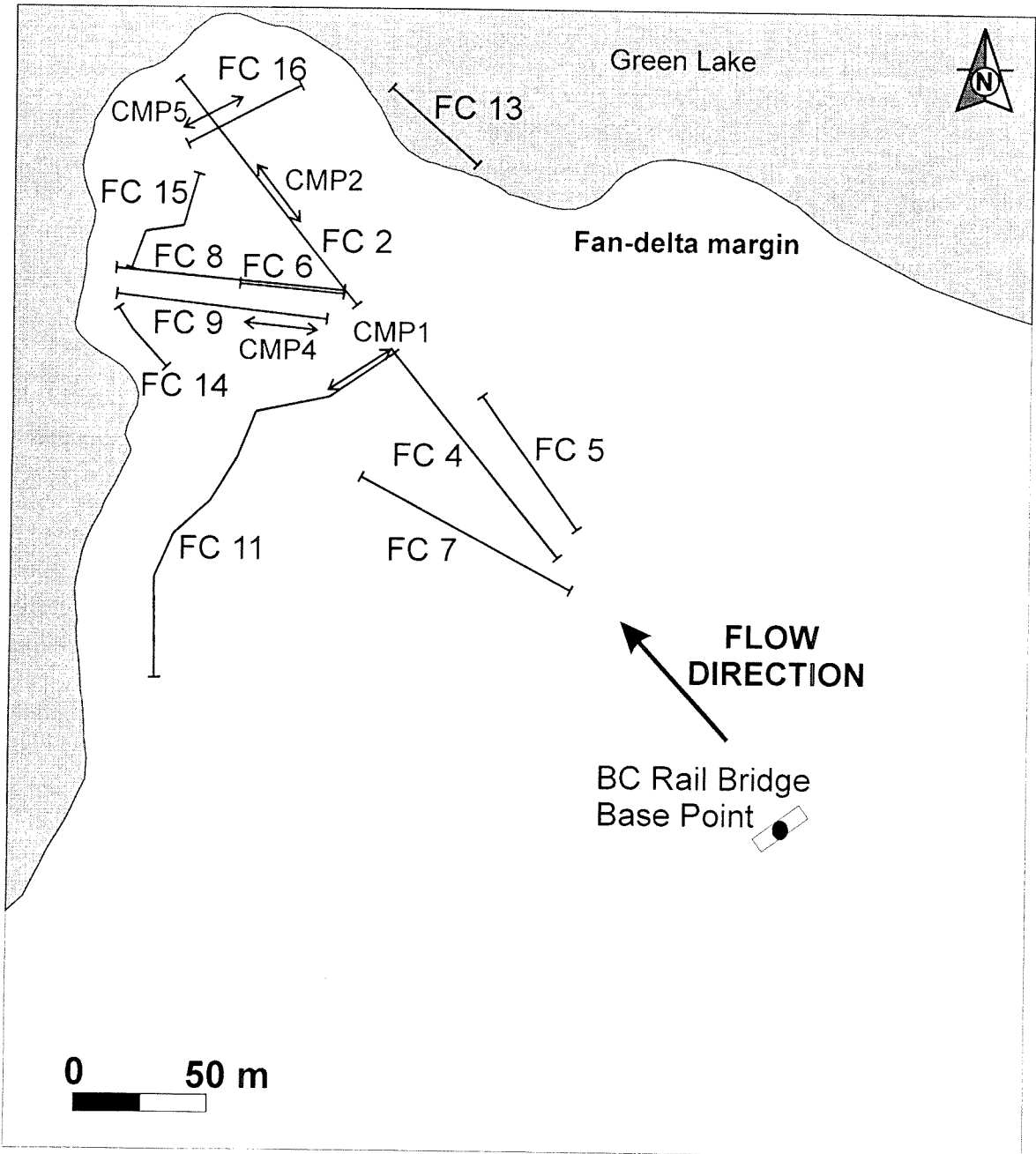


**Figure 2.4** Location of ground penetrating radar (GPR) and CMP profiles on the fan-delta. All profiles were spatially located with reference to the base point.

### 2.3.2.5 Accuracy of Interpretations

Delta topography was taken into consideration before depth estimates were finalized. Profiles were topographically adjusted relative to measured elevation changes. Elevation changes less than half a metre were assumed to be within the limit of measurement precision of depths estimated from GPR profiles ( $\pm 0.5$  metres). Depth precision was assigned as  $\pm 0.5$  metres based on a resolution of 0.5 metres with 50 MHz antennae in coarse fluvial sediment (Huggenberger *et al.*, 1994; Smith and Jol, 1997).

Preliminary bathymetric data indicated that the receiving basin was approximately 20 metres deep in the area of the fan-delta margin. This is well within the operational limit of GPR since gravel-dominated deltas in fresh water environments can be probed to depths ranging to 60 metres using 50 MHz antennae (Smith and Jol, 1997). Table 2.3 illustrates the resolution of GPR depth estimates in various materials.

**Table 2.3** Velocity, wavelength, and theoretical maximum resolution of three frequencies in geologic materials

Parent Material	Velocity (m/ns)	Frequency 25 MHz $\lambda$ (m)	Maximum resolution (m)	Frequency 50 MHz $\lambda$ (m)	Maximum resolution (m)	Frequency 100 MHz $\lambda$ (m)	Maximum resolution (m)
Air	0.3	4	1	2	0.5	1	0.25
dry sand	0.06	2.4	0.6	1.2	0.3	0.6	0.15
saturated sand	0.07	2.8	0.7	1.4	0.35	0.7	0.18
saturated gravel	0.08	3.2	0.8	1.6	0.4	0.8	0.2
freshwater	0.033	1.32	0.33	0.66	0.17	0.33	0.08

(Modified from Sensors and Software, 1996)

## 2.4 Bulk Density Sampling

Bed-material and sediment efflux are conventionally expressed in units of tonnes per annum (Mg per annum) and conversion of volume to a mass requires sediment analysis.

$$\text{Mass (Mg)} = \text{bulk density (kg m}^{-3}\text{)} \times \text{volume (m}^3\text{)} \quad (2.1)$$

A volume-to-mass conversion is calculated from the bulk density of the sediment.

Grid based sampling was not suitable for this study site because of the presence of distributary channels, therefore a radial sampling pattern similar to that adopted for GPR surveying was employed. Sediment on the fan-delta is dominated by gravel and sand.

### 2.4.1 Survey Design

Sample sites were located on the active fan-delta surface at points along a radial grid pattern convergent on a base point (Figure 2.5). A prismatic compass and laser range finder were used to locate sample sites, the positions of which were recorded on a base map.

### 2.4.2 Sampling Procedure

Wolman (1954) introduced a relatively simple and widely utilized method for determining the size distribution of surficial fluvial gravel. Representative sampling of grain sizes greater than 0.05 mm requires a minimum sample size of approximately 10 kg (Coates, 1984). In this study, samples were collected from surface sediment pits on the fan-delta, a combination of methods proposed by Wolman (1954) and Coates (1984).

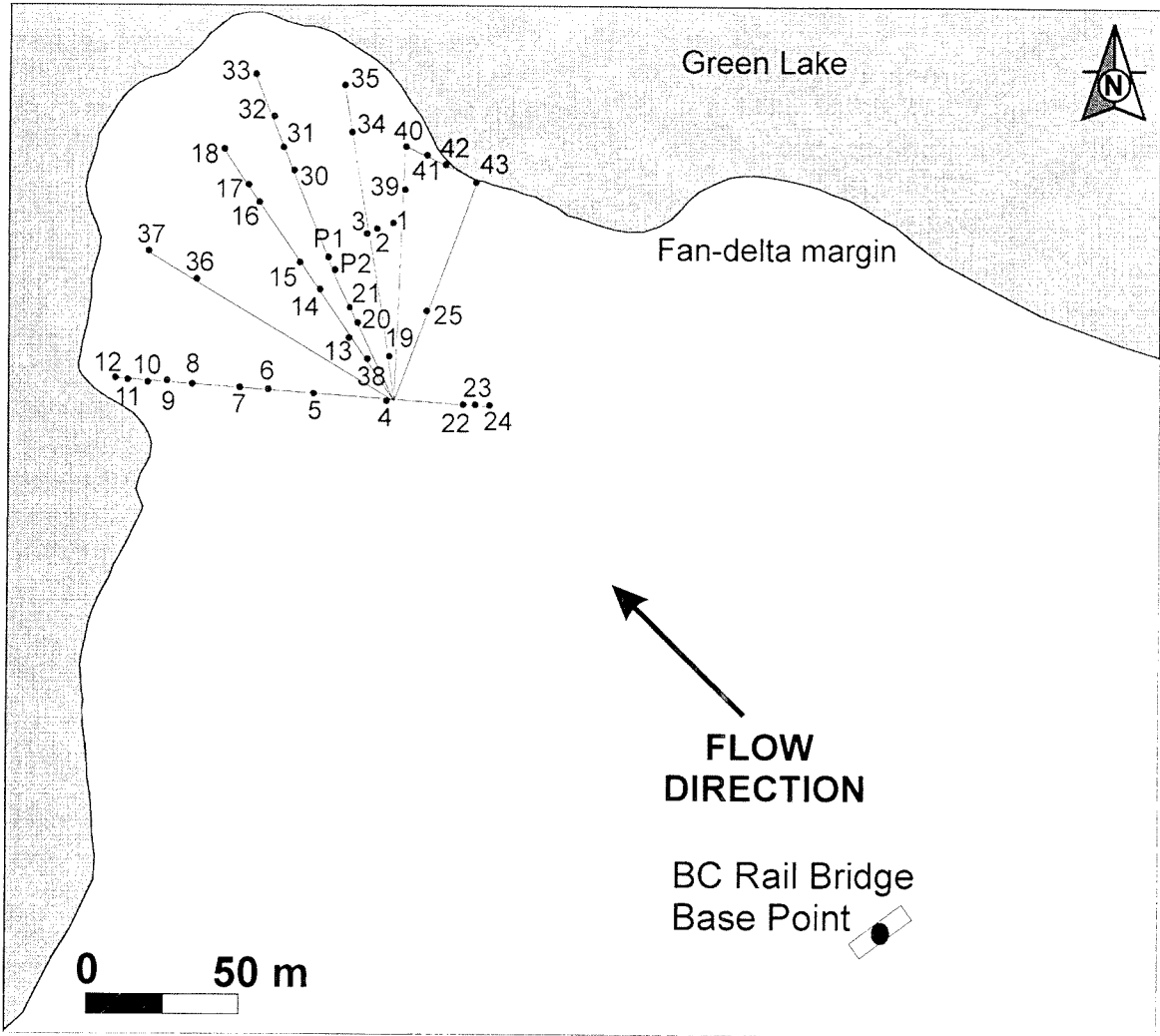


**Figure 2.5** Location of surface sediment core samples on the fan-delta. All sample locations were spatially referenced to the BC Rail bridge base point.

An iron box bulk-sediment sampler (core sampler) was designed and fabricated with an open top and dimensions of 0.20 m x 0.20 m x 0.20 m. This exceeded the largest clast in the sample area. Preparation of each sample site involved excavating and removing surface sediment to the depth of the largest clast within the sample location (Wolman, 1954). The core sampler, placed open side down onto the excavated surface, was manually pressed into the sub-surface until it was completely below grade. The area around the sample location was excavated and the sample plus 0.1 m of sediment below the core sampler were manually extracted and turned open side up. Sediment exceeding the dimensions of the core sampler was sheared off using a surveyor's trowel. Samples were transferred in labeled bags to the lab for analysis.

### **2.4.3 Lab Analysis of Bulk Samples**

Forty-one near-surface core samples of sediment were collected. Each sample was oven dried at 105° C for 24 hours and weighed on a Mettler balance (model H20 accurate within  $\pm 0.001$  g). Bulk density was calculated as the mass of each sample divided by the measured volume of the core sampler (Appendix A-7). The volume of the core sampler was determined by the capacity of water ( $2.039 \times 10^{-3} \text{ m}^3$ ) when filled. The representative bulk density was calculated by dividing the average mass of the forty-one representative core samples by the volume of the core sampler.

Dried samples were sieved to determine the proportions in the Wentworth grain size classes of silt and clay, sand and gravel. Silt and clay include sediment grain sizes less than 0.064 mm, sand includes sediment grain sizes between 0.064 mm and 2 mm, and gravel includes all sediment grain sizes greater than 2 mm (Boggs, 1995). Sieving procedures distinguished grains based on size using three standard sieves and a collection



pan mounted on a Fisher-Wheeler sieve shaker for five minutes. Gravel, sand and silt/clay proportions were individually transferred to bags and weighed on a Mettler balance ( $\pm 0.001$  g).

## **2.5 Application of Geographical Information Systems (GIS)**

Area measurements from successive aerial photographs that form the basis of the incremental volume calculations have been obtained using a GIS program.

### **2.5.1 Measurement of Planimetric Growth**

Successive fan-delta margin locations plotted on a base map were transferred to a GIS program (ArcInfo 3.1) using a standard digitizer tablet. Differences in the areas between the fan-delta margins from sequential aerial photographs were calculated in ArcView (version 3.1). Total planform change over the 52-year period of analysis is the sum of all individual areas.

### **2.5.2 Error Estimation of Planimetric Growth**

Photogrammetric measurements mapped at scales of 1:5000 have been shown to measure the lengths and widths of accumulation zones within  $\pm 0.5$  metres (Roberts and Church, 1986). Planimetric measurements of the fan-delta edge are within  $\pm$  one metre, attributable to measurement error. In order to assess this effect, a buffer of one metre was applied to all GIS line-work digitized on the base map. The absolute areas were calculated and subtracted from the original areas to determine an absolute error estimate for the area calculations.

### **2.5.3 Estimation of Volume**

A paleo-lake contour model of the receiving basin overlain by the fan-delta was constructed based on depth interpretations from a combination of bathymetric and GPR surveys. The purpose of the paleo-lake model is to assign depth estimates of the sediment pile to areas not measured with bathymetry or GPR profiling. Lake bottom contours were visually drafted at one-metre intervals and the paleo-lake contour model was digitally superimposed on the base map of the sequential advancement of the fan-delta margin. The combined paleo-lake contour model and margin location map produced a composite map with sixty-one cells, from which Arc View software generated an attribute table of the sixty-one areas in square metres. Corresponding depth estimates derived from the paleo-lake contour model were added to the attribute table, transferred to an Excel (version 6.0) spreadsheet, and volumes generated. Total volume of the fan-delta was taken as the sum of all the individual volumes.

## **2.6 Sediment Budget**

A sediment rating curve, historic discharge data, and lacustrine rhythmite data were used to determine the sediment budget for Fitzsimmons Creek in order to calculate the percentage contribution of material transported as bed load to the total sediment yield of Fitzsimmons Creek.

### **2.6.1 Sampling Suspended-Sediment**

Suspended-sediment samples were collected between June 16 and July 29, 2000 using a DH<sub>48</sub> depth integrated sediment sampler (hand held version fitted to stream gauging rods). Flow was sampled in the thalweg of the creek. Suspended-sediment samples were collected from a BC Rail bridge at Fitzsimmons Creek, approximately 400 metres upstream from the margin of the fan-delta. Limited replicate samples were collected from a Water Survey of Canada (WSC) stream gauging station (BC 08MG026). A three-metre metal extension rod was retrofitted to the sampler to facilitate collection of suspended-sediment from the WSC cableway. Brian Menounos, Department of Geography, University of British Columbia (UBC), provided supplemental results of suspended-sediment concentrations collected between May 05 and September 20, 2000.

### **2.6.2 Suspended-Sediment Analysis**

Each of the ten suspended-sediment samples were gravity filtered through pre-dried, weighed, and labeled filter paper (0.55 microns), oven dried at 105 °C for 24 hours, and weighed on a Mettler balance ( $\pm 0.001$  g) (Woodward, 1997). Individual weights and volumes were recorded to determine the concentration of suspended-sediment ( $\text{mg L}^{-1}$ ). The same procedure applied to (UBC) data, except that vacuum filtration replaced gravity filtration.

### **2.6.3 Discharge Data**

In order to independently estimate the suspended-sediment load being delivered to Green Lake during the survey periods it is necessary to know the mean daily discharge record of Fitzsimmons Creek for the entire period. Unfortunately, only seven years of

record exist for this stream and it has been necessary to generate a mainly synthetic record based on a linear regression model ( $r^2 = 0.78$ ) utilizing the much longer record of nearby Lillooet River.

#### **2.6.4 Sediment-Rating Curve**

Suspended-sediment data and corresponding discharge data from WSC records were plotted as a log-log graph of the concentration of suspended sediment versus discharge. Best-fit lines and equations of the logarithmic relationship between the concentration of suspended sediment and discharge were generated in Microsoft Excel (2000 edition) and Statview (version 4.5.3). The equation was applied to historic daily discharges of Fitzsimmons Creek and yielded estimates of the mean daily suspended-sediment concentrations. Suspended-sediment concentrations derived from sediment rating curves are biased (Ferguson, 1986; Cohn *et al.*, 1989) and a log to normal bias correction factor recommended by Ferguson (1986) was used to upward adjust calculated daily-suspended sediment concentrations over the 52-year record (Appendix A-5).

#### **2.6.5 Lacustrine Sedimentation**

Lacustrine sedimentation rates in Green Lake for the periods under investigation were obtained from Brian Menounos, Department of Geography, University of British Columbia. Estimates were based on seven, three-inch cores sub-sampled from Ekman dredge cores. Sedimentation rates were based on preliminary examination of rhythmite thickness on a representative area for the lake as a whole as illustrated in Figure 2.6. Estimates are not corrected for organic matter or density differences. Time control is achieved by rhythmite counts and cesium ( $^{137}\text{Cs}$ ) dating to a precision of  $\pm$  two years.

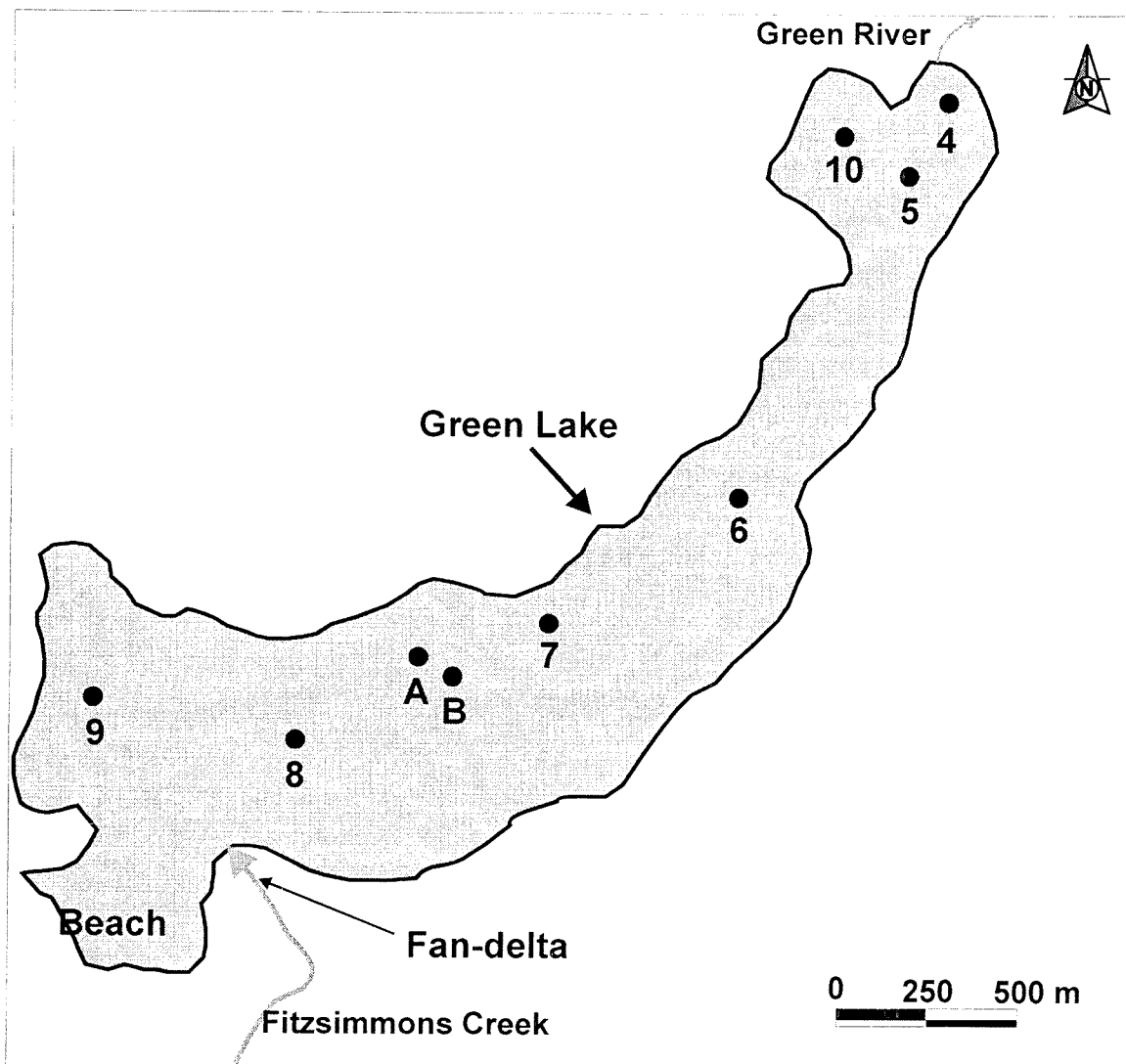


**Figure 2.6** Location of lacustrine sediment core samples in Green Lake.  
 4 - 10 > Location of Ekman dredge cores samples.  
 A & B > Location of vibra-cores samples.  
 Beach indicates the subaqueous accumulation of sediment 10 metres below the water surface.  
 (Data from Menounos, 2000)

# CHAPTER 3:

## RESULTS

The purpose of this chapter is to present the results of the study in terms of three primary objectives: (1) What is the total annual bed-material efflux from Fitzsimmons Creek? (2) How variable is the bed-material efflux? (3) What is the minimum sampling time needed to reliably estimate the 50-year average bed-material efflux from Fitzsimmons Creek? The chapter will also present results of the sediment budget for Fitzsimmons Creek and the percentage of material transported as bed load. Organization of this chapter will be in sections related to the primary objectives and the sediment budget.

### **3.1 Determination of Bed-Material Efflux**

#### ***3.1.1 Planform development: Photo Differencing***

The outline and morphology of the fan-delta derived from eight successive aerial photographs between 1947 and 1999 are illustrated in Figures 3.1a and 3.1b. In the 1947 aerial photograph (Figure 3.1a), an earlier location of the main distributary channel of Fitzsimmons Creek is to the southwest. The 1958 aerial photograph (Figure 3.1b) indicates that the channel shifted after 1947 and a new lobe was under development at that time. The aerial photographs from 1963 to 1999 reveal a rapid accumulation of sediment and pronounced progradation of the fan-delta into the receiving basin during

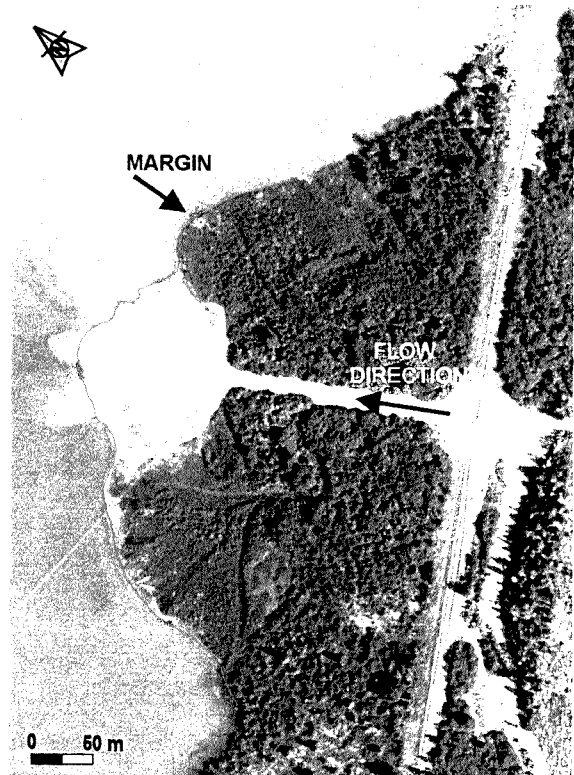
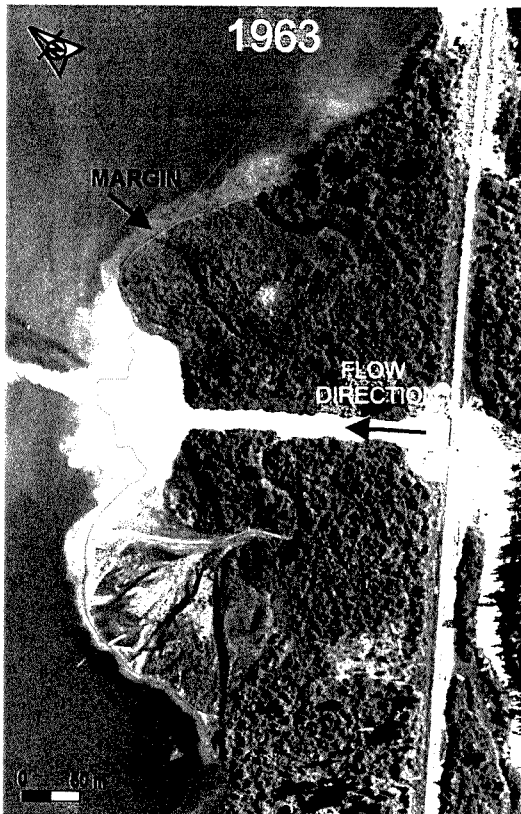
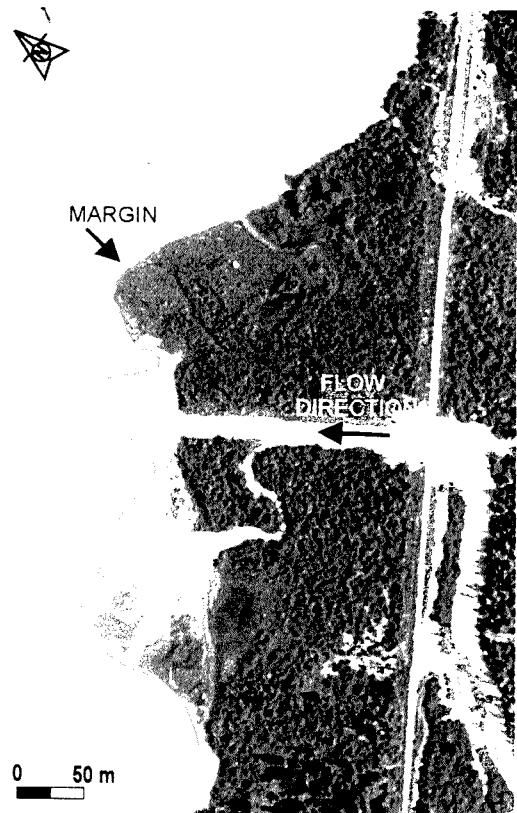
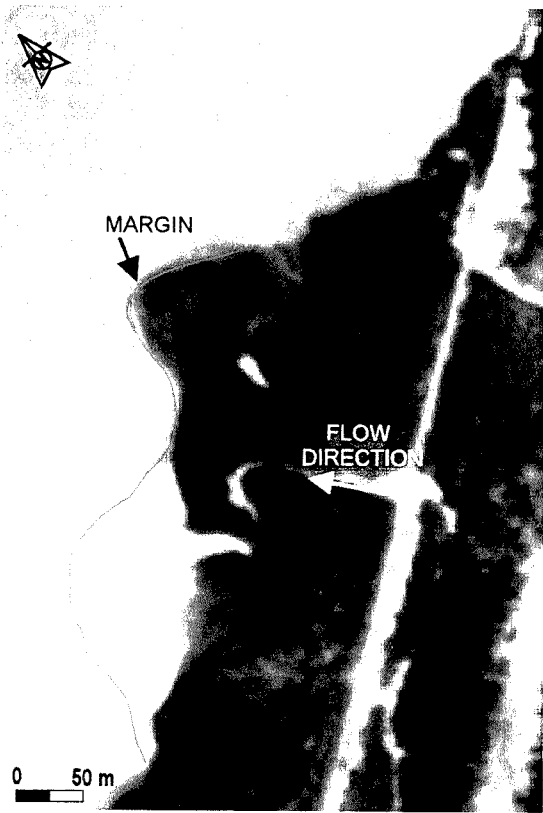


**Figure 3.1a** Time sequential aerial photographs of the study site. Interpreted boundary emphasizes the margin of the fan-delta. (Original photos from Ministry of Environment, Lands and Parks, 1999)

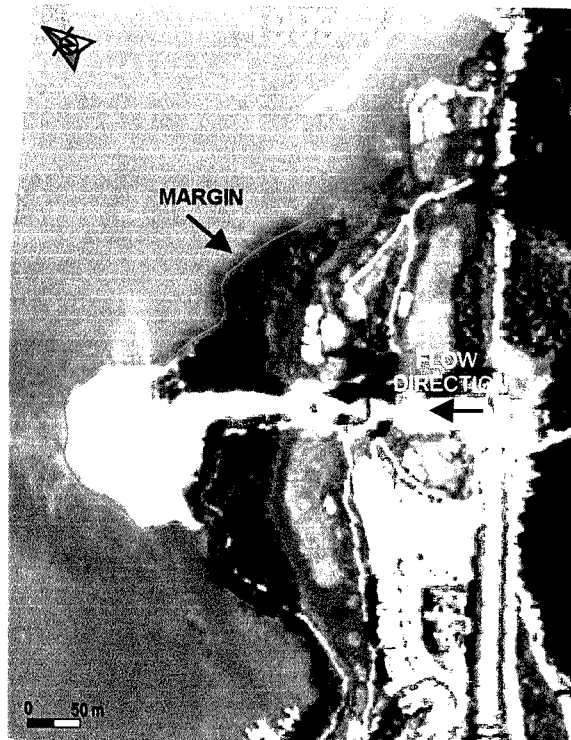
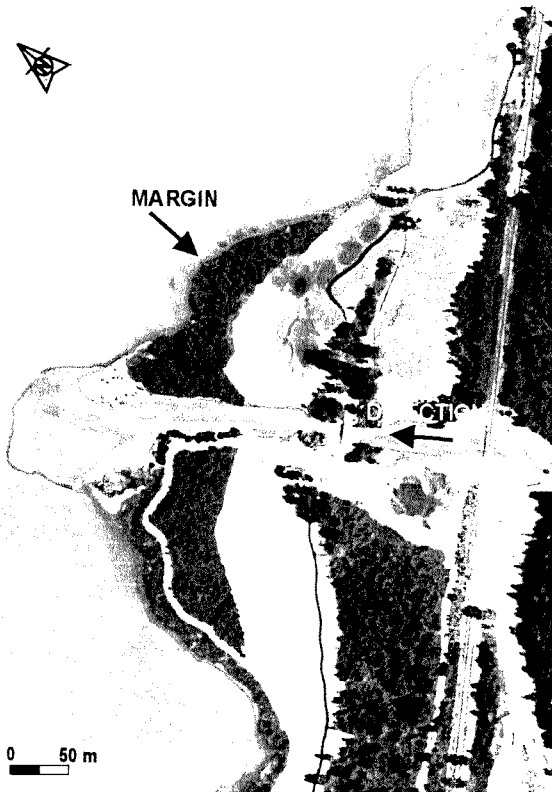
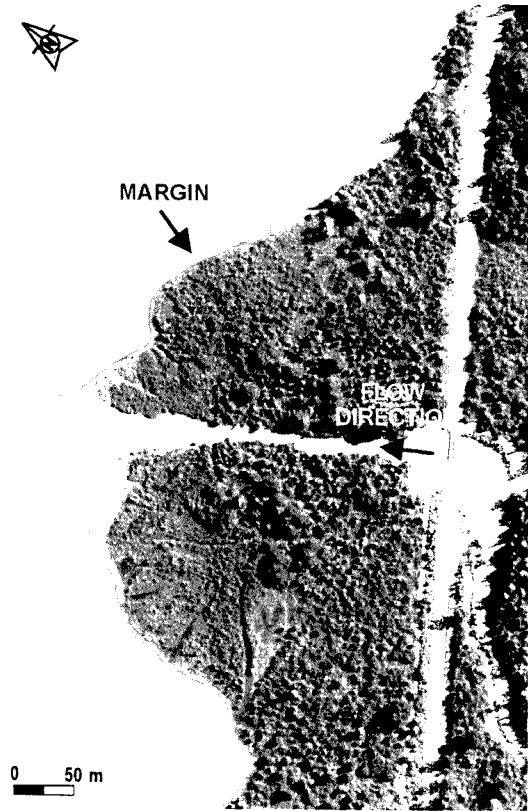
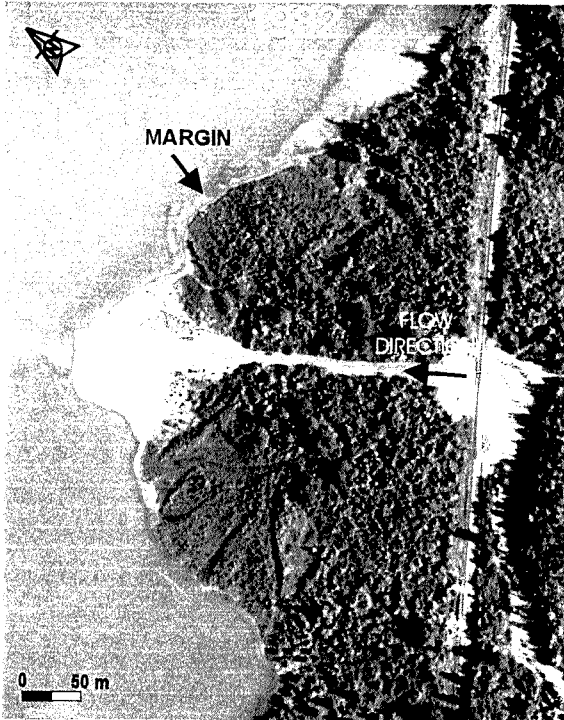


**Figure 3.1b** Time sequential aerial photographs of the study site. Interpreted boundary emphasizes the margin of the fan-delta. (Original photos from Ministry of Environment, Lands and Parks, 1999)



this time interval. Land use changes, evident in the 1994 aerial photograph include the construction of two bridges, and a golf course adjacent to the delta.

The base map (Figure 3.2) showing the delta-front position over the period of record clearly reveals measurable differences in the planimetric development of the fan-delta over periods ranging from four to eleven years between aerial photograph years. Aerial photographs indicate that the main distributary channel flows in the primary direction of fan-delta advancement. Photo differencing of the fan-delta between 1947 and 1958 indicates two areas of growth, also related to the location and re-alignment of the main distributary channel. As Figures 3.2 illustrates, the ten-year period between 1963 and 1973 produced the greatest delta growth, while the nine-year period between 1973 and 1982 exhibits the least growth. Elsewhere in the watershed, however, sediment did accumulate within the channel. Downstream of the BC Rail bridge (Figures 3.1d and 3.1e) the channel narrows over the eight-year period and there is a large accumulation of sediment immediately downstream of the bridge.

Results of photo differencing between 1990 and 1994 reveal accumulation of sediment along the margins of the fan-delta during this four-year period. The fan-delta advanced in two locations between 1994 and 1999. During the summer of 1999, two main distributary channels are apparent on the fan-delta, coincident with lobe development of the fan-delta observed for the last photoperiod.

Successive aerial photographs indicate that the fan-delta developed as a series of three lobes (Figure 3.1 a-h). Relative ages of the lobe features are apparent in aerial photographs because of maturing vegetation and their location with respect to the main distributary channel. The 1947 aerial photograph (Figure 3.1a) shows one

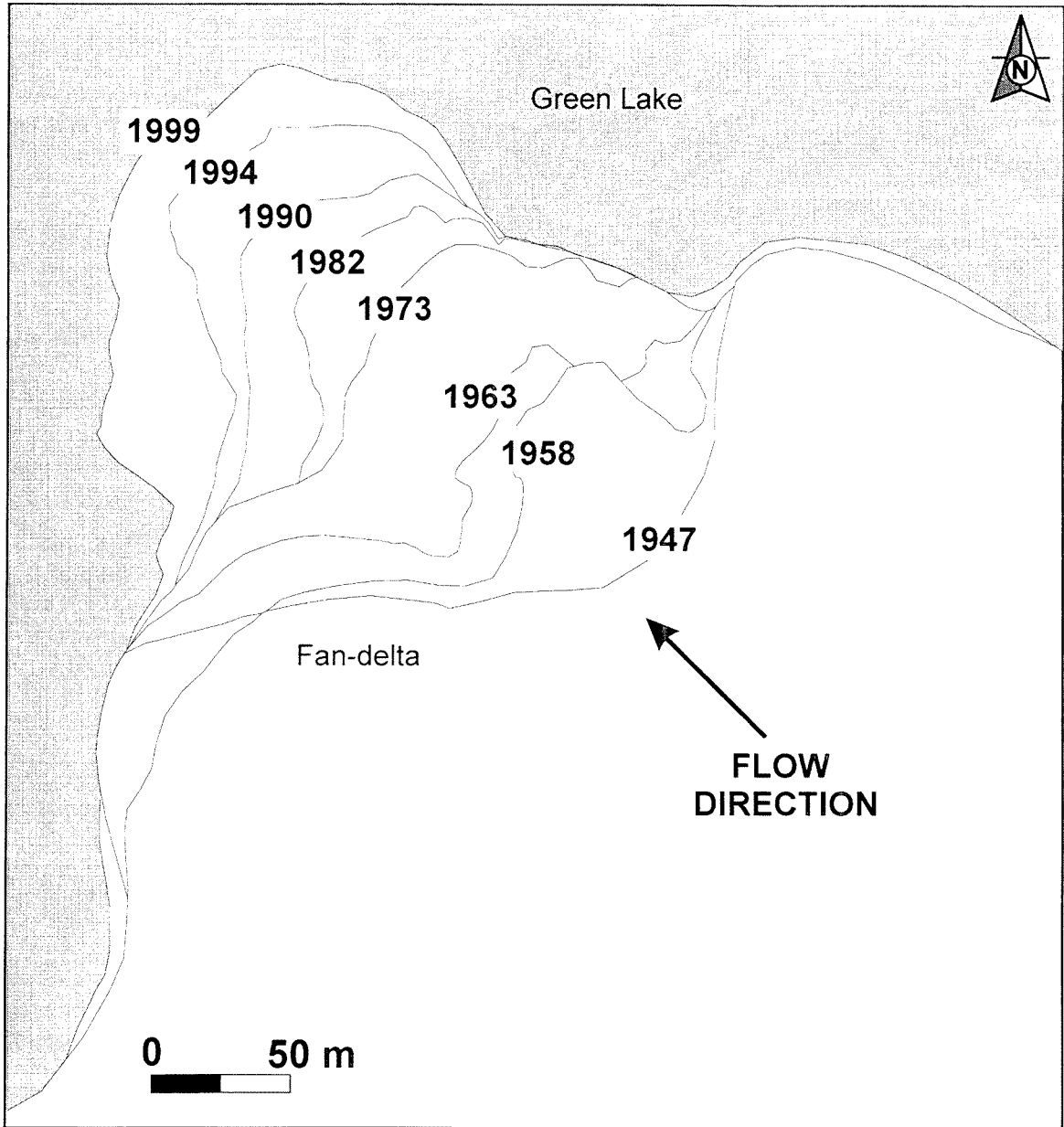


**Figure 3.2** Planform evolution base map revealing the location of time sequential fan-delta margins over the 52-year record. The base map was generated in GIS and the planform measurements were analyzed in ArcView 3.1

established lobe to the southeast of the study site, and another lobe in the preliminary stages of development to the southwest. The established lobe is inferred to have developed in the decades preceding 1947. The 1958 aerial photograph (Figure 3.1b) indicates the realignment of the main distributary channel to its present-day location. Local knowledge, historical accounts, and field examination of the morphology of the main channel reveal that the channel was re-aligned to its present location between 1947 and 1958 for flood maintenance near the BC Rail bridge crossing. A third lobe of the fan-delta developed rapidly following the re-alignment of the channel, advancing the margin of the delta further into the receiving basin.

Aerial photographs highlight the dominant influence of Fitzsimmons Creek on the accumulation of sediment in the receiving basin, Green Lake. The extent of fine sediment contributed from Fitzsimmons Creek to the receiving basin is apparent from the aerial photographs. Colour aerial photographs (Figure 3.1g) highlight the differences of sediment concentration. Almost the entire volume of sediment accumulating in the receiving basin appears to be derived from Fitzsimmons Creek sediment influx and estimates of the sediment budget reported in this study reflect this assumption.

### **3.1.2 Vertical Development: Bathymetry of the Receiving Basin**

Bathymetric profiles indicate depth to the lake bottom. Results from ten transects indicate basin depths proximal to the prodelta ranging from 10 to 18 metres  $\pm$  0.5 metres. Depth estimates calculated from bathymetric profiles point to a shallow basal area in the region immediately northwest of the study site while the deepest area is to the north east of the fan-delta margin (Figure 3.3).

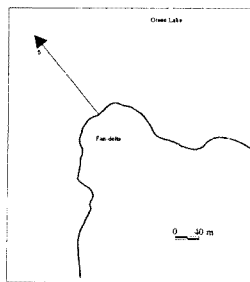
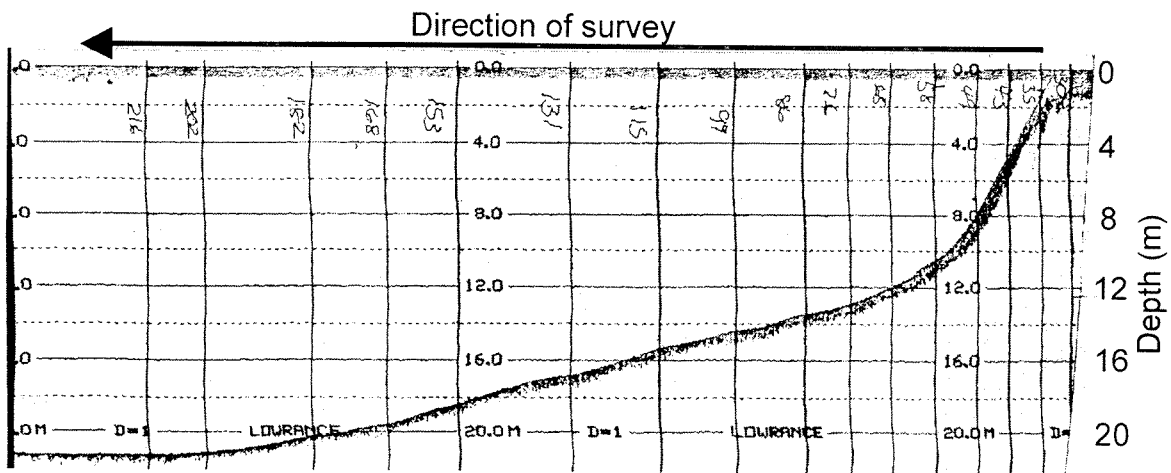


**Figure 3.3** Bathymetry profile illustrating the steep delta front (approximately 25°) and gently sloping pro-delta grading to the receiving basin at a depth approaching 20 metres.

The bathymetric profile reveals the steeply inclined delta-front, close to the fan-delta margin, grading to less steeply inclined sediment, and to sub-horizontal strata into the receiving basin at a depth of approximately 12 metres. The slope of the steepest delta-front approaches 25°. The steepest slopes were observed on bathymetric profiles were parallel to the direction of contemporary river flow and most likely correspond to true dip angles.

### **3.1.3 Vertical Development: Ground Penetrating Radar of the Fan-Delta**

A bathymetric survey conducted to interpret the depth of sediment in the fan-delta revealed significant variation in the elevation of the basal surface of the receiving basin. Ground penetrating radar (GPR) was employed to supplement the bathymetric data and to provide estimates of sediment thickness in the fan-delta.

Three common mid-point (CMP) surveys were performed to determine the average near-surface velocity of the EM waves. Velocities of EM waves calculated from the inverse slope of the ground wave in repeated CMP surveys ranged from 0.06 to 0.08 m ns<sup>-1</sup> (Appendix A-2a – A-2c). Average near-surface velocity was calculated as 0.07 m ns<sup>-1</sup> and is consistent with previous examinations of coarse-grained deltaic sediments (Jol and Smith, 1992; Smith and Jol, 1997).

Attenuation of the GPR signal is illustrated by profiles at two-way travel times of 140 to 260 ns, corresponding to depths ranging between 10 - 18 metres (Figure 3.4a-d and Appendix B-3a – B-3i). The attenuation of the GPR signal occurs in the area below the bottomset facies. Profiles conducted in the apparent direction of dip include FC2, FC4, FC5, FC6, FC8 and FC9, all highlighting the three principal sedimentary facies (topset, forest, and bottomsets).

Topset facies are horizontal and range in thickness from three to four metres. Foreset facies in the apparent dip direction range in thickness from six to eight metres. Sub-horizontal bottomset facies range in thickness from two to five metres. Topset facies consist of horizontally stratified gravel and sand, foreset facies consist of inclined coarse-grained facies at an apparent dip approaching 25°, and the bottomset facies likely consist of fine-grained sediments deposited nearly horizontally (Jol and Smith, 1991). The FC2 profile (Figure 3.4a) indicates less steeply inclined slopes of the delta-front at the horizontal distance of 110 m. Here the more gently dipping foresets overlie a lenticular package of reflectors.

The steepest slopes measured from the GPR profiles have an apparent dip of 25°. A migration calculation (Reynolds, 1997) was applied (Appendix A-6), and produced an adjustment from 25° to 25.003°. The vertical displacement of the two-way travel time was calculated as 0.05 ns, which is equivalent to a change in depth of just 0.0035 metres, significantly less than the error associated with depth estimates. Migration of each profile was therefore not undertaken.

Error estimates associated with sediment thickness were based on visual interpretation of depth from GPR profiles. The assigned error of  $\pm 0.5$  metres was within the accepted resolution for 50 MHz antennae in a coarse grained environment (Sensors and Software, 1996). Results from GPR profiles (Figures 3.4a – 3.4d and Appendix B-3) indicate the depth of sediment accumulated in the fan-delta ranges between 10 - 18 metres ( $\pm 0.5$  metres).

Although GPR profiles are commonly topographically corrected to take into account variations in surface topography, the study area has little relief and this

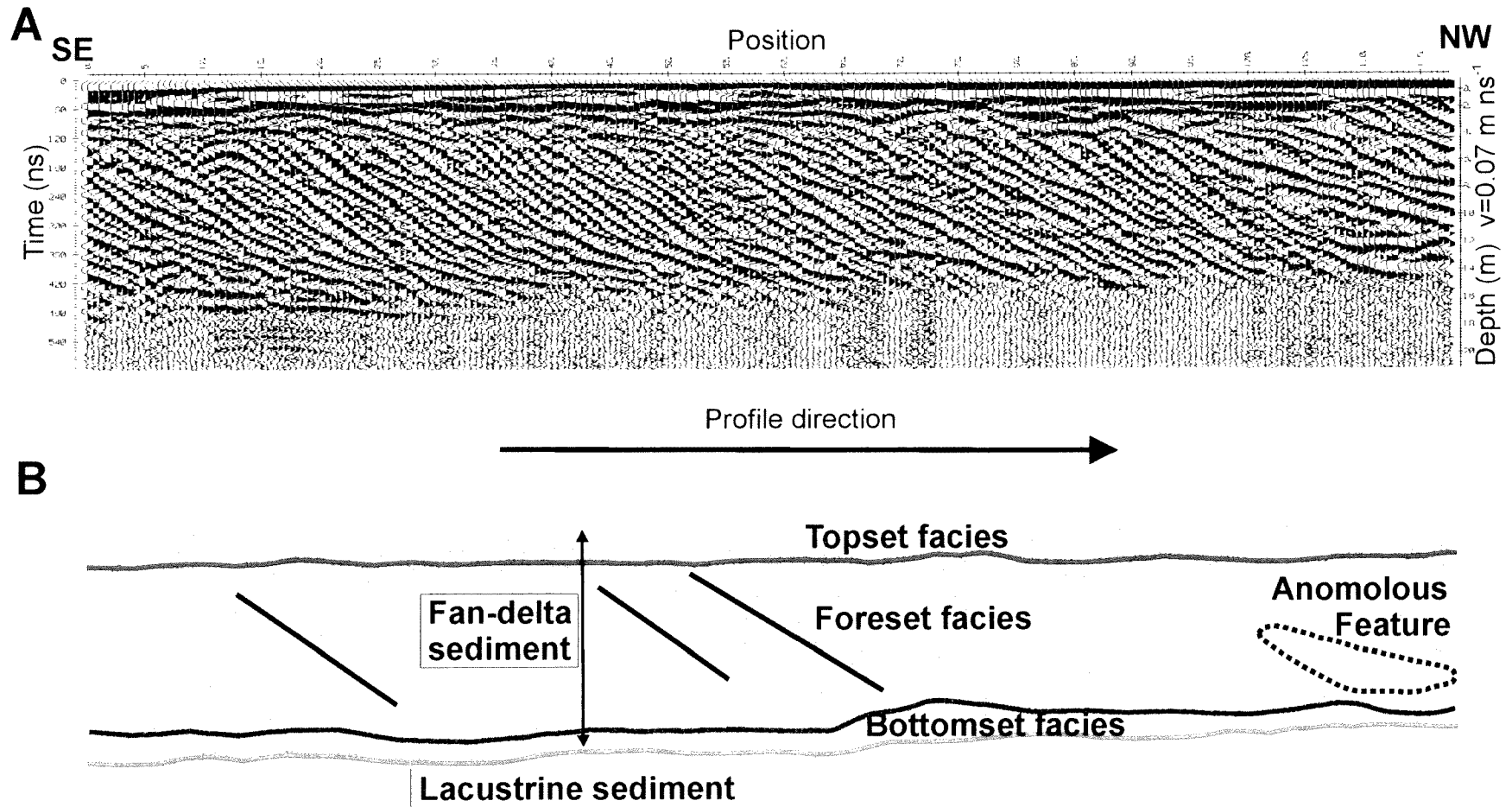


**Figure 3.4a** (A) Radar profile FC2 in the direction of dip. (B) Interpreted boundaries. Linework emphasizes the major reflections and reveals the thickness of fan-delta sediment as well as the estimated radar facies. Anomalous feature most probably illustrates the sedimentary record of shifting distributary channels.

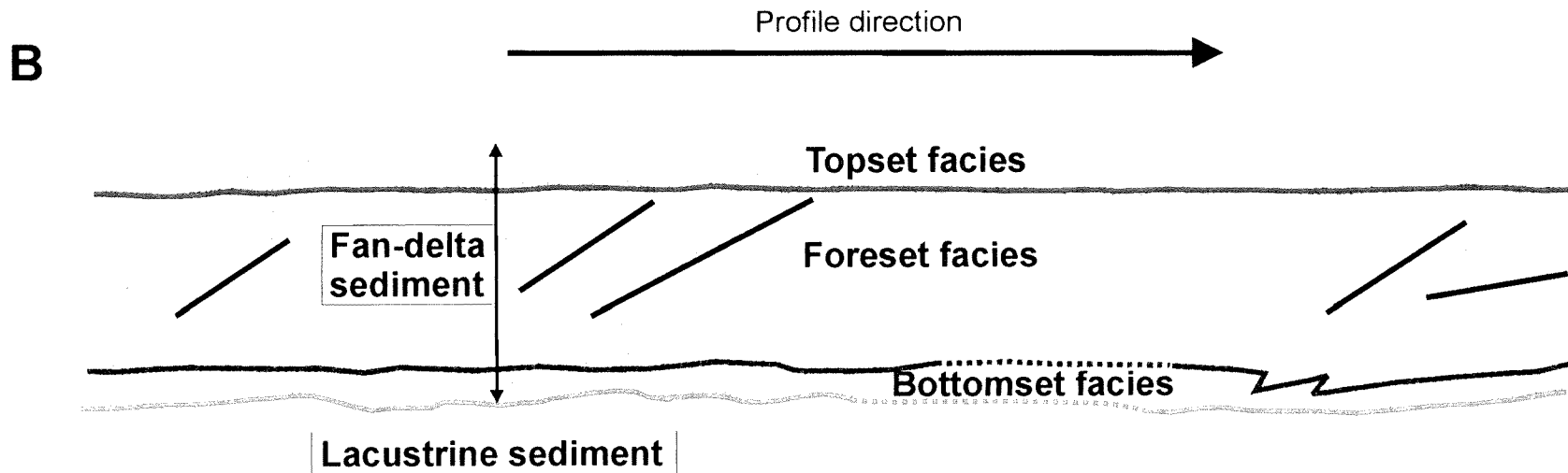
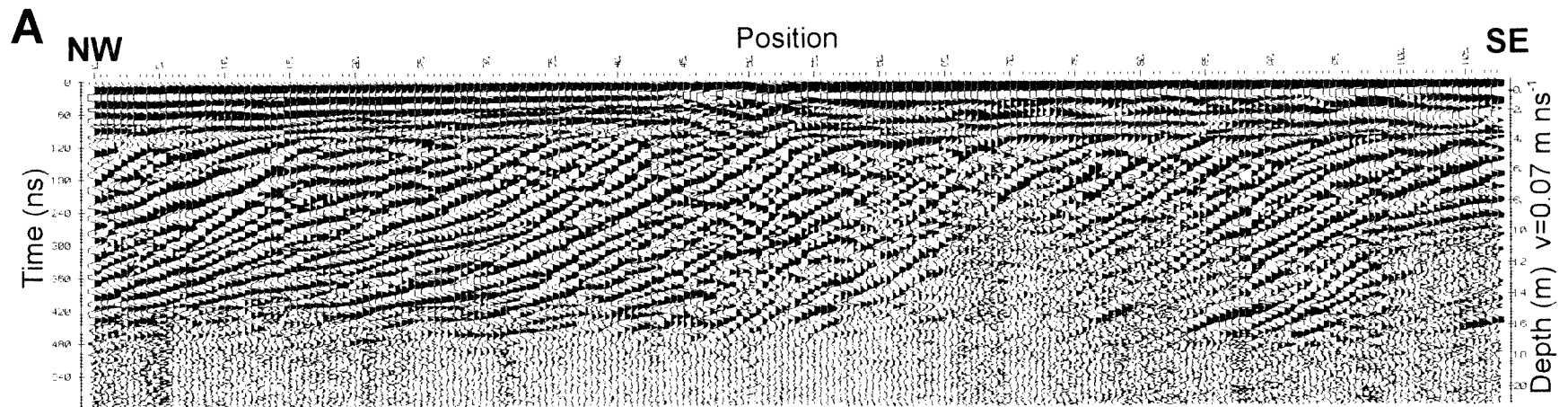


**Figure 3.4b** (A) Radar profile FC4 opposite the direction of dip. (B) Interpreted boundaries. Linework emphasizes the major reflections and reveals the thickness of fan-delta sediment as well as the estimated radar facies. Shifting distributary channels are interpreted from changes in foreset facies slopes in the SE end of the transect.



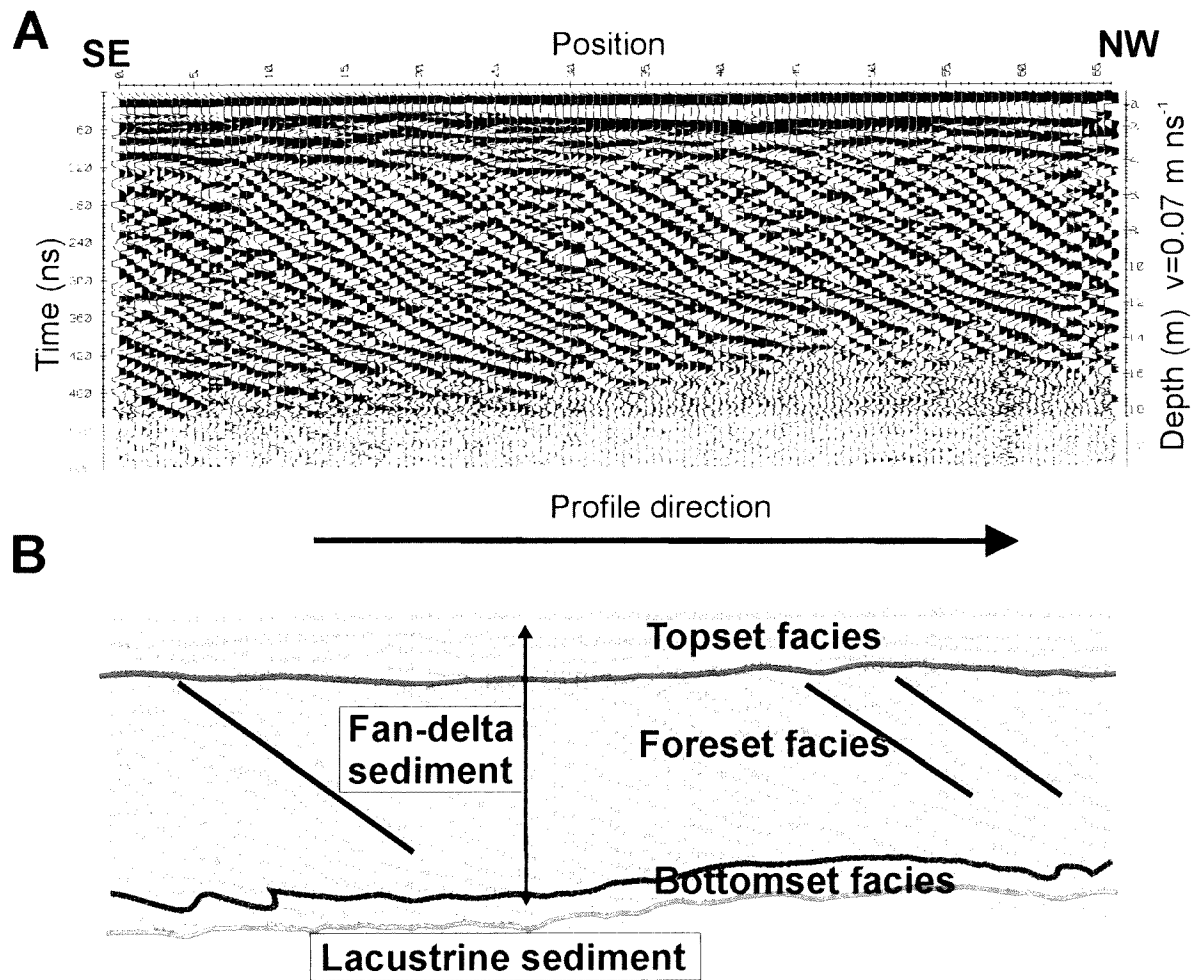


**Figure 3.4c** (A) Radar profile FC5 in the direction of dip. (B) Interpreted boundaries. Linework emphasizes the major reflections and reveals the thickness of fan-delta sediment as well as the estimated radar facies.

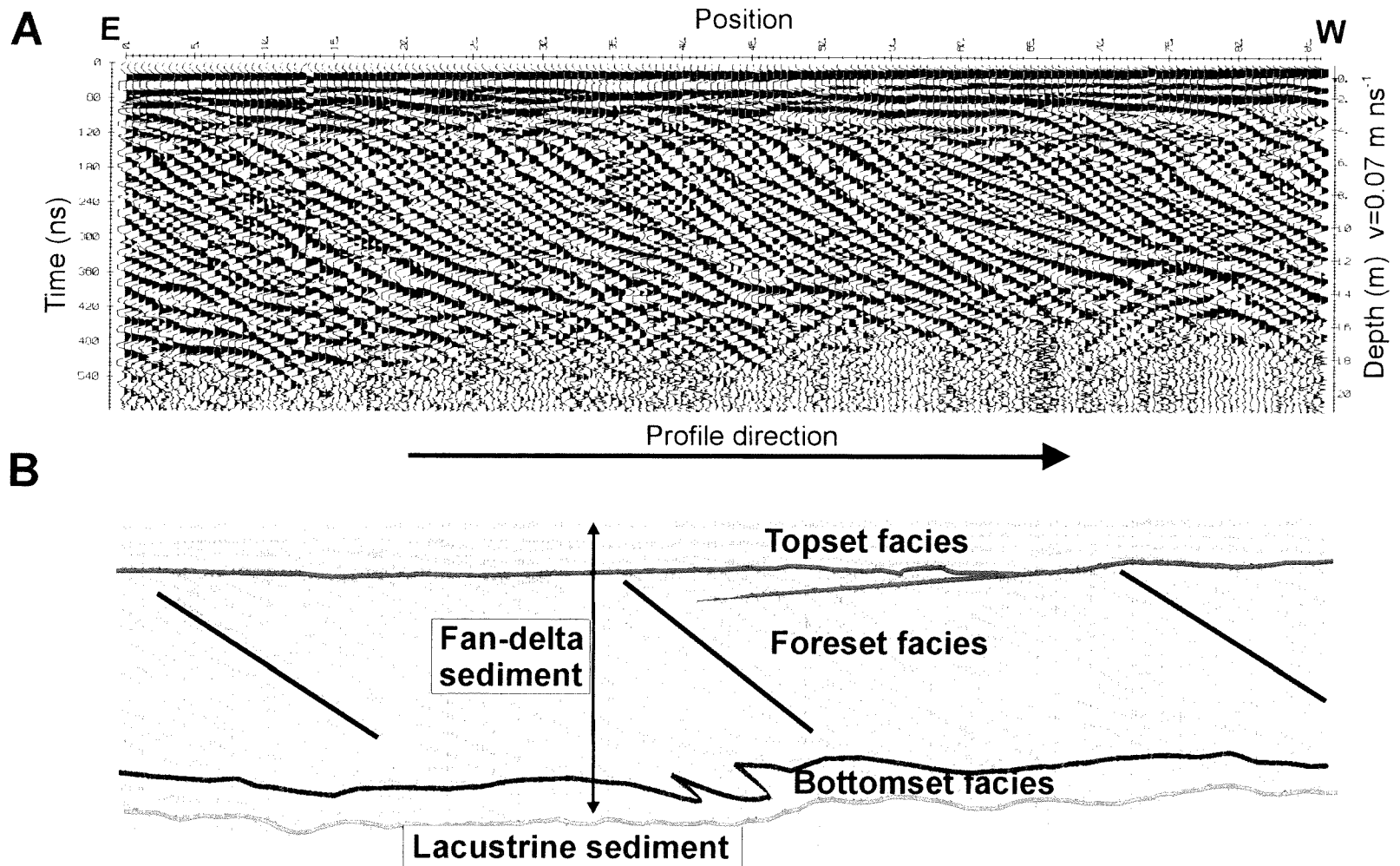


**Figure 3.4d** (A) Radar profile FC8 in the direction of dip. (B) Interpreted boundaries. Linework emphasizes the major reflections and reveals the thickness of fan-delta sediment as well as the estimated radar facies.

correction was unnecessary. Areas of the study site with vegetation corresponded to the highest elevation, approximately 0.75 metres above the lake surface. The active fan-delta area exhibits very little topographic variation ( $\pm 0.30$  metres).

GPR and bathymetry survey results were combined in a paleo-lake contour model of the receiving basin under the contemporary fan-delta. Figure 3.5 illustrates the one-metre contours ranging from 10 to 18 metres. This map shows the relatively shallow sediment surface in the southwest area of the fan-delta and the greatest depth at the northeast area of the fan-delta.

#### **3.1.4 Bulk Density**

In order to determine the sediment yield from volume estimates, the average bulk density of the delta sediment pile must be specified. It is useful to consider this average value as an integration of three components of possibly contrasting local bulk density: the near-surface topset facies deposited by the river, the underlying foreset facies deposited, and the basal bottomset facies.

The near-surface component is directly accessible and is the subject of a sediment survey. Forty-one core samples of sediment were collected and measured for mass and the percentage composition of silt, sand, and gravel (Appendix B-4). Mass of samples ranged from  $2.88 \times 10^3$  to  $4.13 \times 10^3$  g ( $\pm 2$  g) and averaged  $3.66 \times 10^3$  g ( $\pm 0.3 \times 10^3$  g) with a median of  $3.68 \times 10^3$  g.

Sediment samples from surface test pits consist of coarse fluvial material dominated by large gravel intermixed with coarse sand. Measurements summarized in

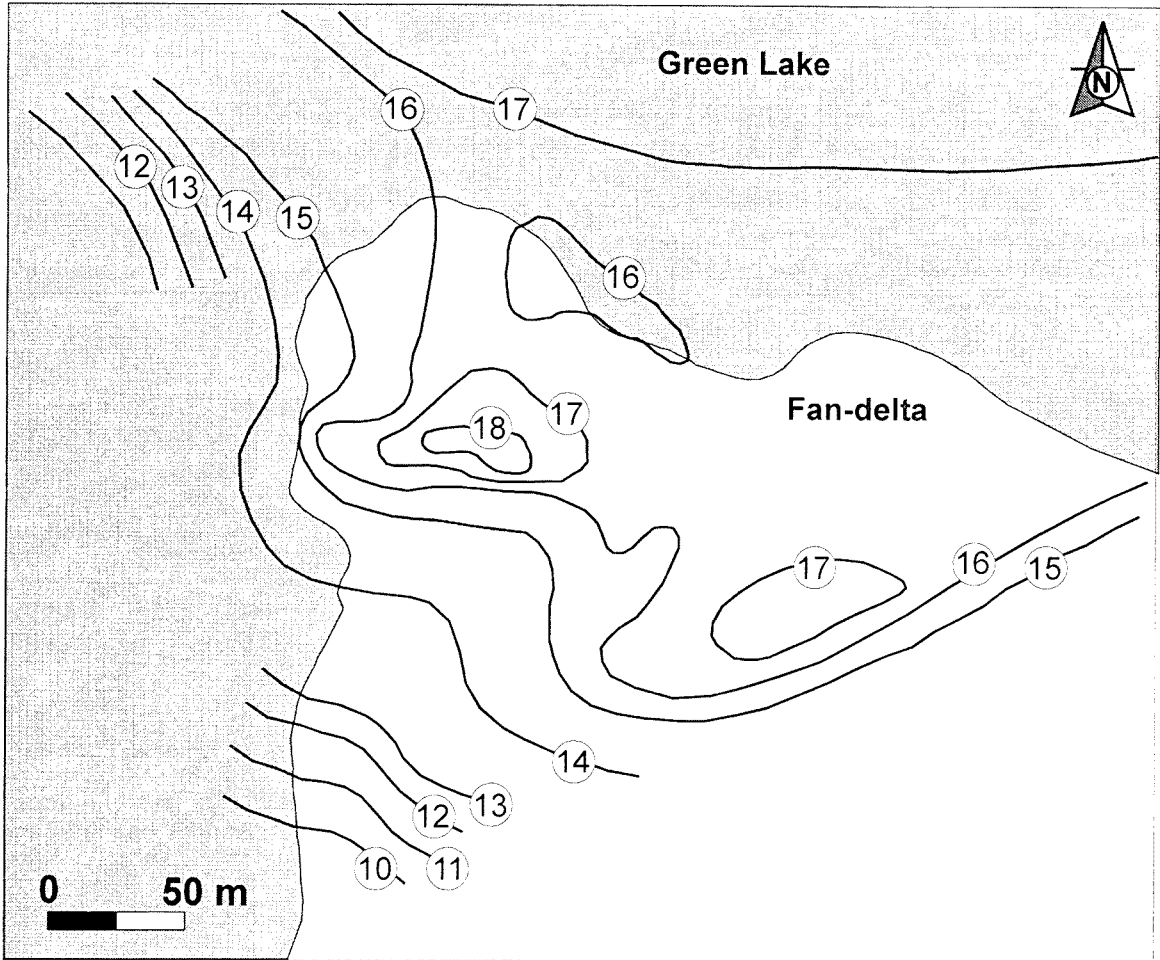


**Figure 3.5** Paleo-lake contour model. Contours shown in metres based on combined results from GPR and bathymetry surveys. Lake bottom contours are shown with respect to the location of the fan-delta August 30, 1999.

Table 3.1 indicate the average percent gravel in surface samples was 58% with a standard deviation of 25%. The silt and clay fraction made up less than 1% of the total weight. Samples exhibit gravel composition ranging from 4.1 % to 84.1% and sand ranging from 14.3% to 96.6%.

**Table 3.1** Summary of surface sediment samples  
Average total mass was used to determine the bulk density conversion factor.

	<b>Average Mass (g)</b>	standard deviation	<b>percent of total volume</b>
<b>Total Mass</b>	<b>3655 ± 2</b>	293	
<b>Silt/Clay</b>	<b>22.06 ± 0.01</b>	39.06	<b>1</b>
<b>Sand</b>	<b>1459.14 ± 0.01</b>	691.12	<b>41</b>
<b>Gravel</b>	<b>2173.65 ± 0.01</b>	925.59	<b>58</b>

The bulk density of near-surface sediment samples is  $1.79 \times 10^3 \text{ kg m}^{-3}$  based on the average mass of the surface sediment samples. This bulk density value has been assigned to the topset facies component of the sediment pile.

A bulk density of  $1.58 \times 10^3 \text{ kg m}^{-3}$  has been assigned to the foreset component of the sediment pile based on literature reviews of comparative bulk densities in neighbouring rivers such as the Lillooet River,  $1.4 \times 10^3 \text{ kg m}^{-3}$  (Gilbert, 1975) and the Squamish River,  $1.45 \times 10^3$  (Hickin, 1989). These values were combined with calculations from United States Geological Survey tables of sub-aqueous sand and gravel bulk densities (Chow, 1964). These computations are detailed in Appendix A-7.

A bulk density of  $1.39 \times 10^3 \text{ kg m}^{-3}$  has been assigned to the bottomset component of the sediment pile based on results from United States Geological Surveys of sub-aqueous sediment (Chow, 1964) and comparative estimates with neighbouring systems, also detailed in Appendix A-7. The average bulk density for the fan-delta sediment body is based on the weighted average of each of the three components. Weighting is based on the 1:2.5:0.5 ratio of the topset, foreset, and bottomset thickness evident in the GPR profiles. The result of this integration (see Appendix A-7) is an average bulk density for the entire fan-delta sediment body of  $1.60 \pm 0.10 \times 10^3 \text{ kg m}^{-3}$ , a value adopted here for all volume to mass conversions.

### **3.1.5 Estimates of Bed-Material Efflux**

The base map was divided into 61 cells bounded by the one-metre contour lines of the paleo-lake basal surface and the measured sequential fan-delta margin locations (Figure 3.6). Area and volume estimates were calculated (Appendix A-3) and are summarized based on photo differencing in Tables 3.2a & 3.2b. Due to differences in the time scale between sequential photographs (four to eleven years), comparisons are based on average annual rates for each of the photoperiods.

Annual average bed-material efflux volumes range between  $0.61 \pm 0.08 \times 10^4 \text{ m}^3 \text{ yr}^{-1}$  and  $1.78 \pm 0.21 \times 10^4 \text{ m}^3 \text{ yr}^{-1}$  (Table 3.2a). The total volume of bed-material measured over the 52-year period is  $5.22 \pm 0.84 \times 10^5 \text{ m}^3$ , which translates to an average annual volume of  $1.00 \pm 0.16 \times 10^4 \text{ m}^3 \text{ yr}^{-1}$ .

The variation of accumulated sediment volume for the photoperiods is illustrated in Figure 3.7. An upward trend in the average annual volume of bed-material efflux is suggested in the plot of average annual efflux over the sequential decadal periods of

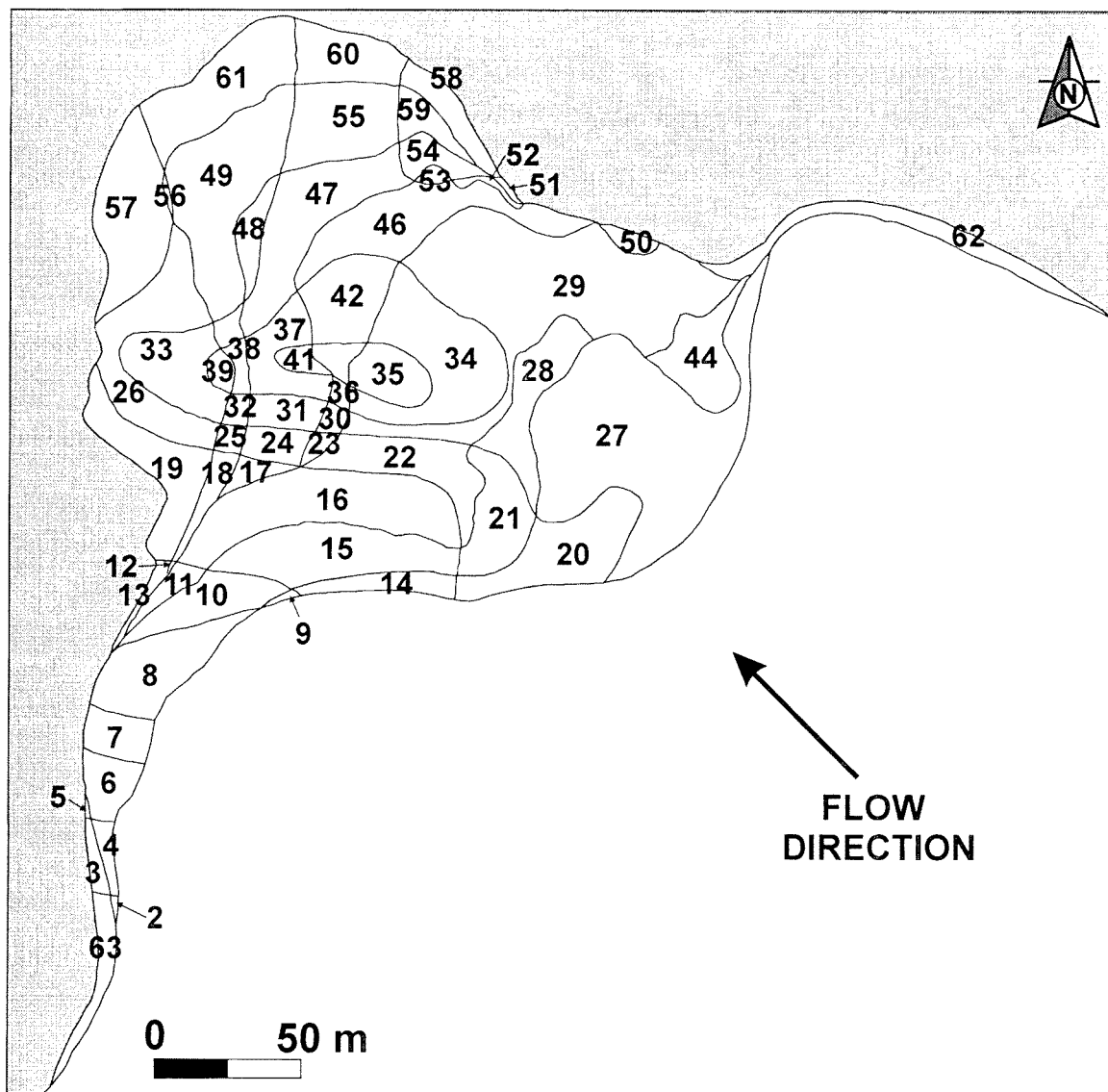


**Figure 3.6** Base map created using GIS to calculate areas and volumes for photo-differencing. Linework is a combination of boundary lines in Figure 3.2 and Figure 3.5. Refer to Appendix A-3 for depths associated with each cell.

**Table 3.2a** Bed-material efflux and total volume with time

<b>Period</b>	<b>Annual Volume<sup>1</sup> (m<sup>3</sup> yr<sup>-1</sup>)</b>	<b>Annual Volume<sup>1</sup> error %</b>
<b>1947 - 1958</b>	<b>9053</b>	<b>± 12.61</b>
<b>1958 - 1963</b>	<b>11314</b>	<b>± 15.79</b>
<b>1963 - 1973</b>	<b>12548</b>	<b>± 8.04</b>
<b>1973 - 1982</b>	<b>4010</b>	<b>± 15.95</b>
<b>1982 - 1990</b>	<b>6089</b>	<b>± 13.8</b>
<b>1990 - 1994</b>	<b>15998</b>	<b>± 18.47</b>
<b>1994 - 1999</b>	<b>17798</b>	<b>± 11.78</b>

<b>Period</b>	<b>Total Volume<sup>1</sup> (m<sup>3</sup>)</b>	<b>Annual Volume (m<sup>3</sup> yr<sup>-1</sup>)</b>	<b>Annual Volume error (m<sup>3</sup> yr<sup>-1</sup>)</b>
<b>1947 - 1999</b>	<b>521797</b>	<b>10014</b>	<b>± 1614</b>

1- volume of bed material accumulated in the fan-delta

analysis. Sediment efflux exhibits a major fluctuation over the measurement period, centred on the 1973 – 1990 low. The average sediment efflux increases  $3.5 \times 10^3 \text{ m}^3 \text{ yr}^{-1}$  between the 1947 - 1958 period and the 1963 - 1973 period to a maximum of  $1.25 \times 10^4 \text{ m}^3 \text{ yr}^{-1}$ . There is a sharp decline after 1973 to comparatively low annual average bed-material transport rates of  $0.40 \pm 0.06 \times 10^4 \text{ m}^3 \text{ yr}^{-1}$  from 1973-1982, and  $0.61 \pm 0.08 \times 10^4 \text{ m}^3 \text{ yr}^{-1}$  from 1982-1990. The average bed-material efflux increases significantly during 1990 – 1994 and reaches its greatest average value in the period of 1994 – 1999.



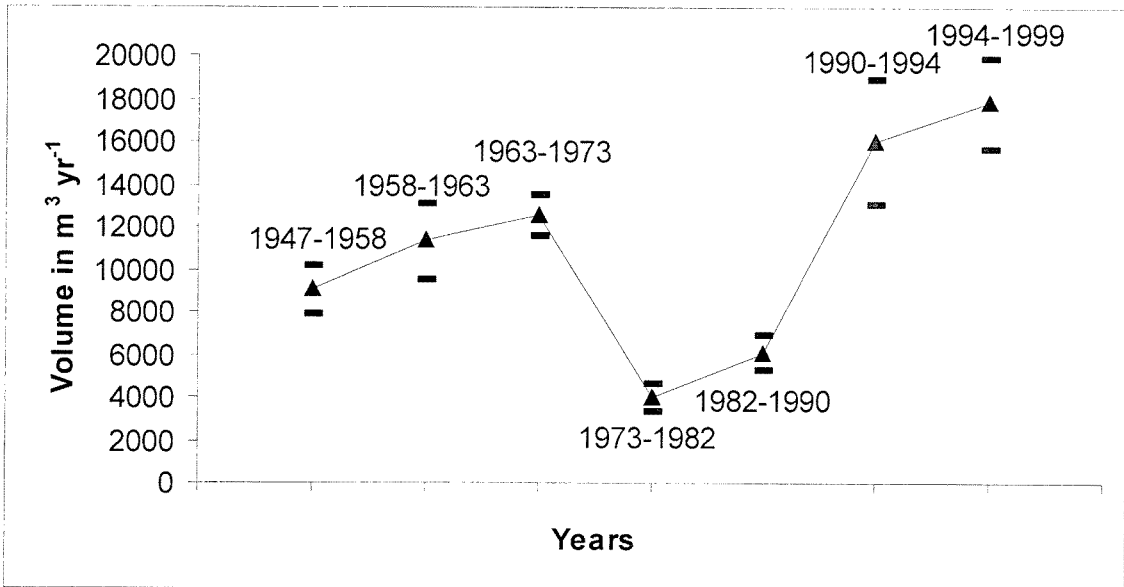


**Figure 3.7** Average annual bed-material efflux ( $\text{m}^3 \text{yr}^{-1}$ ) illustrating variability of average annual estimates based on decadal periods of time over the 52-year record.

Since volume estimates are multiplied by the same conversion factor, the relationship by weight remains the same, with the addition of increased error associated with the conversion factor (Table 3.2b). The total mass of sediment measured over the period August 2<sup>nd</sup>, 1947 to August 30<sup>th</sup>, 1999 is  $8.35 \pm 1.44 \times 10^5$  Mg, which translates to an average annual bed-material transport rate of  $1.60 \pm 0.28 \times 10^4$  Mg yr<sup>-1</sup>. The specific bed-material efflux from August 2<sup>nd</sup> 1947 to August 30<sup>th</sup> 1999 (19059 days), based on a drainage basin of 100 km<sup>2</sup>, is  $0.44 \pm 0.08$  Mg km<sup>-2</sup> day<sup>-1</sup>.

**Table 3.2b** Bed-material efflux and total yield (mass) over time

<b>Period</b>	<b>Annual Bed-Material Efflux (Mg yr<sup>-1</sup>)</b>	<b>Annual Bed-Material Efflux Error %</b>
<b>1947 - 1958</b>	<b>14485</b>	<b>± 14.07</b>
<b>1958 - 1963</b>	<b>18102</b>	<b>± 16.98</b>
<b>1963 - 1973</b>	<b>20077</b>	<b>± 10.18</b>
<b>1973 - 1982</b>	<b>6416</b>	<b>± 17.13</b>
<b>1982 - 1990</b>	<b>9742</b>	<b>± 15.15</b>
<b>1990 - 1994</b>	<b>25597</b>	<b>± 19.50</b>
<b>1994 - 1999</b>	<b>28477</b>	<b>± 13.34</b>

<b>Period</b>	<b>Total Bed-Material Efflux (Mg)</b>	<b>Annual Bed-material Efflux (Mg yr<sup>-1</sup>)</b>	<b>Annual Bed-Material Efflux Error (Mg yr<sup>-1</sup>)</b>
<b>1947 - 1999</b>	<b>834875</b>	<b>16022</b>	<b>± 2770</b>

A comparison of the variability of average bed-material efflux for each photo period to the average bed-material sediment efflux based on the increasing length of record is illustrated in Figure 3.8. Clearly, the variation apparent in the average annual bed-material efflux over shorter periods is not as pronounced over the long-term. That is, relatively high average bed-material transport rates during the periods 1990 – 1994 and 1994 – 1999 are buffered when averaged over a longer record.

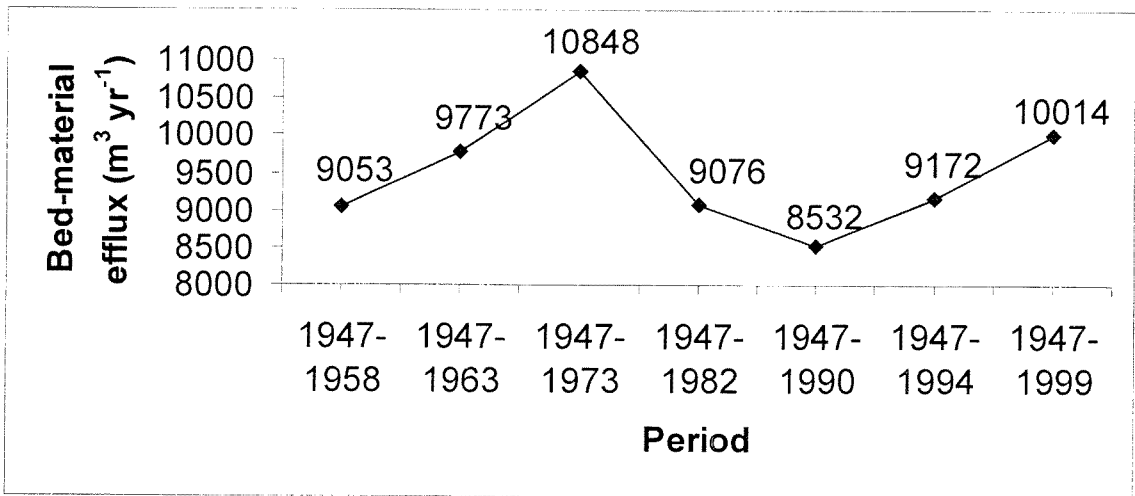


**Figure 3.8** Average bed-material efflux with increasing length of record. Vertical scale has been adjusted to illustrate variability.

## 3.2 Sediment Budget

### 3.2.1 Suspended-Sediment Settling in the Receiving Basin

Lacustrine sedimentation data compiled by Brian Menounos, Department of Geography, UBC are summarized with precision specifications in Table 3.3. Average sedimentation rates range from 1.64 to 4.15 mm yr<sup>-1</sup> depending on the period of record, with spatial standard deviation ranging from 1.05 to 4.09 mm yr<sup>-1</sup> respectively. The error assigned to these measurements is 15% based on average expected error determined elsewhere (Evans and Church, 2000).

The average annual sedimentation rate of fine sediment in the lake ranges between 3.36 – 8.51 x 10<sup>3</sup> m<sup>3</sup> yr<sup>-1</sup>. The lowest rates occur during the period 1963 to 1990, while the highest rate occurs during the 1990 – 1994 period. Area of the lake was 2.05 km<sup>2</sup> determined using GIS software.

**Table 3.3** Lacustrine sedimentation rates

Period	sedimentation rate mm yr <sup>-1</sup>	standard deviation* mm yr <sup>-1</sup>	total volume** m <sup>3</sup> yr <sup>-1</sup>
1947 - 1958	2.05	0.69	4203
1958 - 1963	2.31	0.93	4736
1963 - 1973	1.90	0.54	3895
1973 - 1982	2.01	0.60	4121
1980 - 1990	1.64	1.05	3362
1990 - 1994	4.15	4.09	8508
1994 - 1999	3.78	1.43	7749

(Data from Brian Menounos, Department of Geography, UBC, 2000)

\* based on rhythmite thickness variability for decadal estimates

\*\* based on lake area of 2.05 km<sup>2</sup>

### 3.2.2 Suspended-Sediment Modeling ( $DH_{48}$ )

Summary data from suspended-sediment samples collected between May 05 and November 13, 1999 and their corresponding discharges are reported in Table 3.4 and plotted as a sediment-rating curve in Figure 3.9. Concentrations of the thirty-one suspended sediment samples ranged from 10 to 2290 mg L<sup>-1</sup> for discharges ranging from 1 to 26 m<sup>3</sup> s<sup>-1</sup> respectively. The sediment-rating curve is described by the linear regression equation (with 0 intercept):

$$\text{Log } C_{SS} = 2.2507 \times \text{Log } Q_{\text{Fitz}} \quad (3.1)$$

where  $C_{SS}$  is the concentration of suspended-sediment, and  $Q_{\text{Fitz}}$  is the discharge of Fitzsimmons Creek. The coefficient of variation is  $r^2 = 0.673$  indicating that 67% of the variation in the concentration of suspended-sediment is statistically attributable to changes in discharge. For unknown reasons, one measured concentration of suspended sediment is anomalous. Figure 3.9 illustrates the anomalous point and its relative position with respect to the best-fit line. In accordance with accepted methods, the anomalous point was not considered in the calculation of the best-fit line (Milliman and Syvitski, 1992).

Concentrations of suspended-sediment predicted from a log-transformed regression analysis must be converted to account for the anti-log transform bias (Ferguson, 1986). This has been achieved using a method outlined by Ferguson (1986) and shown in Appendix A-5; in this case the upward correction of about 48% is appropriate.

**Table 3.4** Suspended-sediment samples (DH<sub>48</sub>)

<b>Date of Sample</b>	<b>Concentration (mg L<sup>-1</sup>)</b>	<b>Daily Discharge** (m<sup>3</sup> s<sup>-1</sup>)</b>
14-May-99*	293.43	2.40
25-May-99*	600.50	9.00
29-May-99*	43.33	4.70
5-Jun-99*	292.71	8.00
14-Jun-99*	284.71	11.00
16-Jun-99	2289.82	26.00
18-Jun-99	316.53	13.90
18-Jun-99	330.40	13.90
18-Jun-99	319.48	13.90
29-Jun-99*	20.27	5.61
1-Jul-99*	39.25	6.88
2-Jul-99*	64.24	6.65
07-Jul-99	233.58	8.56
12-Jul-99	301.69	13.10
13-Jul-99	187.62	14.70
13-Jul-99	170.18	14.70
13-Jul-99	169.48	14.70
14-Jul-99*	241.50	15.10
29-Jul-99	443.12	9.07
16-Aug-99*	21.50	10.60
25-Aug-99*	1117.56	18.00
25-Aug-99*	1757.43	18.00
25-Aug-99*	1816.50	18.00
29-Aug-99*	124.22	11.30
29-Aug-99*	126.13	11.30
18-Sep-99*	11.47	4.06
20-Sep-99*	26.67	4.61
20-Sep-99*	26.67	4.61
28-Oct-99	11.00	1.71
28-Oct-99	10.25	1.71
13-Nov-99	70.50	4.11
13-Nov-99	75.14	4.11

(\* Data from Brian Menounos, Department of Geography,  
University of British Columbia, 2000)

(\*\*Water Survey of Canada, 1999)

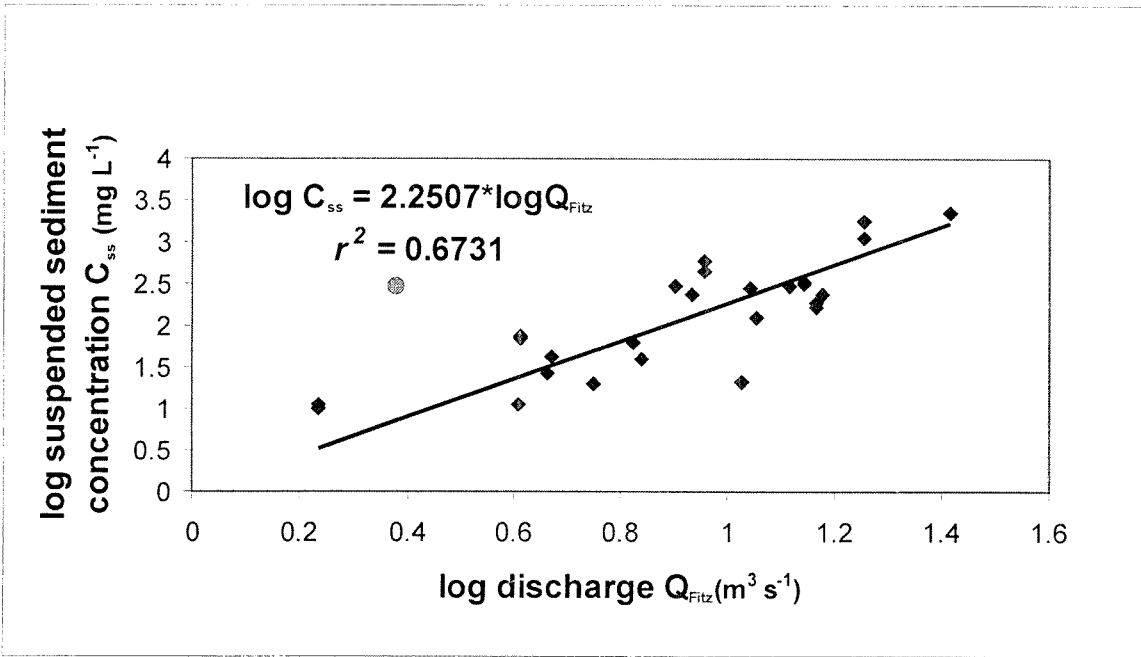


**Figure 3.9** Sediment rating curve showing the relationship between suspended-sediment concentration and mean daily discharges. The equation of the best-fit line excludes one data point, represented by ●. Explanation of the omission is explained within the text Section 3.6.2.



Synthesized historical daily discharges of Fitzsimmons Creek were based on a correlation with historical daily discharges of the Lillooet River. The linear regression of the available daily discharge record from Fitzsimmons Creek versus the corresponding daily discharge records from the Lillooet River produced a variance  $r^2 = 0.78$ . Figure 3.10 illustrates the scattergram plot, demonstrating a reasonably close distribution of points around the best-fit line:

$$Q_{\text{Fitz}} = 0.026268Q_{\text{Lillooet}} + 0.648591 \quad (3.2)$$

This equation was used to synthesize historical daily discharges for Fitzsimmons Creek beginning August 2<sup>nd</sup>, 1947. The daily record over the 52-year period contains some gaps (Figure 3.11). The largest gap (1996) is evident in the long-term record, although, smaller gaps also occur in other years during periods of low discharge. The daily discharges from 1997 were assumed to represent a reasonable estimate of the 1996 data, and were therefore, replicated to fill the missing record. The synthesized long-term record illustrated in Figure 3.11 indicates no significant trend. However, three prominent discharges (greater than  $25 \text{ m}^3 \text{ s}^{-1}$ ) occurred in the later part of the record.

The regression models (equation 3.1 and 3.2) estimated annual suspended sediment transport between  $1.33 \pm 0.89 \times 10^4 \text{ Mg yr}^{-1}$  and  $2.01 \pm 1.35 \times 10^4 \text{ Mg yr}^{-1}$ . The lowest value corresponds with the period 1982 – 1990, while the greatest rate of accumulation corresponds with the period 1990 – 1994. Errors associated with the modeled rates of suspended sediment range between 42% and 65% based on a

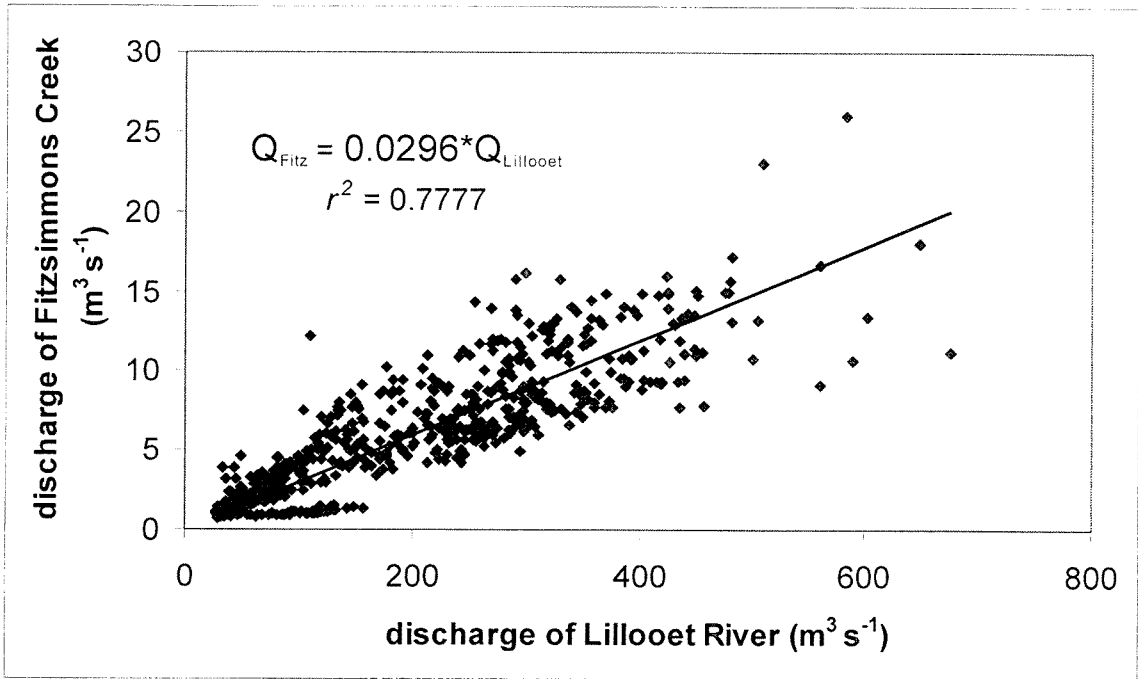


**Figure 3.10** Scattergram plot illustrating correlation between measured daily discharges of the Lillooet River and Fitzsimmons Creek. (Data from Water Survey of Canada, 1999)

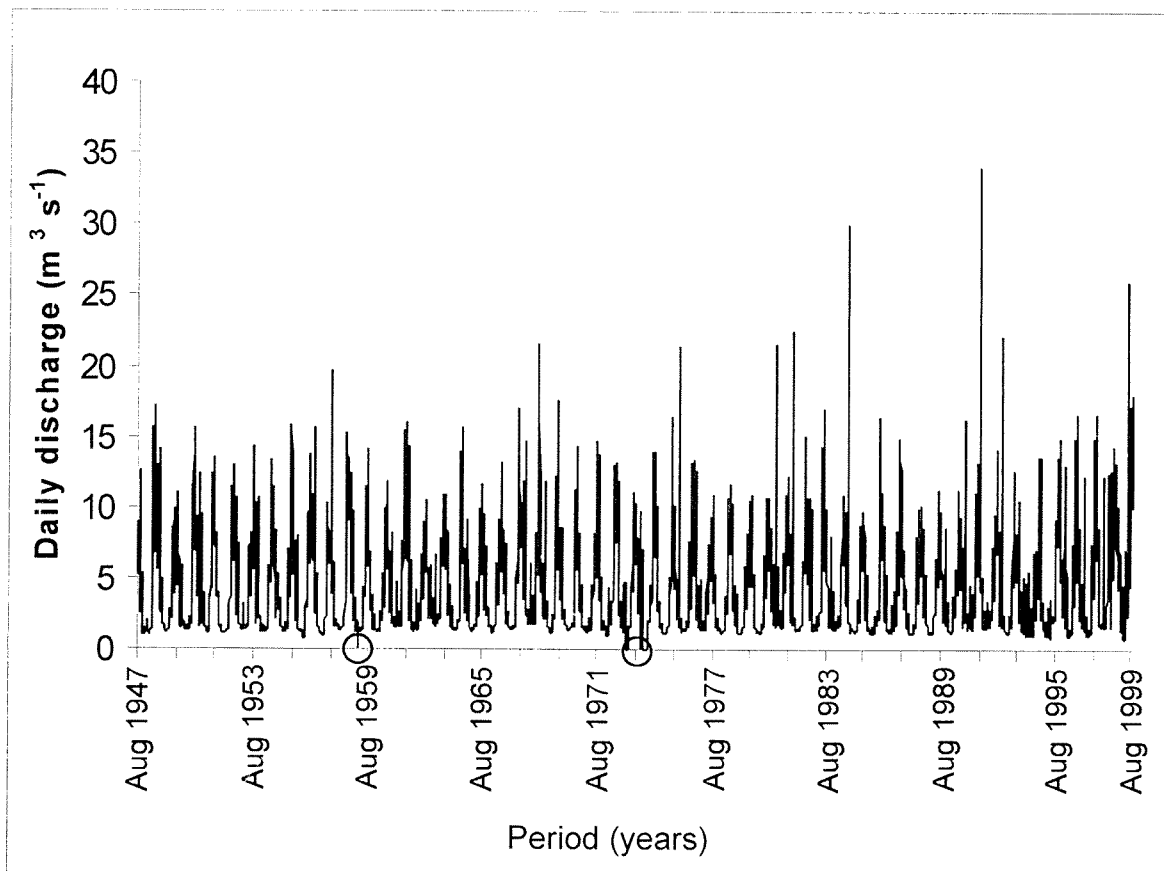


**Figure 3.11** Synthesized and measured daily discharges of Fitzsimmons Creek, British Columbia from August 02, 1947 to August 30, 1999.

○ indicates minor gaps in discharge record.

(Data from Water Survey of Canada, 1999).

combination (product rule) of the standard errors associated with the sediment-rating curve and synthesized daily discharge records for Fitzsimmons Creek. Table 3.5 reveals

**Table 3.5** Minimum and total sediment yields over sequential periods

<b>Period</b>	<b>Delta Bed-material (Mg)</b>	<b>Lake (Mg)</b>	<b>Total Minimum Sediment Yield (Mg)</b>	<b>Suspended Sediment DH<sub>48</sub> (Mg)</b>	<b>Total Sediment Yield (Mg)</b>
<b>1947 - 1958</b> error ±	<b>157530</b> 22164	<b>45702</b> 8236	<b>203232</b> 46581	<b>186151</b> 93280	<b>343681</b> 178878
<b>1958 - 1963*</b> error ±	<b>92014</b> 15624	<b>24071</b> 4338	<b>116085</b> 28812	<b>94490</b> 43304	<b>186504</b> 91151
<b>1963 - 1973*</b> error ±	<b>202579</b> 20623	<b>39301</b> 7082	<b>241880</b> 50238	<b>189260</b> 86678	<b>391839</b> 183836
<b>1973 - 1982*</b> error ±	<b>58462</b> 10015	<b>37542</b> 6765	<b>96004</b> 23924	<b>146696</b> 78242	<b>205158</b> 114928
<b>1982 - 1990</b> error ±	<b>76317</b> 11562	<b>26335</b> 4746	<b>102652</b> 24226	<b>103966</b> 67293	<b>180283</b> 119844
<b>1990 - 1994</b> error ±	<b>103229</b> 20130	<b>34311</b> 6183	<b>137540</b> 36586	<b>81226</b> 34633	<b>184455</b> 86482
<b>1994 - 1999</b> error ±	<b>144749</b> 19310	<b>39388</b> 7098	<b>184137</b> 41431	<b>84548</b> 35197	<b>229297</b> 100237
<b>1947 - 1999*</b> error ±	<b>834875</b> 144350	<b>246649</b> 44446	<b>1081524</b> 270057	<b>886337</b> 446922	<b>1721217</b> 917503

**NOTE:**

Delta (Bed-material) is defined as all material accumulated in the fan-delta of Fitzsimmons Creek

Lake is defined as sediment mass from core samples (rhythmite records)

Total minimum sediment yield is the minimum mass of sediment accumulated over the periods based on the mass of sediment accumulated in the fan-delta + mass of sediment estimated from core samples.

Suspended sediment (DH<sub>48</sub>) is defined as the mass of sediment delivered to the receiving basin based on modeled data.

\* original discharge record contains minor gaps

the contribution of suspended sediment to the total yield of the river for individual

periods and over the 52-year period. Appendix A-8 documents the calculation and methods used to determine the error associated with the suspended-sediment samples.

### **3.2.3 Sediment Transported as Bed-load**

The sediment accumulated in the fan-delta is a combination of gravel, sand, and silt and clay, although surface sediment pits reveal silt and clay presence is negligible at less than 1% by weight. Analysis of lacustrine sediment samples reveals that they are largely composed of silt and clay (Personal Communication, Brian Menounos, Department of Geography, UBC, 2000). Fine sediment is transported past the fan-delta and distributed throughout the receiving basin, carried in the outflow river of Green Lake, and reworked into beach sediments along the margins of the lake. Survey differencing of bathymetric profiles from 1969 and 2000 indicate sub-aqueous accumulation of sediment in the southwest region of the lake, herein referred to as the “beach” deposit.

The combination of sediment accumulated in the fan-delta and the sediment measured in the receiving basin provide a minimum estimate of sediment yield over the study period, based on the assumption that an undetermined amount of sediment has accumulated as beach deposits, as well as sediment lost in the outflow river of the receiving basin. Since the estimate of sediment yield is a minimum amount, the total percentage of sediment transported as bed load represents the maximum estimate. The maximum contribution of bed load varies between  $61 \pm 30\%$  and  $84 \pm 23\%$  as shown in Table 3.6. Over the 52-year period of the study, the maximum contribution of bed load in this system is  $77 \pm 30\%$ , based on the total minimum sediment yield of  $0.57 \pm 0.14 \text{ Mg km}^{-2} \text{ day}^{-1}$ .

The results of the suspended sediment modeling (DH<sub>48</sub>) suggest that a significant amount of suspended sediment is not accounted for in direct measurements based on lacustrine sedimentation rates. Table 3.6 shows the percentage contribution of bed load to the total sediment yield based on the DH<sub>48</sub> estimates. The percentage contribution of bed load varies between 28 ± 59% and 63 ± 46%. The contribution of bed load to the total sediment yield over the entire 52-year record is estimated to be 49 ± 56% (22 – 76%). Sediment yield for Fitzsimmons Creek based on DH<sub>48</sub> estimates and direct measurement of bed material is 0.90 ± 0.48 Mg km<sup>-2</sup> day<sup>-1</sup>.

**Table 3.6** Maximum contribution of bed load and estimate of bed load proportion of the total sediment yield in Fitzsimmons Creek

<b>Period</b>	<b>Maximum Bed Load (%)</b>	<b>Bed Load (%)</b>
<b>1947 - 1958</b> error	<b>78</b> ± 27	<b>46</b> ± 54
<b>1958 - 1963*</b> Error	<b>79</b> ± 30	<b>49</b> ± 52
<b>1963 - 1973*</b> Error	<b>84</b> ± 23	<b>52</b> ± 48
<b>1973 - 1982*</b> Error	<b>61</b> ± 30	<b>28</b> ± 59
<b>1982 - 1990</b> Error	<b>74</b> ± 28	<b>42</b> ± 68
<b>1990 - 1994</b> Error	<b>75</b> ± 33	<b>56</b> ± 51
<b>1994 - 1999</b> Error	<b>79</b> ± 26	<b>63</b> ± 46
<b>1947 - 1999*</b> Error	<b>77</b> ± 30	<b>49</b> ± 56

\* original discharge record contains minor gaps

## CHAPTER 4:

# DISCUSSION

In section 4.1 of this chapter the technique of photo differencing as an indirect method of determining sediment efflux is discussed. Section 4.2 outlines the results of the study in the context of the primary and secondary objectives. Section 4.3 focuses on the average annual bed-material efflux of Fitzsimmons Creek and its variability over time, and the length of record required to accurately estimate average bed-material efflux in a debris-flow influenced system. Section 4.4 discusses the sediment budget for Fitzsimmons Creek based on the data collected. Results as they pertain to landform evolution and engineering applications are discussed in Section 4.5 of this chapter.

### 4.1 Photo Differencing

The long-term minimum specific sediment yield is  $0.57 \pm 0.14 \text{ Mg km}^{-2} \text{ day}^{-1}$  based on direct measurements and a representative estimate of the sediment yield for this system is  $0.90 \pm 0.48 \text{ Mg km}^{-2} \text{ day}^{-1}$ . Both estimates fall within the range of yields determined from short-term regional records of sediment yield ( $0.2 - 1.2 \text{ Mg km}^{-2} \text{ day}^{-1}$ ) in British Columbia (Church *et al.*, 1989). More important is the fact that they fall in the “disturbed” domain. Church *et al.*, (1989) define disturbed as those drainage basins with land-use transitions or having prolific local sediment sources. The consistency of the minimum and estimated sediment yields with the regional norms and with the results of Gilbert (1987) and Hickin (1989) further support the use of photo differencing as a

reliable technique for determining the sediment efflux of a river. Three considerations must be taken into account when using the photo-differencing technique. First, the sediment accumulated in the delta over the period of record must be sufficient to provide measurable differences. Secondly, an estimate must be made of the sediment transported past the fan-delta and deposited throughout the receiving basin, and of that lost via the outflow. Thirdly, large variability of sediment efflux in these alpine rivers means that reliable averages must be based on long records. The length of record used by Gilbert (1975), Hickin (1989), and in this study were 57, 54 and 52 years respectively. The respective record of aerial photograph coverage and historical bathymetric surveys represents a basic limit for the techniques of photo and survey differencing.

Development of lobes and advancement of the fan-delta into the receiving basin was directly related to the location of the main and secondary distributary channels. Sequential aerial photographs revealed the main distributary channel discharged water and sediment in the direction of delta progradation. Sediment transport in distributary channels appears to be the primary contributor to delta progradation rather than extensive deposition over the whole delta front. Delta-front progradation as affected by bed load deposition at the river mouth best describes the process of basin infilling by sediment from Fitzsimmons Creek (Syvitski and Daughney, 1992). The results of the planimetric growth of the fan-delta in this study are consistent with Wood and Ethridge's (1988) argument that the isopach map of the delta-front in Gilbert-type fan-deltas displays a lobate geometry. As studies of fan-deltas indicate (Nemec and Steel, 1988; Wood and Ethridge, 1988; Postma, 1990), a coarse-grained alluvial fan prograding into a standing body of water from an adjacent highland is the ideal environment for the formation of a



fan-delta. The fan-delta formed by Fitzsimmons Creek displays a lobate geometry, has clearly visible topset, foreset and bottomset facies, is coarse-grained, and forms in close proximity to adjacent mountains. Classification of the study site as a fan-delta is therefore supported on the basis of geomorphic setting and planform evolution.

## **4.2 Vertical Dimension of the Fan-delta: Survey Results**

### **4.2.1 Bathymetric Surveys**

Bathymetry profiles reveal irregular subsurface morphology at the base of steeply inclined sediment of the fan-delta that may relate to slumping or shifting distributary channels. Postma (1984) argues that most failures in steeply sloped sub-aqueous beds are deposited immediately proximal to the delta-front. The GPR profile FC2 (Figure 3.4a) illustrates a depositional feature along a semicircular plane, at the base of the fan-delta front. Although the feature may be described as a slope failure, it is more probable that the depositional feature may be the result of shifting distributary channels and their resulting depositional patterns. Examination of bathymetric profiles in numerous locations of the delta-front reveal a consistent delta slope (approaching  $25^\circ$ ), except in the shallower southwest area of the study site adjacent to the sub-aqueous beach. The reason for the absence of low-slope planform development in the fan-delta is not known.

### **4.2.2 Ground Penetrating Radar(GPR) Surveys**

Bathymetry and GPR results provide estimates of the vertical thickness of sediment in the fan-delta. Initially, bathymetry surveys were conducted and the results provided an estimate of the depth of sediment accumulated in the fan-delta and revealed

the steep delta front topography. Results from GPR profiles were instrumental in corroborating bathymetric evidence and provided an increased degree of accuracy to estimates of the vertical dimension of sediment. GPR profiles (Figures 3.4a-d) clearly indicate a loss of signal at a two-way travel time approaching 360 ns. The loss of radar waves (GPR) in profiles was attributable to the attenuation of the signal at the fine sediment interface. Significant differences between the dielectric properties of coarse-grained sediment in the fan-delta and fine-grained sediment in the receiving basin result in strong boundary reflections. Bottomset facies of the fan-delta identified in GPR profiles overlies lacustrine sediment. Results from preliminary examination of lacustrine core samples indicate the fine sediment is largely composed of silt and clay (Brian Menounos, U.B.C., personal communication, 2000). Since silt and clay strongly attenuate electromagnetic waves, this interface is described as the lower boundary of the fan-delta.

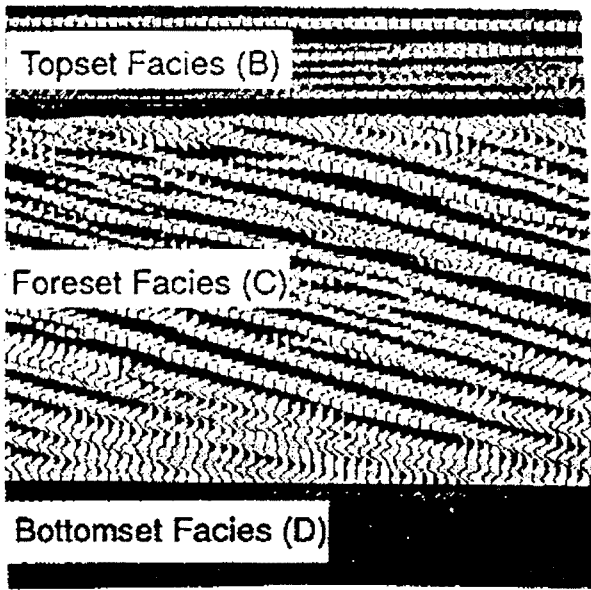
The accuracy of the depth scale applied to GPR profiles relies on the estimate of the velocity of radar waves. Previous GPR studies on sub-aqueous coarse-grained deltas in alpine environments suggest velocities of  $0.07 \text{ m ns}^{-1}$  (Jol, 1993). Verification of the depth of subsurface lithology from GPR profiles is commonly made with outcrops, core samples, or well data. Information of this nature was not available for the study area. Nevertheless calculated average near-surface velocity of  $0.07 \text{ m ns}^{-1}$  is in agreement with previous studies of coarse-grained deltas and bathymetry data provide an independent verification of the vertical dimension of sediment accumulated in the fan-delta.

The depth at which signal attenuation occurred in GPR profiles is comparable to estimates of the depth of the receiving basin from bathymetry profiles. Bathymetry and GPR profiles confirmed that sediment thickness in the southwest area of the study site is

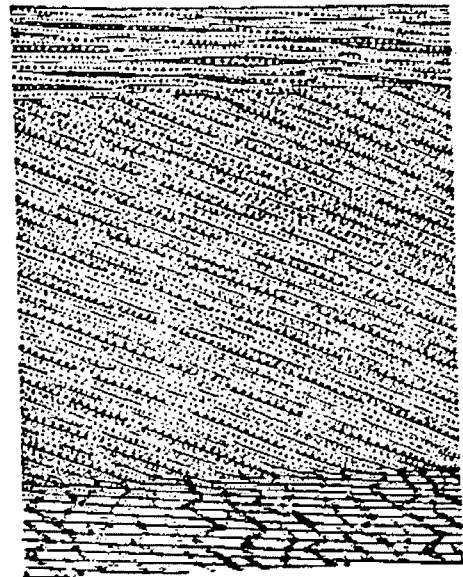
approximately ten metres, less than all other areas. The relatively shallow sediment thickness (10 m) imaged in GPR profiles indicate that the shallow area apparent in bathymetry profiles existed prior to the accumulation of sediment in the fan-delta at this site, and is the ancestral basal morphology of the receiving basin. A one-metre paleo-lake contour map integrated the results of both survey techniques to provide an overall estimate of the subsurface morphology of the receiving basin prior to the accumulation of sediment in the fan-delta constructed by Fitzsimmons Creek.

GPR provides data on the subsurface structure that can be used to interpret the depositional environment. GPR imagery of steeply inclined foreset facies was consistent with the steeply inclined delta front from bathymetric surveys, confirming the assumption of steeply inclined sediment throughout the fan-delta as it prograded into the receiving basin over the 52-year period.

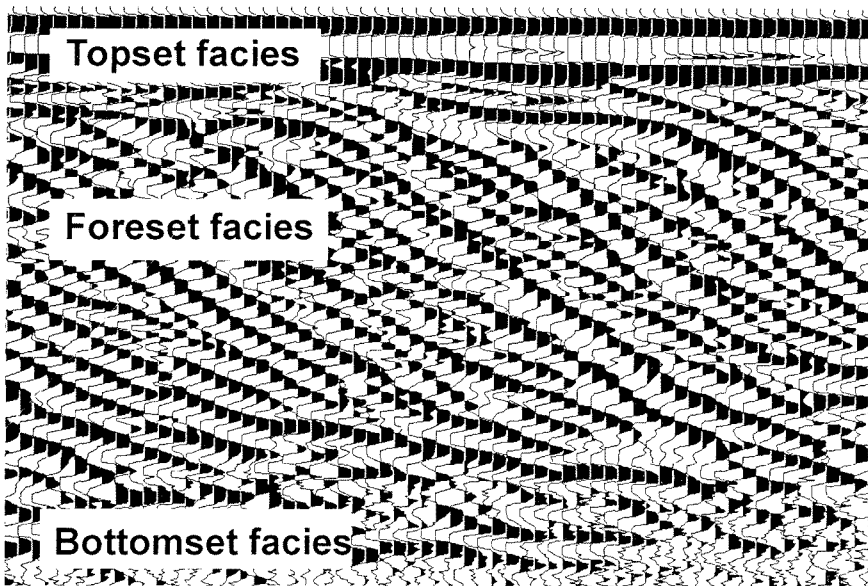
GPR results (Figures 3.4a-d) reveal three principal facies; topset facies, steeply inclined foreset facies with an apparent dip of  $25^{\circ}$ , and sub-horizontal bottomset facies, confirming the fan-delta is a Gilbert type delta (Figure 4.1). Topset facies (0 – 4 m thick) were interpreted to be largely composed of gravels and coarse sand based on surficial examination of the fan-delta and distributary channels. GPR profiles provided data on the internal thickness of facies. Surface test pits provided the evidence of the general composition of fluvial sediments (58% gravel, 41% sand, 1% silt/clay). The low percentage of silt and clay on the surface of the fan-delta is most likely due to the ability of Fitzsimmons Creek to transport silt and clay in suspension beyond the delta margin.



Peyto Delta (Smith and Jol, 1997)



Bonneville Delta (Gilbert, 1890)



Fitzsimmons Creek Delta (this study)

**Figure 4.1** Comparison of the sub-surface architecture of deltaic systems. Note the presence of three distinct facies, topset, foreset, and bottomsets.

(Modified from Smith and Jol, 1997)

The extent of gravel within foreset facies is unknown, although one large-scale pit excavation on the study site (Caterpillar Excavator) indicated a scarcity of coarse gravel below four metres. This observation combined with a review of the composition of sediment in the neighbouring Lillooet and Squamish River deltas, and interpretation of GPR profiles was the rationalization for assuming foreset facies are sand dominated. Results from GPR profiles and surface test pits suggest that silt and clay is negligible (less than 1% by weight) in the topset facies of the fan-delta. Strong GPR reflectors at depth are unlikely if extensive silt and clay in the upper-most sediment of the fan-delta were present because silt and clay attenuate GPR signals. This result combined with a lack of silt and clay (less than 0.064 mm) in surface sediment samples suggests that sediment less than 0.064 mm is predominantly transported to the receiving basin, results consistent with lacustrine sediment accumulation in similar environments (Gurnell, 1987).

In review, gravel is largely contained within the topset facies of the delta and to some degree in the foreset facies. Topset facies contain a significant proportion of sand, although foreset facies appear to contain the greatest proportion of sand. Bottomset composition is not specified, but assumed to be comprised of sand and silt and clay as the finer sediment falls out of suspension as the flow from Fitzsimmons Creek enters Green Lake.

## 4.3 Variability and Estimate of Bed-Material Efflux

### 4.3.1 Long-Term Estimate of Bed-Material Efflux

Total volume of sediment accumulated in the fan-delta in the 52-year period of this study is  $5.22 \pm 0.31 \times 10^5 \text{ m}^3$  and this volume was not adjusted for compaction. The coarse-grained fan-delta in this study formed rapidly over a period of 52-years and any correction for compaction of sediment in the fan-delta would be small and likely within the margin of measurement error. An average bulk density of  $1.60 \pm 0.1 \times 10^3 \text{ kg m}^{-3}$  was calculated for sediment accumulated in the fan-delta corresponding to a bed-material transport rate of  $8.35 \pm 1.44 \times 10^5 \text{ Mg}$  for Fitzsimmons Creek over the 52-year period.

### 4.3.2 Variability of Bed-Material Efflux

Temporal variability of the average bed-material efflux is evident over the 52-year record with estimates ranging between  $0.64 \pm 0.11 \times 10^4$  and  $2.85 \pm 0.38 \times 10^4 \text{ Mg yr}^{-1}$ . The results reveal that bed-material transport rates in an alpine environment are variable by an order of magnitude. The effect of landscape change on the variability of sediment transport revealed over sequential decadal periods is likely attributable to both anthropogenic and natural influences in the drainage basin of Fitzsimmons Creek.

Average bed-material efflux increases  $5.4 \times 10^3 \text{ Mg yr}^{-1}$  between the period 1947 to 1958 and 1963 to 1973. The increase is coincident with logging activity in the upper watershed of Fitzsimmons Creek. The effect of logging versus natural processes of erosion in the upper watershed of Fitzsimmons Creek on the sediment yield during this period of increased yield remains uncertain. Nevertheless logging has increased sediment yield elsewhere (Patric *et al.*, 1984), so logging activities may have contributed a

component of the sediment yield of Fitzsimmons Creek over this period. The plot of average bed-material efflux over time shows a relatively low sediment transport rate in the periods 1973 to 1982, and 1982 to 1990 (Figure 3.7). The lowest average bed-material efflux coincides with periods of no active logging in the upper watershed. The synthesized discharge record of Fitzsimmons Creek indicates discharges during the period of relatively low sediment efflux were consistent with those in the period of higher efflux (1947-1973). Low bed-material transport rates may be due in part to a lack of sediment availability, deposition of sediment within the channel, the inability of the river to mobilize sediment, or a combination of many factors governing sediment transport in alpine basins such as climate, geology, relief, and land use (Meade *et al.*, 1990).

The greatest increase in bed-material transport was observed between the periods 1982 to 1990 and 1990 to 1994. Part of this increase in bed-material transport is undoubtedly explained by a major debris flow event in August 1991. The most interesting result is a comparison of the bed-material transport rate in the period following the debris flow. Although there was no documented flood event between 1994 and 1999, this was the period of greatest bed-material accumulation in the fan-delta. This result may be explained by the availability of sediment following the debris flow event in August 1991. Results of this study indicate that the estimated volume of sediment supplied during the debris flow was not transported in its entirety to the fan-delta. Clearly, the primary sediment source for the fan-delta in this study is the alluvial fan. Coarse sediment is largely stored along the alluvial fan of Fitzsimmons Creek, predominantly confined along and within the existing channel. Observations of the channel along its entire length indicate sediment is readily available, but transport of coarse material is discharge

limited. The highest transport rate during the 1994 – 1999 period may be explained by a combination of high discharges in the later part of the record and the availability of sediment directly upstream from the fan-delta. Variation in discharge alone does not explain the variation in the transport rate of bed-material in this system. Ashmore and Church (1998) state that there may be influences other than gross hydraulic conditions on the mean bed-material transport rate. In the case of Fitzsimmons Creek, land use, such as construction of parking lots, residential development, and engineering of the creek channel during the last decade may have increased peak discharges and thus enhanced the transport of coarser sediment (Pizzuto *et al.*, 2000).

Sediment transport rates are influenced by four factors: climate, geology, relief, and land use (Meade *et al.*, 1990). In theory, predictive models should be able to indicate the impact of each factor on sediment transport. In practice, the influence of an individual factor is difficult to discriminate (Meade *et al.*, 1990). Owens and Slaymaker (1992) suggest that smaller drainage basins can be used to test the response of sediment transport rates to catchment disturbances, both natural and anthropogenic. Identification of the relative contribution of each factor to the variability of sediment transport rates is beyond the scope of this study, however, historical data, anecdotal evidence, and comparative literature suggest that landslides, logging, floodplain development, and river training with dikes have likely increased the rate of sediment delivery and availability of sediment to the fan-delta.

This study examined bed-material efflux over seven sequential periods for a total of 52-years. Combining sequential years improves the estimate of the long-term average annual sediment transport rates. Variability of sediment transport rates may be due to



erosion and deposition of sediment along the river channel. Sediment storage within the channel and along the bed is expected to vary both spatially and temporally over time. The peak average bed-material efflux of the period marked by a debris-flow event (1990-1994), and the period following the event (1994-1999) were masked when the time scale was increased. Inclusion of debris flow events in long-term estimates appears to be essential, a view argued by Church and Kellerhal's (1979) who note that most sediment in small streams is transported during short duration storm events and may escape representative sampling.

The variability of bed-material transport is apparent, even when based on 10-year averages. Indeed, it is not entirely clear from the present data that 52 years is long enough to fully integrate the variability present in the bed-material transport rate of Fitzsimmons Creek. It is clear, however (Figure 3.7), that even a 10-year mean may significantly deviate from the 50-year mean on this system, which appears to respond strongly to discrete debris-flow events. It would appear that the length of record required as a basis for a stable long-term mean sediment discharge estimate depends on the frequency, timing and magnitude of debris-flow events. Church *et al.* (1985) and Ashmore and Church (1998) have recommended that examinations of bed-material transport in highly variable systems such as Fitzsimmons Creek be conducted over the "long-term". On Fitzsimmons Creek this minimum length of record appears not to be less than 50 years.

## 4.4 Sediment Budget

### 4.4.1 Overview

In order to determine the total sediment yield, a sediment budget must be constructed based on sediment input, storage, and output from Fitzsimmons Creek's receiving basin. Green Lake has three tributary systems, however, Fitzsimmons Creek dominates sediment input, as evidenced from aerial photographs of the sediment plumes over the period of the study. Fitzsimmons Creek appears to have a high concentration of sediment in suspension, while 19 Mile Creek and Alta Creek (refer to Figure 1.9) transport relatively insignificant volumes. Any contribution is assumed to be negligible and within measurement error.

### 4.4.2 Resolving the Sediment Budget

Sediment input was measured at the fan-delta and throughout the lake. The specific sediment yield calculated from the combined fan-delta and lacustrine estimates is  $0.57 \pm 0.14 \text{ Mg km}^{-2} \text{ day}^{-1}$ , an estimate well below the expected specific sediment yield from a comparison with Church *et al.*, (1989) and with long-term yields on the Lillooet and Squamish Rivers. The comparatively low result suggests this value may underestimate the suspended sediment proportion of the sediment budget. Lacustrine core samples did not account for sediment accumulated in the beach at the southwest end of the lake (Figure 2.6). Estimation of the volume of sediment transported in the outflow tributary (Green River) of the receiving basin also remains unspecified. Sediment input to Green Lake should be equivalent to the sediment stored within the lake plus that sediment transported through to the outflow, all things being equal. Sediment volumes based on

lacustrine core estimates are significantly less than those estimated from suspended sediment modeling, but the uneven distribution and small number of lake core sites suggest that they have not accounted for all the sediment accumulated throughout the lake. Also, no estimate of sediment concentrations in the outflow of the lake are known, but literature reviews demonstrate that outflow rivers may carry greater than 10% of the sediment input (Heinemann, 1984).

In this case the sediment budget would therefore be:

$$\text{Total sediment yield} = \text{DH}_{48} + \text{Delta} = \text{Delta} + \text{Lake} + \text{Beach} + \text{Outflow} \quad (4.1)$$

where “DH<sub>48</sub>” is the sediment carried in suspension based on modeled data, “Delta” is the sediment accumulated in the fan-delta, “Lake” is the sediment accumulated in the lake based on varve records, “Beach” refers to sediment accumulated in the sub-aqueous southwest end of the lake, and “Outflow” refers to sediment remaining in suspension and transported out of the receiving basin. This equation can be further reduced:

$$\text{Total sediment yield} = \text{DH}_{48} = \text{Lake} + \text{Beach} + \text{Outflow} \quad (4.2a)$$

Equation 4.2a is assumed to represent the sediment budget for Green Lake. Substituting known estimates into the equation for the 52-year study period:

$$\text{Total sediment yield} = 886\,337 \text{ (Mg)} = 246\,649 + \text{Beach} + \text{Outflow (Mg)} \quad (4.2b)$$

The sediment budget implies Beach and Outflow account for 639 688 Mg of sediment. There is a significant degree of error associated with the modeled suspended sediment estimate, so caution is warranted when seeking balance to the sediment budget (equation 4.2b). Sediment unaccounted for in the Beach component may be as high as  $3.0 \pm 1.5 \times 10^5$  Mg based on cursory differencing of bathymetric surveys between 1969 and 2000. If Outflow sediment is 10% of the suspended sediment entering the receiving basin, this accounts for an additional 88 634 Mg. Approximately  $2.5 \times 10^5$  Mg of sediment remains unaccounted for in this sediment budget estimate, but this is within measurement error.

The specific sediment yield of  $0.90 \pm 0.48$  Mg km<sup>-2</sup> day<sup>-1</sup> based on the bed load + modeled suspended sediment estimate falls within the specific-sediment yield range ( $0.12 - 1.0$  Mg km<sup>-2</sup> day<sup>-1</sup>) from disturbed, 100 km<sup>2</sup>, glacierized basins in British Columbia and supports the short-term results of Church *et al.*, (1989). The short-term data was based suspended sediment samples with the assumption that bed load accounts for less than 5% percent of the total load. As Figure 4.2 shows, the specific sediment yield including modeled suspended sediment samples for Fitzsimmons Creek is in the upper portion for small alpine basins. The expanding indices for small basins (100 km<sup>2</sup> and less) indicate the uncertainty of the data based on suspended-sediment data to estimate sediment yields in small basins with higher than average bed-load transport rates. The average annual sediment yield of  $3.3 \times 10^5$  kg km<sup>-2</sup> yr<sup>-1</sup> is only slightly less than the average yield for the Lillooet River ( $3.5 \times 10^5$  kg km<sup>-2</sup> yr<sup>-1</sup>) and the within an order of magnitude of the Squamish River ( $5.0 \times 10^5$  kg km<sup>-2</sup> yr<sup>-1</sup>) (Gilbert, 1987; Hickin, 1989), suggesting the larger basins transport more sediment per kilometer of drainage basin. Combined with the short-term data by Church *et al.*, (1989), the comparison provides some indication that

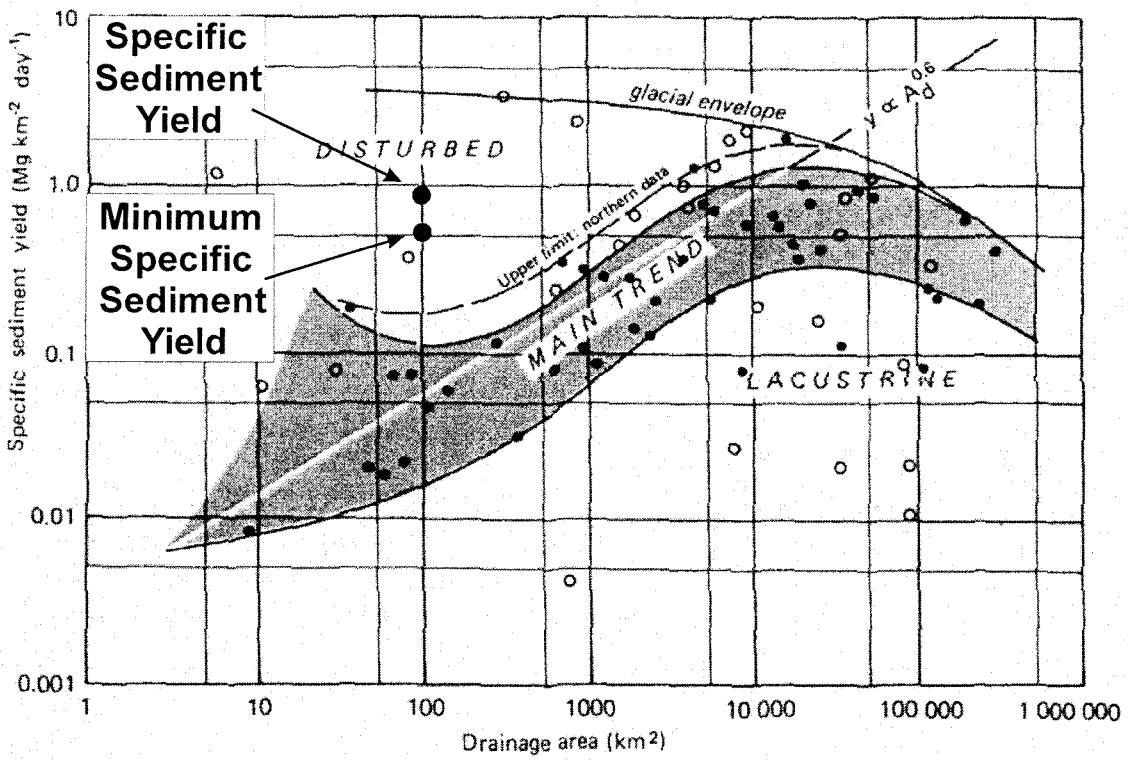


**Figure 4.2** Correlation of specific sediment yield and drainage basin area and the corresponding estimates of specific sediment yield of Fitzsimmons Creek.  
(Modified from Church *et al.*, 1989)

the specific sediment yield estimate for Fitzsimmons Creek is reasonable.

Sediment yield is comprised of material transported in suspension and bed load. While geomorphologists are able to estimate the sediment yield, it is difficult to accurately determine the mechanism of transport due to spatial and temporal variation. Determination of the contribution of suspended-sediment required synthesizing data for suspended-sediment concentrations and discharges on Fitzsimmons Creek, since no historical data was available. Estimates are based on a sediment rating curve model, model of historical discharge based on a comparative data set (Lillooet River), and estimates of the lacustrine sedimentation rate during each sequential period. The precision of estimates in this section is reflected by the errors in calculation outlined in Table 3.5. The errors associated with the suspended sediment data are compounded by the fact that the rating approach obscures unsteadiness in transport rates unrelated to hydraulic conditions (Ashmore and Church, 1998). Therefore, the total sediment load may be underestimated during a period including a debris flow event.

Studies have demonstrated the power function relation between the concentration of suspended sediment and discharge, which implies most sediment is transported during high discharge events (Meade *et al.*, 1990). Results of sediment yield variability, however, over the period of analysis are not adequate in the absence of other information to provide causality between total sediment load and discharge events. The greatest average value may be attributable to increased peak discharge events, availability of sediment, or a combination of both. Fitzsimmons Creek drains a glacial valley occupied by terraces, sparse vegetation, numerous tributaries, and lateral moraines in the headwater reaches. Large flood events may transport a considerable amount of the sediment, but the

relatively short duration of these events regulates the magnitude to a large degree.

Historical daily discharge data for Fitzsimmons Creek was synthesized from the equation of the best-fit line between available discharges of Fitzsimmons Creek and the corresponding daily discharges from the Lillooet River. A correlation ( $r^2 = 0.78$ ) between these systems is most likely due to the fact that they are both located in the same mountain range, and have similar hydrological models driven by snowmelt and fall rainstorm events. The distribution of points along the best-fit line of the correlation (Figure 3.10) indicates standard errors which, when combined and taken to one standard deviation, account for a large margin of error associated with the modeled suspended sediment estimates.

The relatively high rates of bed-load transport in this study are linked to the geomorphic setting of the study site. The fan-delta is a repository for coarse sediment transported from the alluvial fan of Fitzsimmons Creek as it emerges from the constrained valley between Whistler and Blackcomb Mountains. The alluvial fan remains the primary source of coarse sediment to the fan-delta. Bed load remains only a partial component of the sediment yield in this system. Studies of rivers with similar geology and climate in Switzerland indicate river basins draining glacierized regions with low concentrations of suspended sediment during normal runoff, but substantial concentrations during large-magnitude flood events (Bogen, 1992). This may be the case for very fine sediments carried in suspension and distributed throughout the lake. The estimate of suspended sediment during the period 1990 – 1994 may underestimate the actual magnitude of material carried in suspension during the debris flow event. Even so, the average annual estimate of the suspended-sediment transport rate during this period is

the greatest, in comparison to the period following the debris flow event that had the greatest measured bed-load transport rate. It is unclear whether the results from this study corroborate Bogen's (1992) assertion, since the greatest average sediment yield was largely due to a combination of the availability and ability to transport sediment in Fitzsimmons Creek. The occurrence of the greatest average bed-material transport rate in the decade following the greatest average suspended-sediment transport rate is intuitively in accordance with the notion that bed-material transport will lag suspended sediment.

The fan-delta is largely composed of sediment sand sized and greater. Various sizes of sediment were mobilized and transported as bed load on the fan-delta during low discharges, therefore, estimates of bed-material efflux may in fact represent the bed-load transport of sediment along the last reach of Fitzsimmons Creek, from the BC Rail bridge to the fan-delta at Green Lake. In this reach, sand sized sediment and greater is likely transported as bed load. Studies of fan-delta progradation into receiving basins in Switzerland identify all sediment accumulated in the fan-delta as bed load (Gurnell, 1987). For discussion of the sediment budget, all sediment accumulated in the fan-delta will herein be referred to as bed load.

Studies show that in steep alpine environments, bed load contributes as much as 30% of the total sediment yield (Gurnell, 1987). In this study, bed load in Fitzsimmons Creek accounts for a maximum of 77% and likely, 49% of the total sediment yield. While this estimate is higher than Gurnell's (1987) findings, it remains probable. Small rivers are more susceptible to flash floods and have larger contributions from bed load because of their steeper gradients and proximity to source material (Milliman and Syvitski, 1992). Results of this study support the assumption that sediment yields in alpine environments



are highly influenced by bed-load transport. Determination of the extent of bed-load transport in steep alpine environments is essential because of its influence on channel morphology and stability.

## 4.5 Engineering Applications

Although sediment yields provide useful information on variations in sediment transport, the effects of suspended-sediment ( $< 0.062$  mm) on engineering applications are not substantial since the bed-material is more pertinent for studies of river channel stability (Ashmore and Church, 1998). The bed-material in this case is largely transported as bed load and presents the greatest challenge to river engineers.

The use of fan-delta morphology to determine the bed-material transport rate in Fitzsimmons Creek provides a direct linkage between hydraulic processes and the geomorphology of rivers. The bed load transport rate and variation of the bed load also provides a measure of the channel stability and can be applied to engineering objectives.

The BC Rail train bridge crossing at Fitzsimmons Creek presents a significant problem because of seasonal aggradation of bed-material in response to the decreased stream gradient (Figure 4.3). Estimates of gravel recruitment from the creek have been documented since a debris flow event in 1991. Records estimate the total volume of sediment removed from the creek over the 52-year period to be as high as  $1.7 \times 10^5 \text{ m}^3$ .

Presently we are unable to predict, with acceptable levels of accuracy, the transport and storage of sediment particles within river channels (Meade *et al.*, 1990). Sediment storage within the river becomes a consideration in the examination of sediment yield. Gravel extraction volumes were not included in final sediment yield

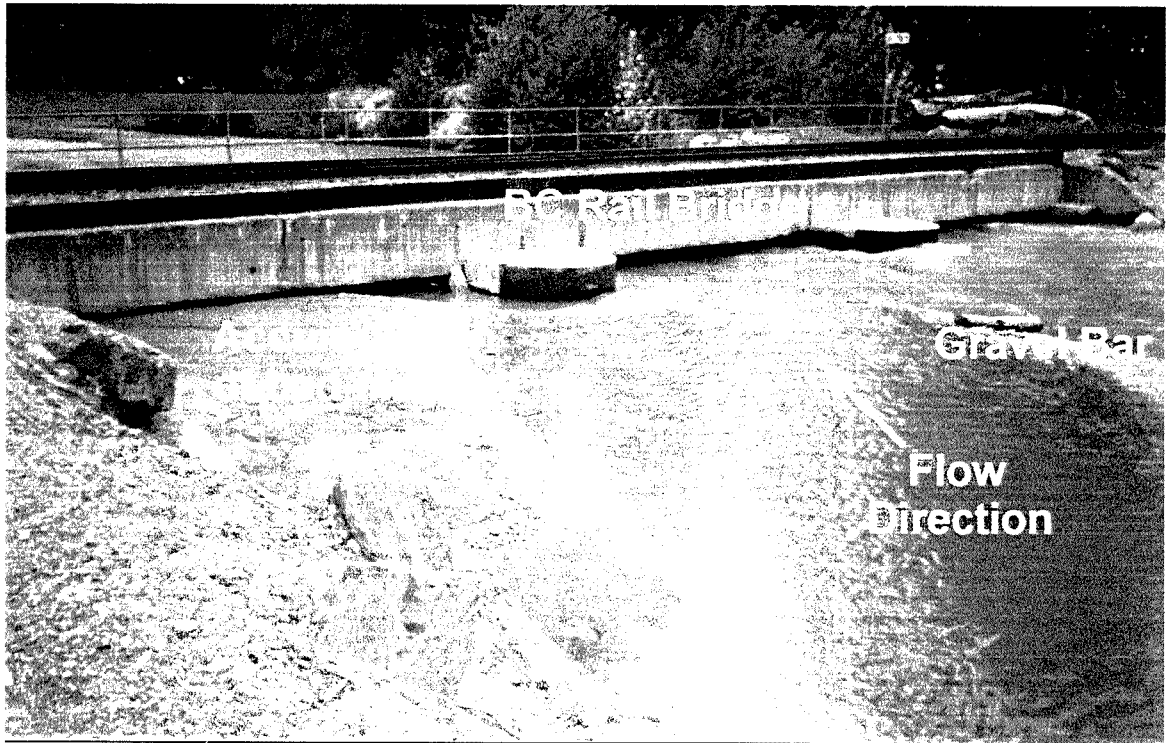


**Figure 4.3** Flooding hazard associated with bed-material accumulating on the up-stream side of the BC Rail bridge in Fitzsimmons Creek. The bridge is located approximately 400 metres upstream of the fan-delta margin August 1999.

estimates because the extraction has been relatively recent (commencing September 1991) and the mobility of sediment in the entire system is unknown. If gravel extraction values were included in recent sediment yield estimates, the percentage of material transported as bed load would increase. Since a large amount of gravel and sand was removed in the summer of 1999, the data would suggest that the fan-delta would experience a drastic reduction in growth. Removal of sediment from accumulation zones may in fact accelerate the movement of sediment from sources further upstream in the river. Examination of river morphology following gravel extraction programs and fall storm events indicates rapid infilling of the cavities, most likely due to the availability of major sediment sources along the riverbanks and valley walls of Fitzsimmons Creek as a consequence of the Quaternary glacial history (Church *et al.*, 1989; Church and Slaymaker, 1989).

Fitzsimmons Creek is redistributing and transporting glacial sediments to the fan-delta and receiving basin. Development along the floodplain of Fitzsimmons Creek and placement of riprap may reduce access to the floodplain, increasing the creek's efficiency as a transport mechanism. Urbanization results in greater peak discharge events, which can influence the volume of sediment supplied to stream channels (Pizzuto *et al.*, 2000). Observations of the river channel immediately upstream of the fan-delta indicate that coarse sediment is readily available. Sediment mobilized as bed load is available to be continually supplied during peak discharges. Variability of the bed material component in glacier-fed rivers arises from the fact that in rivers draining alpine environments, differences in the proportion of the total sediment load attributable to bed load are closely linked to variations in the rate at which sediment is supplied (Gomez, 1987).

# CHAPTER 5:

## CONCLUSIONS

### 5.1 The Bed-Material Efflux

This study provides the first estimate of the long-term bed-material transport rate for a small alpine drainage basin (approximately 100 km<sup>2</sup>), in the Coast Mountains of British Columbia. Aerial photography combined with bathymetric and ground penetrating radar surveys are the basis of a reliable and convincing method of measuring bed-material efflux over a 52-year period.

Three primary objectives were addressed in this study:

1. *What is the annual bed-material efflux from Fitzsimmons Creek?*

The average annual bed-material efflux over the 52-year record is  $1.60 \pm 0.28 \times 10^4$  Mg yr<sup>-1</sup> for Fitzsimmons Creek. This estimate is based on a combination of data including aerial photograph differencing, bathymetric and ground penetrating radar investigations and analysis of the sediment composition in the fan-delta.

2. *How variable is the bed-material efflux from Fitzsimmons Creek?*

As expected, the bed-material efflux for a river draining a steep alpine environment with an abundant sediment supply is highly variable. Average annual bed-material transport rates vary over decadal-scales by an order of magnitude. The greatest average annual transport rate was measured in the decade following a debris flow event, most likely explained by a combination of the availability of sediment in the alluvial fan immediately upstream of the fan-delta, and discharges capable of mobilizing sand and

gravel sized sediment. Variability of average annual transport rates was evident in a comparison of records as long as 10-years. Clearly, in a system such as Fitzsimmons Creek, determining the bed-material transport rate over a period even as long as 10 years is not sufficient. The cause of the variability of bed-material transport in this system is beyond the scope of this study. Literature review and site investigation, however, would support the influence of discharge and periodic flood induced debris-flow events to the highly variable bed-material transport rates.

*3. What is the minimum sampling time to reliably estimate the 50-year average bed-material efflux from Fitzsimmons Creek?*

The variability associated with average bed-material transport rates estimated over shorter time periods has been clearly demonstrated, supporting the belief that sediment transport in steep alpine systems require measurements over a long time period. Based on the frequency of debris-flow events and the effect on the bed-material transport rate, the minimum length of record appears to be not less than 50 years for Fitzsimmons Creek.

## **5.2 Sediment Yield and the Proportion of Bed Load**

Bed load is commonly assumed to contribute a small percentage of the total sediment yield from rivers. In alpine environments, however, the proportion is expected to be higher. A secondary objective of this study was to determine the proportion of sediment yield composed of material transported as bed load. Surface sediment core samples revealed that less than 1% of the fan-delta at the surface was composed of silt and clay. As well, ground penetrating radar resolution at depth was exceptional,

corroborating the belief that the fan-delta is largely composed of sediment equal to or greater than sand-sized material. The suspended sediment was estimated using two methods, lacustrine core samples, and modeled relationships based on sediment-rating and synthetic discharge curves.

Results from lacustrine core samples collected in a parallel study (Personal Communication, Brian Menonous, Department of Geography, UBC, 2000) provided an estimate of the sediment accumulation rate in Green Lake, however, not all the sediment delivered to the receiving basin was considered. Two other possible suspended-sediment sinks, “Beach” and “Outflow” were recognized. Consequently, addition of the bed-material in the fan-delta and suspended sediment in the lake provides an estimate of the minimum specific sediment yield of  $0.57 \pm 0.14 \text{ Mg km}^{-2} \text{ day}^{-1}$ . The modeled suspended sediment estimates should be equal to or greater than the measured values determined from lacustrine core samples. Modeled volumes however, greatly exceeded measured volumes, even beyond the margin of error. Although this error represents an unbalanced sediment budget equation, the difference can possibly be made up if the mass of suspended sediment accumulated in the beach and transported in the outflow river were taken into consideration. Totaling the modeled suspended sediment with the bed-load estimates gives a specific sediment yield of  $0.90 \pm 0.48 \text{ Mg km}^{-2} \text{ day}^{-1}$ . Both estimates fall within the specific sediment yield of  $0.2 - 1.0 \text{ Mg km}^{-2} \text{ day}^{-1}$  for disturbed,  $100 \text{ km}^2$ , glacierized basins from short-term estimates of sediment yield by Church *et al.*, (1989). The long-term sediment yields determined in this study are consistent with short-term results of sediment yield in British Columbia and with the two long-term results from larger basins in the Coast Mountains, providing some confirmation of the final estimates.

Based on sediment yield estimates, bed load accounts for  $49 \pm 56$  % on average of the total sediment yield in Fitzsimmons Creek over the 52-year record. Transport of bed load may be, however, as high as  $63 \pm 46$  % for a decadal period. The importance of calculating the relatively high contribution of bed load in this system is the effect of coarse material on channel form and pattern, such as widening of the channel due to deposition of sediment in the last reach of Fitzsimmons Creek.

Ground penetrating radar (GPR) was found to be very useful as a shallow geophysical tool in this study. Determination of the vertical dimension of sediment accumulated in the fan-delta was improved with GPR. In this study, the fan-delta advanced into a narrow alpine lake concealing the irregular lake bottom, an irregularity, which would not have otherwise been accounted for using traditional techniques such as bathymetric profiling to estimate sediment thickness. Progradation of the delta on the side of the lake also conceals the sloping lake bottom. Clearly, bathymetry alone would have failed to accurately estimate the volume of sediment accumulated in the delta, and thus the average bed-material transport rate.

The sedimentary features of the delta, specifically horizontal coarse-grained topsets, steeply inclined foresets approaching  $25^\circ$ , and sub-horizontal bottomset facies, are features synonymous with a Gilbert-type delta. This result, combined with the morphological shape of the delta, clearly define it as a Gilbert-type fan-delta.

If one assumes that a comparison of this study with the long-term studies of Gilbert (1975) and Hickin (1989), as well as the short-term study by Church *et al.*, (1989) provide a reliable test of the technique, then this study is the first of its kind to combine

survey differencing and GPR to indirectly determine bed-material transport rates and sediment efflux.

### **5.3 Suggestions for Future Research**

The need for additional information warrants comparative research on similar basins in British Columbia. Further research on mechanisms of sediment transport, specifically bed-load transport must be long-term due to seasonal and temporal inactivity of coarse fluvial sediments.

Many standard bed-load transport rate equations were formulated in environments that are not characteristic of the Coast Mountains of British Columbia. Therefore, the appropriateness of those bed-load transport equations could be tested against the known bed-material transport rate as Fitzsimmons Creek empties into Green Lake since the application of traditional bed-load formulae are believed to underestimate the true transport rate. The purpose of testing traditional formulae against a known rate is to resolve if bed-load transport can be estimated using conventional formulas for rivers draining steep alpine environments. This method can also be applied to testing morphological methods based on differencing cross sections (Martin and Church, 1995; Ham and Church, 2000) since there are few cases where the true bed-load transport rate is known for comparison (Ashmore and Church, 1998).

In order to estimate the contribution of sediment transported as bed load to some degree of accuracy, an accurate and all encompassing sediment budget estimate is necessary. The sediment budget in this study, however, includes components, which were not fully specified. Determining these variables is fundamental to strengthening the



estimate of sediment yield and the proportion of sediment transported as bed load in Fitzsimmons Creek.

# **APPENDIX A**

## **CALCULATIONS**

- A-1 Aerial Photo Enlargement Scale Calculations
- A-2a Velocity Calculations from Common Mid-Point GPR Profiles
- A-2b Velocity Calculations from Common Mid-Point GPR Profiles
- A-2c Velocity Calculations from Common Mid-Point GPR Profiles & Average Velocity Calculation
- A-3 Area and Volume calculation from GIS base map
- A-4 Sample calculation of daily suspended-sediment
- A-5 Suspended-Sediment Log-Log Bias Correction
- A-6 GPR Migration Calculation
- A-7 Bulk Density Calculations
- A-8 Error Calculation for Decadal Suspended-Sediment Estimates

## Appendix A-1 Aerial Photo Enlargement Scale Calculations

Preamble: Aerial photographs enlargements were scaled based on ground-truthing. Distances between structures and geomorphic features were measured on each photo and on the study site to determine scales. Features include the BC Rail bridge, BC Rail buildings, triple culvert crossing, stream crossings, power lines, pedestrian bridges, and trail crossings.

Note:

Ground - true distance in mm

Photo - distance on aerial photograph in mm

Scale - scale estimate

194			195		
Ground	Photo	Scale	Ground	Photo	Scale
208000	53.5	1:3888	81000	26.25	1:3086
314000	81	1:3877	208000	68.5	1:3036
370000	96.5	1:3834	314000	101.75	1:3086
			370000	122	1:3033
	<b>scale</b>	<b>1:3866</b>		<b>scale</b>	<b>1:3060</b>

196			197		
Ground	Photo	Scale	Ground	Photo	Scale
81000	27.5	1:2945	53000	14.25	1:3719
208000	71	1:2930	81000	21.75	1:3724
314000	106	1:2962	208000	56	1:3714
			314000	84.5	1:3716
	<b>scale</b>	<b>1:2946</b>		<b>scale</b>	<b>1:3718</b>

**1982**

Ground	Photo	Scale
53000	12.25	1:4327
81000	19	1:4263
196000	45.5	1:4308
208000	48.75	1:4267
314000	72.5	1:4331
370000	85.75	1:4315
<b>scale</b>		<b>1:4302</b>

**1990**

Ground	Photo	Scale
53000	14.75	1:3593
81000	22.5	1:3600
196000	54	1:3630
208000	57.75	1:3602
314000	87	1:3609
370000	103.5	1:3575
<b>scale</b>		<b>1:3602</b>

**1994**

Ground	Photo	Scale
81000	28.25	1:2842
114000	40	1:2850
196000	68.75	1:2861
208000	73	1:2849
314000	110	1:2868
<b>scale</b>		<b>1:2854</b>

**1999**

Ground	Photo	Scale
81000	21.5	1:3767
114000	30.25	1:3800
196000	51.5	1:3806
208000	55	1:3782
314000	83	1:3783
370000	97.75	1:3795
<b>scale</b>		<b>1:3789</b>

## Appendix A-2a Velocity Calculation from Common Mid-Point (CMP2) GPR Profile

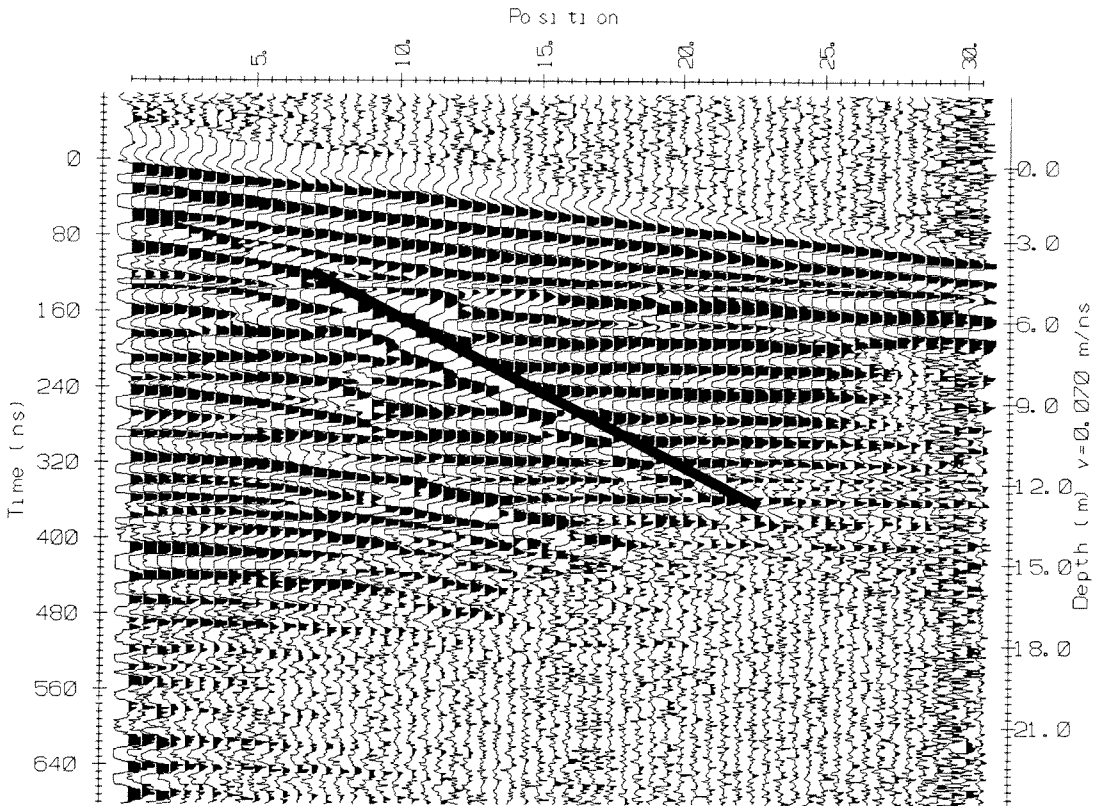


Figure A-2.1 CMP2 GPR profile

Velocity of ground wave calculation:

$$v = \text{time} / \text{depth} = (18.25 - 8.95) \text{ m} / (289 - 146) \text{ ns}$$

$$v = 0.065 \text{ m/ns}$$

## Appendix A-2b Velocity Calculation from Common Mid-Point (CMP4) GPR Profile

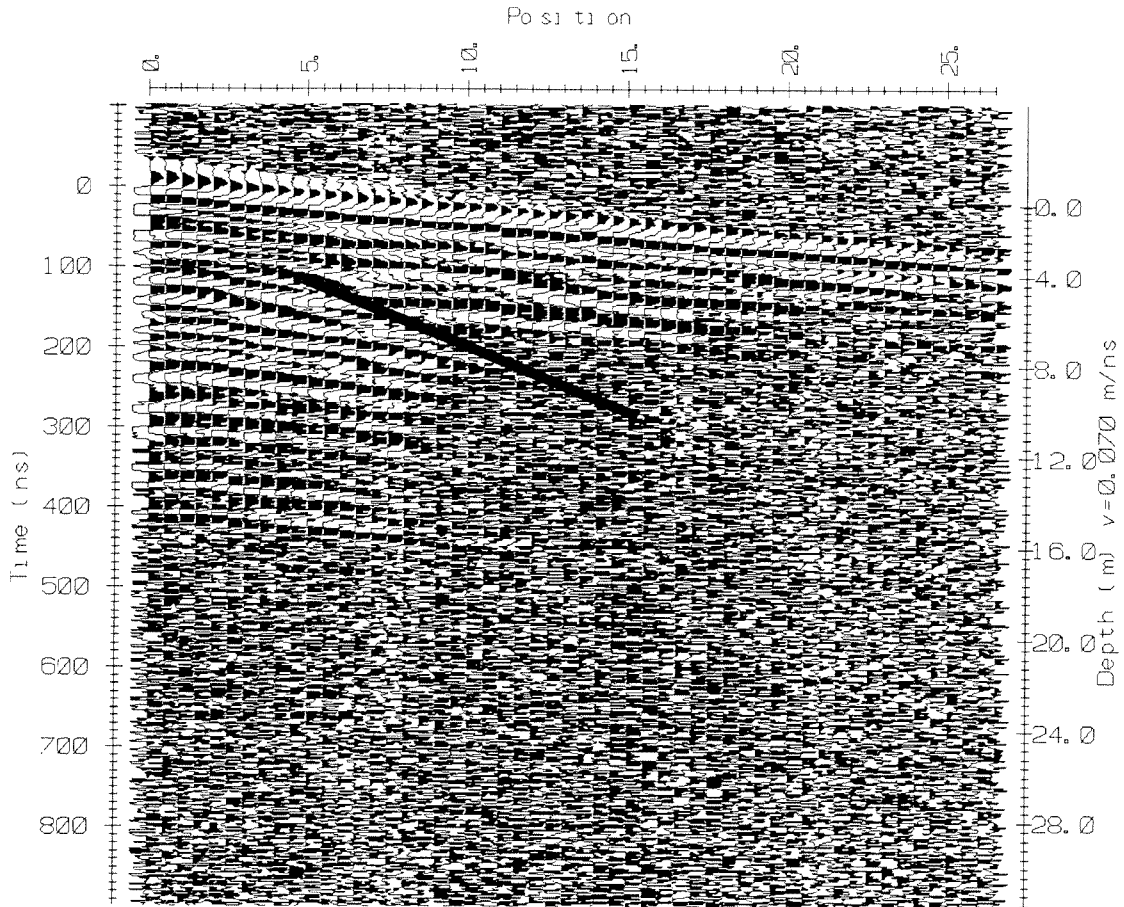


Figure A-2.2 CMP4 GPR profile

Velocity of ground wave calculation

$$\text{velocity} = \text{depth} / \text{time} = (10.25 - 5.15) \text{ m} / (182 - 111) \text{ ns}$$

$$v = 0.072 \text{ m/ns}$$

**Appendix A-2c Velocity Calculation from Common Mid-Point (CMP5) GPR Profile & Average Velocity Calculation**

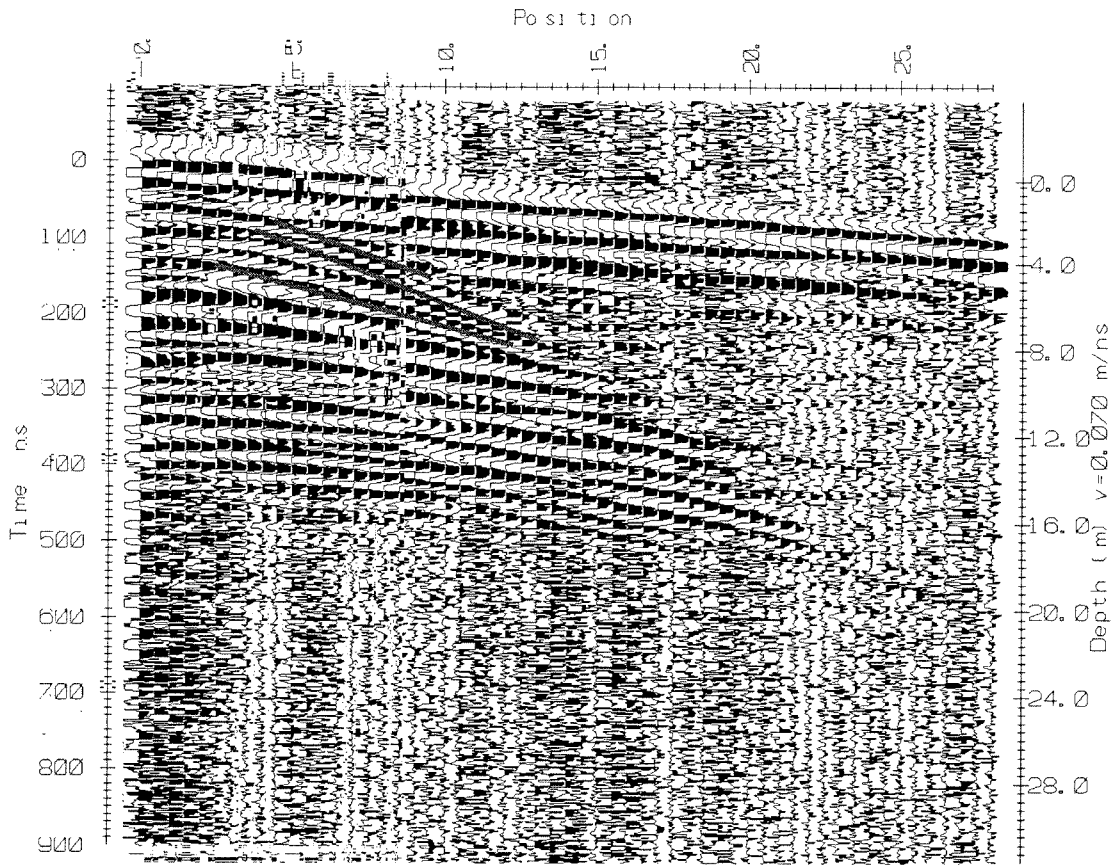


Figure A-2.3 CMP5 GPR profile

Velocity of ground wave calculation

$$\text{velocity} = \text{depth} / \text{time} = (12.50 - 7.45) \text{ m} / (175 - 107) \text{ ns}$$

$$v = 0.074 \text{ m/ns}$$

**Average CMP Velocity Calculation**

(values from CMP velocities in Fig 2.3, Fig A-2.1, A-2.2, A-2.3)

$$\text{average velocity} = 0.065 + 0.065 + 0.072 + 0.074 \text{ m/ns}$$

$$\text{average velocity} = 0.069 \text{ m/ns} \sim 0.070 \text{ m/ns}$$

## Appendix A-3

### Area and Volume Calculation from GIS Base Map

Table A-3 Area and Volume Calculations from GIS (Figure 3.6)

Area ID	Area (m <sup>2</sup> )	Depth (m)	Volume (m <sup>3</sup> )	Area ID	Area (m <sup>2</sup> )	Depth (m)	Volume (m <sup>3</sup> )	
61	1098	15.5	17026	39	95	17.5	1662	
60	561	16.5	9250	19	801	14.5	11615	
58	310	16	4968	36	54	17.5	944	
55	862	16.5	14223	31	257	16.5	4236	
49	1560	15.5	24185	32	75	16.5	1230	
59	225	16	3602	30	66	16.5	1085	
57	1103	14.5	16000	25	79	15.5	1230	
54	239	16	3824	24	225	15.5	3482	
47	1157	16.5	19092	23	72	16	1150	
53	52	16	834	22	752	16	12038	
56	16	14.5	237	21	669	16	10697	
48	235	15.5	3641	18	184	14.5	2668	
52	43	16.5	709	17	134	15	2017	
51	20	16.5	329	16	1545	15	23182	
46	1127	16.5	18597	20	983	16	15734	
62	625	16.5	10314	15	1109	14.5	16083	
29	3341	17	56803	13	77	14	1084	
26	1113	15.5	17255	12	6	13.5	81	
50	98	16	1568	11	138	13.5	1862	
27	3452	17	58683	10	557	13.5	7523	
42	663	17.5	11606	14	271	15	4058	
34	1365	17.5	23889	9	23	13.5	309	
44	639	17	10866	8	818	13.5	11043	
37	500	17.5	8747	7	310	12.5	3877	
43	83	16.5	1370	6	311	11.5	3579	
28	726	17	12340	5	7	11.5	82	
33	684	16.5	11278	3	101	10.5	1061	
38	90	17.5	1572	4	102	10.5	1074	
35	404	18	7269	63	266	10	2663	
40	129	18	2323	2	10	10	99	
41	108	18	1952					
<b>Total area</b>					<b>32729</b>	<b>Total volume</b>		<b>521798</b>

Total area of fan-delta = 32 729 m<sup>2</sup>

Total volume of fan-delta = 521 798 m<sup>3</sup>

## Appendix A-4



## Sample Calculation of Daily Suspended Sediment

Table A-4 Example of Daily Suspended Sediment Calculation

Lillooet Q (m <sup>3</sup> s <sup>-1</sup> )	Fitz Q (m <sup>3</sup> s <sup>-1</sup> )	Css (mg L <sup>-1</sup> )	Corrected Css (mg L <sup>-1</sup> )	Daily Mass (Mg day <sup>-1</sup> )
277	7.92	105.53	156.35	107
242	7.01	79.95	118.46	72
233	6.77	74.01	109.65	64
233	6.77	74.01	109.65	64
242	7.01	79.95	118.46	72

<b>total contribution for the 5 day period (Mg) =</b>	<b>379</b>
---	------------

**Where**

**Lillooet Q** - daily discharge from Lillooet River

**Fitz Q** - daily discharge from Fitzsimmons Creek from equation 3.2

**Css** - concentration of suspended sediment from equation 3.1

**Corrected Css** - concentration estimate corrected for log-log bias (48.16%)

**Daily Mass** - daily mass of suspended sediment (mg L<sup>-1</sup> --> Mg day<sup>-1</sup> --> x 0.0864)

## Appendix A-5 Suspended-Sediment Log-Log Bias Correction

Table A-5 Bias Correction for modeled suspended sediment data

Date	Css	Q	log Q	log Css	log C'	s <sup>2</sup> calculation
14/5/99	293.43	2.4	0.3802	2.4675	0.8557	anomoly
25/5/99	600.50	9	0.9542	2.7785	2.1477	0.0137
29/5/99	43.33	4.7	0.6721	1.6368	1.5127	0.0005
06/05/99	292.71	8	0.9031	2.4664	2.0326	0.0065
06/14/99	284.71	11	1.0414	2.4544	2.3439	0.0004
29/6/99	20.27	5.61	0.7490	1.3068	1.6857	0.0050
01/07/99	39.25	6.88	0.8376	1.5938	1.8852	0.0029
02/07/99	64.24	6.65	0.8228	1.8078	1.8519	0.0001
14/7/99	241.50	15.1	1.1790	2.3829	2.6535	0.0025
16/8/99	21.50	10.6	1.0253	1.3324	2.3077	0.0328
25/8/99	1117.56	18	1.2553	3.0483	2.8252	0.0017
25/8/99	1757.43	18	1.2553	3.2449	2.8252	0.0061
25/8/99	1816.50	18	1.2553	3.2592	2.8252	0.0065
29/8/99	124.22	11.3	1.0531	2.0942	2.3702	0.0026
29/8/99	126.13	11.3	1.0531	2.1008	2.3702	0.0025
18/9/99	11.47	4.06	0.6085	1.0596	1.3696	0.0033
20/9/99	26.67	4.61	0.6637	1.4260	1.4938	0.0002
20/9/99	26.67	4.61	0.6637	1.4260	1.4938	0.0002
16/06/99	2289.82	26	1.4150	3.3598	3.1847	0.0011
18/06/99	316.53	13.9	1.1430	2.5004	2.5726	0.0002
18/06/99	330.4	13.9	1.1430	2.5190	2.5726	0.0001
18/06/99	319.48	13.9	1.1430	2.5044	2.5726	0.0002
07/07/99	233.58	8.56	0.9325	2.3684	2.0987	0.0025
12/07/99	301.69	13.1	1.1173	2.4796	2.5146	0.0000
13/07/99	187.62	14.7	1.1673	2.2733	2.6273	0.0043
13/07/99	170.18	14.7	1.1673	2.2309	2.6273	0.0054
13/07/99	169.48	14.7	1.1673	2.2291	2.6273	0.0055
29/07/99	443.12	9.07	0.9576	2.6465	2.1553	0.0083
28/10/99	11	1.71	0.2330	1.0414	0.5244	0.0092
28/10/99	10.25	1.71	0.2330	1.0107	0.5244	0.0082
13/11/99	70.5	4.11	0.6138	1.8482	1.3816	0.0075
13/11/99	75.14	4.11	0.6138	1.8759	1.3816	0.0084
					<b>s<sup>2</sup>=</b>	<b>0.1483488</b>

log C' = logQ x 2.2507

Css=Q^(2.2507)

Equation to synthesize SS concentration from discharge

Ferguson's (1986) bias correction factor =  $\exp(2.65 \cdot s^2) = 1.481602488$

**Therefore, estimates of daily suspended sediment must be multiplied by the bias correction factor of 48%**

## Appendix A-6 GPR Migration Calculation (from Reynolds, 1997)

Preamble: GPR profiles were not corrected for dip angle electronically. In order to determine the true dip angle, a manual migration calculation was completed. The following outlines the calculation and the conclusion.

$d_t$  - Vertical time displacement  
 $\theta_t$  - apparent dip angle  
 $\theta_T$  - dip angle after migration  
 $V$  - material velocity  
 $t$  - two-way travel time

Given:  $\theta_t = 25^\circ$   
 $V = 0.07$  m/ns

Equation 1.  $d_t = t\{1-[1-(V^2 \tan^2\theta_t)/4]^{1/2}\}$

$$d_t = 400\{1[1-(0.07)^2(\tan^2(25))/4]^{1/2}\}$$
$$d_t = 400\{0.000133192\}$$
$$d_t = 0.053 \text{ ns}$$

Equation 2.  $\tan \theta_T = \tan\theta_t/[1-(V^2 \tan^2\theta_t)/4]^{1/2}$

$$\tan \theta_T = \tan(25)/[1-(0.07)^2(\tan^2(25))/4]^{1/2}$$
$$\tan \theta_T = 0.466307658/0.999866807$$
$$\theta_T = 25.0029^\circ$$

The vertical displacement associated with this study is  $\pm 0.053$  ns which translates to  $\pm 0.00371$  metres, an error well within the assigned error of  $\pm 0.5$  metres from interpretations of GPR profiles.

The dip angle after migration has been shown to increase  $0.0029^\circ$ . The original apparent dip of  $25^\circ$  will be adopted as the true dip in this study.

## Appendix A-7 Bulk Density Calculations

Table A-7 Bulk Densities of Geologic Materials

Grain Size	Permanently Submerged (kg m <sup>-3</sup> )	Aerated (kg m <sup>-3</sup> )
Clay	641 – 961	961 – 1281
Silt	881 – 1201	1201 – 1362
Clay-silt mixtures	641 – 1041	1041 – 1362
Sand-silt mixtures	1201 – 1522	1522 – 1762
Clay-silt-sand mixtures	801 – 1281	1281 – 1602
Sand	1362 – 1602	1362 – 1602
Gravel	1362 – 2002	1362 – 2002
Poorly sorted sand and gravel	1522 – 2082	1522 – 2082

(modified from Chow, 1964)

### **Part I. Topset Facies**

Bulk density of topsets is based on the average mass of surface sediment samples divided by the volume of the core sampler.

$$\text{Topset bulk density} = 3.655 \text{ kg} / 2.039 \times 10^{-3} \text{ m}^3$$

$$\text{Topset bulk density} = 1793 \text{ kg m}^{-3}$$

### **Part II. Foreset Facies**

Bulk density of foresets is based on values from Chow (1964), which compare well with the bulk densities associated with neighbouring deltas.

It is assumed that foresets consist of less gravel than topsets, and a higher percentage of sand. The proportions are therefore estimated to be 40% gravel and 60% sand.

Given the assumption that 1682 kg m<sup>-3</sup> approximates the gravel proportion of sediment (from the median bulk density of aerated sand-silt mixtures in the above table) and 1450 kg m<sup>-3</sup> approximates the bulk density of sand sized sediment (based on the aerated sand bulk density from Chow (1964)), it follows that:

$$\text{Foreset bulk density} = 0.40 \times 1682 \text{ kg m}^{-3} + 0.60 \times 1450 \text{ kg m}^{-3}$$

$$\text{Foreset bulk density} = 1543 \text{ kg m}^{-3}$$

### Part III. Bottomset Facies

Bulk density of bottomsets is based on the average of

USGS reservoir data (58% sand, 42% silt/clay)	- 1400 kg m <sup>-3</sup>
Hickin (1989) lower estimate for the Squamish R.	- 1400 kg m <sup>-3</sup>
Gilbert (1975) lower estimate for the Lillooet R.	- 1365 kg m <sup>-3</sup>
Average bulk density	= 1388 kg m <sup>-3</sup>

**Bottomset bulk density = 1388 kg m<sup>-3</sup>**

### Overall Bulk Density for the Sediment Pile

GPR profiles in the direction of apparent dip reveal the beds in a ratio of 1:2.5:0.5 for topset:foreset:bottomset facies. Assuming this is the case, a representative overall bulk density based on the ratio of stratigraphy is:

$$\begin{aligned}\text{Topset bulk density} &= 1793 \text{ kg m}^{-3} \times 1.0 = 1793 \text{ kg m}^{-3} \\ \text{Foreset bulk density} &= 1543 \text{ kg m}^{-3} \times 2.5 = 3858 \text{ kg m}^{-3} \\ \text{Bottomset bulk density} &= 1388 \text{ kg m}^{-3} \times 0.5 = 694 \text{ kg m}^{-3}\end{aligned}$$

$$\begin{aligned}\text{Overall average bulk density} &= 6345 \text{ kg m}^{-3} / 4 \\ &= 1586 \text{ kg m}^{-3}\end{aligned}$$

Accounting for the error associated with the assumed bulk densities, the representative value has been rounded off to the nearest 100 kg m<sup>-3</sup>.

**Therefore, the bulk density to represent the sediment pile is 1600 ± 100 kg m<sup>-3</sup>.**

## **Appendix A-8**

### **Error Calculation for Decadal Suspended-Sediment Estimates**

**(Based on DH<sub>48</sub> samples)**

#### **Part 1: Standard Error of Suspended-Sediment Concentration**

Sediment Rating Curve was plotted as two linear relationships

Rating curve part i - based on 27 observations the standard error = 129.37 mg L<sup>-1</sup>

Rating curve part ii - based on 4 observations the standard error = 387.61 mg L<sup>-1</sup>

(from MicroSoft Excel calculations)

**Weighted standard error of suspended-sediment concentration =**

$$\frac{(\text{error part i}) \times (\text{number of observations}) + (\text{error part ii}) \times (\text{number of observations})}{(\text{total number of observations})}$$

Therefore weighted standard error of suspended-sediment concentrations =

$$\begin{aligned} & \frac{(129.37 \times 27) + (387.61 \times 4)}{31} \\ = & 5043.43 / 31 \\ = & \pm 162.6912903 \end{aligned}$$

**Weighted standard error of suspended-sediment concentrations**

$$= \pm 162.69 \text{ mg L}^{-1}$$

## Part 2: Standard Error of Daily Discharge Measurements

### **Standard error of discharge record for Fitzsimmons Creek**

$$= \pm 1.671567 \text{ m}^3 \text{ s}^{-1}$$

(from MicroSoft Excel Calculation)

### Overall Error of Daily Suspended-Sediment Concentrations

$$= \text{Standard error (daily discharge)} \times \text{standard error (suspended sediment)} \\ \times 0.0864$$

Where

0.0864 is the conversion factor from  $\text{mg L}^{-1}$  to  $\text{Mg day}^{-1}$

**Therefore, overall error of daily suspended-sediment concentrations is:**

$$= 162.69 \times 1.671567 \times 0.0864 \\ = \pm 23.496 \text{ Mg day}^{-1}$$

Note: The errors associated with daily suspended-sediment concentrations ( $\text{DH}_{48}$ ) in Table 3.5 are based on the overall error ( $\pm 23.496 \text{ Mg day}^{-1}$ ) multiplied by the number of days in the period of observation.

### Sample Calculation:

For the period 1982 - 1990 there were 2864 days

$$\text{Therefore total error} = 2864 \text{ days} \times 23.496 \text{ Mg day}^{-1} \\ = \pm 67\,293 \text{ Mg}$$

Therefore, the error on the estimate of suspended-sediment for the period 1982 - 1990 is  $\pm 67\,293 \text{ Mg}$

# APPENDIX B

## SUPPLEMENTARY DATA

B-1 Summary of Depths from Bathymetric Profiles

B-2a Bathymetry Profile 1 - B-2k Bathymetry Profile 11

B-3a GPR Profile (FC1)

B-3b GPR Profile (FC6)

B-3c GPR Profile (FC7)

B-3d GPR Profile (FC9)

B-3e GPR Profile (FC11)

B-3f GPR Profile (FC13)

B-3g GPR Profile (FC14)

B-3h GPR Profile (FC15)

B-3i GPR Profile (FC16)

B-4 Sediment Core Composition Data



## **Appendix B-1**

### **Summary of Depths from Bathymetric Profiles**

**(Profile Numbers refer to Locations on Figure 2.1)**

<b>Transect 1 (81°) True north</b>		<b>Transect 2 (96°) True north</b>	
Depth (m)	Distance(m)	Depth (m)	Distance(m)
141	149	134	152
128	133	115	137
114	116	100	120
100	99	87	101
94	82	70	82
78	68	59	67
66	55	48	55
56	44	37	44
46	34	32	37
37	27	27	32
30	20	20	27
25	16	0	20
17	14	0	0
16	0	0	0
		0	0
		0	0
<b>Transect 3 (111°) True north</b>		<b>Transect 4 (126°) True north</b>	
Depth (m)	Distance(m)	Depth (m)	Distance(m)
179	181	172	166
166	170	149	152
155	151	137	138
135	135	126	128
126	117	115	110
110	105	100	99
81	91	87	88
65	79	79	77
56	66	69	67
46	58	59	57
37	48	53	51
29	41	44	45
22	32	38	37
15	27	27	33
0	20	0	27
0	15	0	0

\*distance - refers to distance from start of bathymetric survey line

<b>Transect 5 (141°) True north</b>		<b>Transect 6 (156°) True north</b>	
Depth (m)	Distance(m)	Depth (m)	Distance(m)
143	198	178	188
144	185	167	164
115	166	154	144
92	154	142	127
91	140	129	109
56	120	119	91
61	105	96	78
47	91	99	70
39	79	90	61
34	69	82	59
27	62	72	0
0	53	68	0
0	45	64	0
0	39	59	0
0	32		
0	27		
<b>Transect 7 (171°) True north</b>		<b>Transect 8 (186°) True north</b>	
Depth (m)	Distance(m)	Depth (m)	Distance(m)
155	185	165	183
156	173	143	146
118	150	111	123
113	125	98	101
98	106	78	89
79	88	70	76
67	77	54	64
56	59	43	53
48	47	33	42
40	37	27	33
0	0	18	25
0	0	16	17
<b>Transect 9 (201°) True north</b>		<b>Transect 9 (201°) True north</b>	
Depth (m)	Distance(m)	Depth (m)	Distance(m)
199	169	61	53
170	156	46	39
149	141	35	30
127	123	26	19
106	101	17	3
86	82	16	0
72	65		

# Appendix B-2a Bathymetry Profile 1

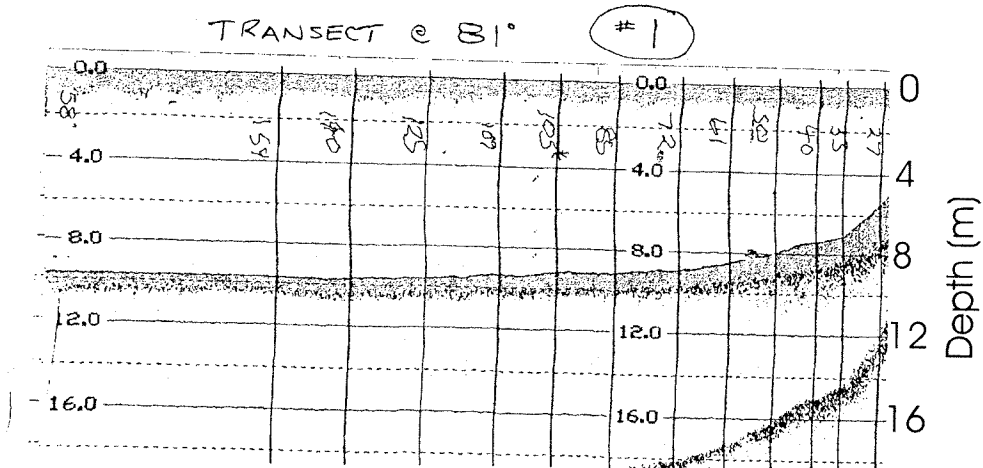
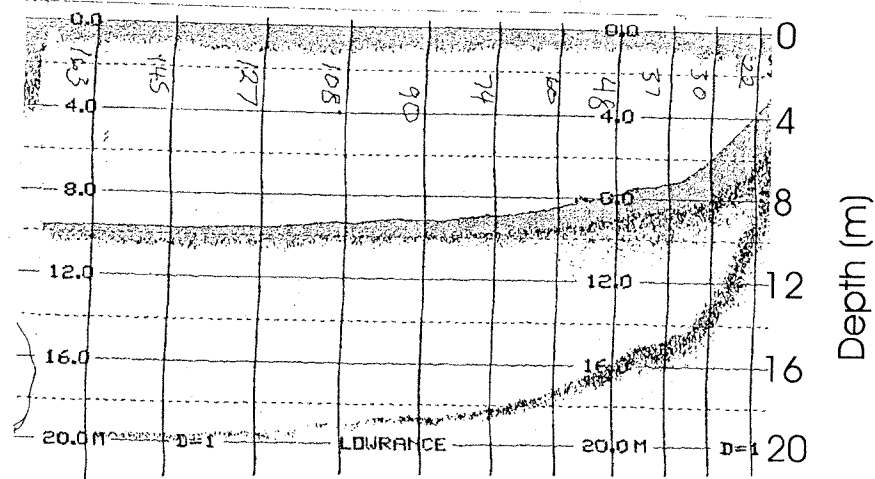


Figure B-2a Bathymetric profile at 81° true north. Two replicates shown, distance in yards.

## Appendix B-2b Bathymetry Profile 2

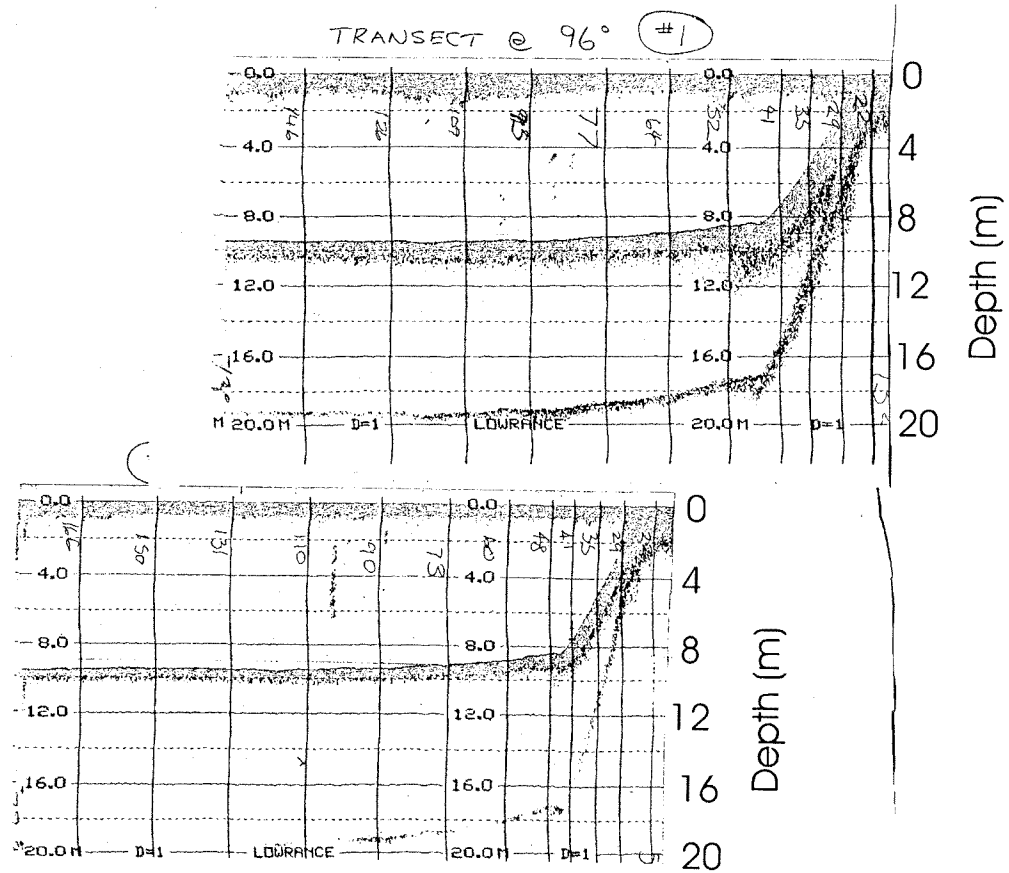


Figure B-2b Bathymetric profile at 96° true north. Two replicates shown, distance in yards.

### Appendix B-2c Bathymetry Profile 3

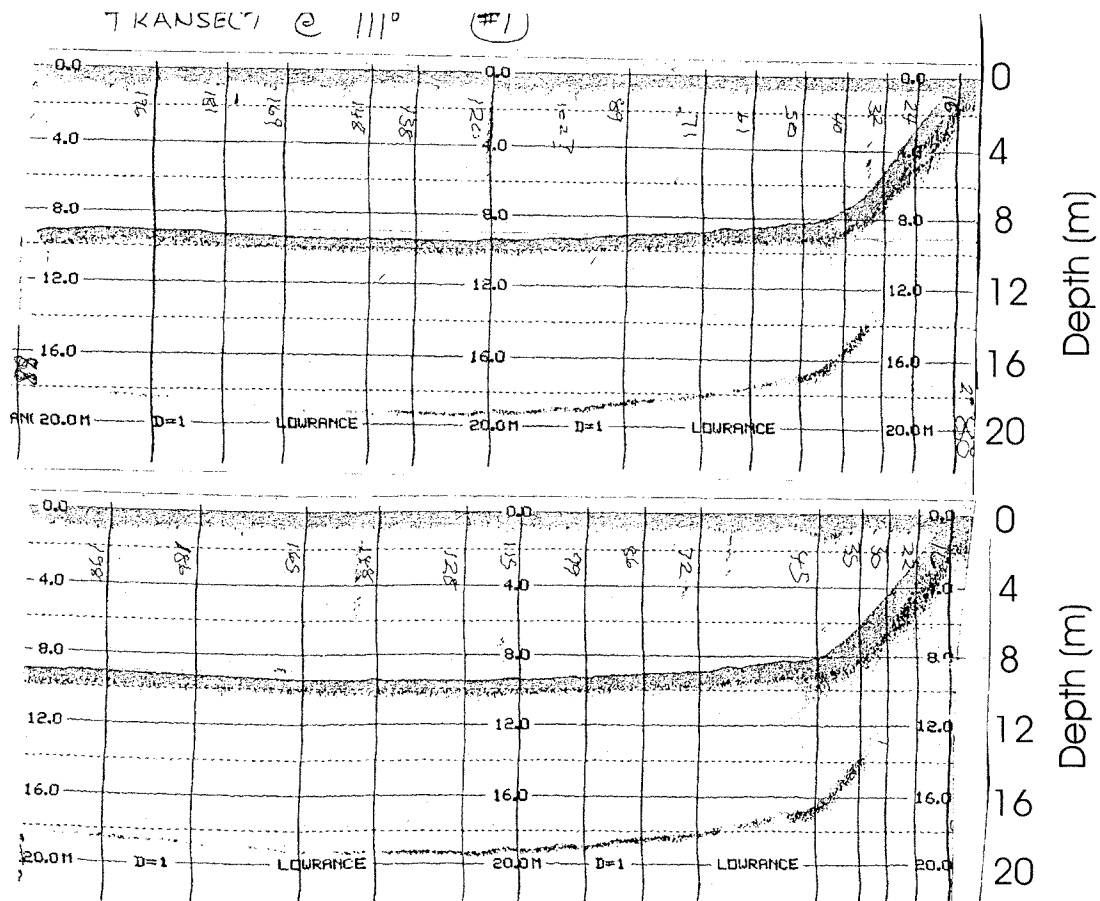


Figure B-2c Bathymetric profile at 111° true north. Two replicates shown, distance in yards.

# Appendix B-2d Bathymetry Profile 4

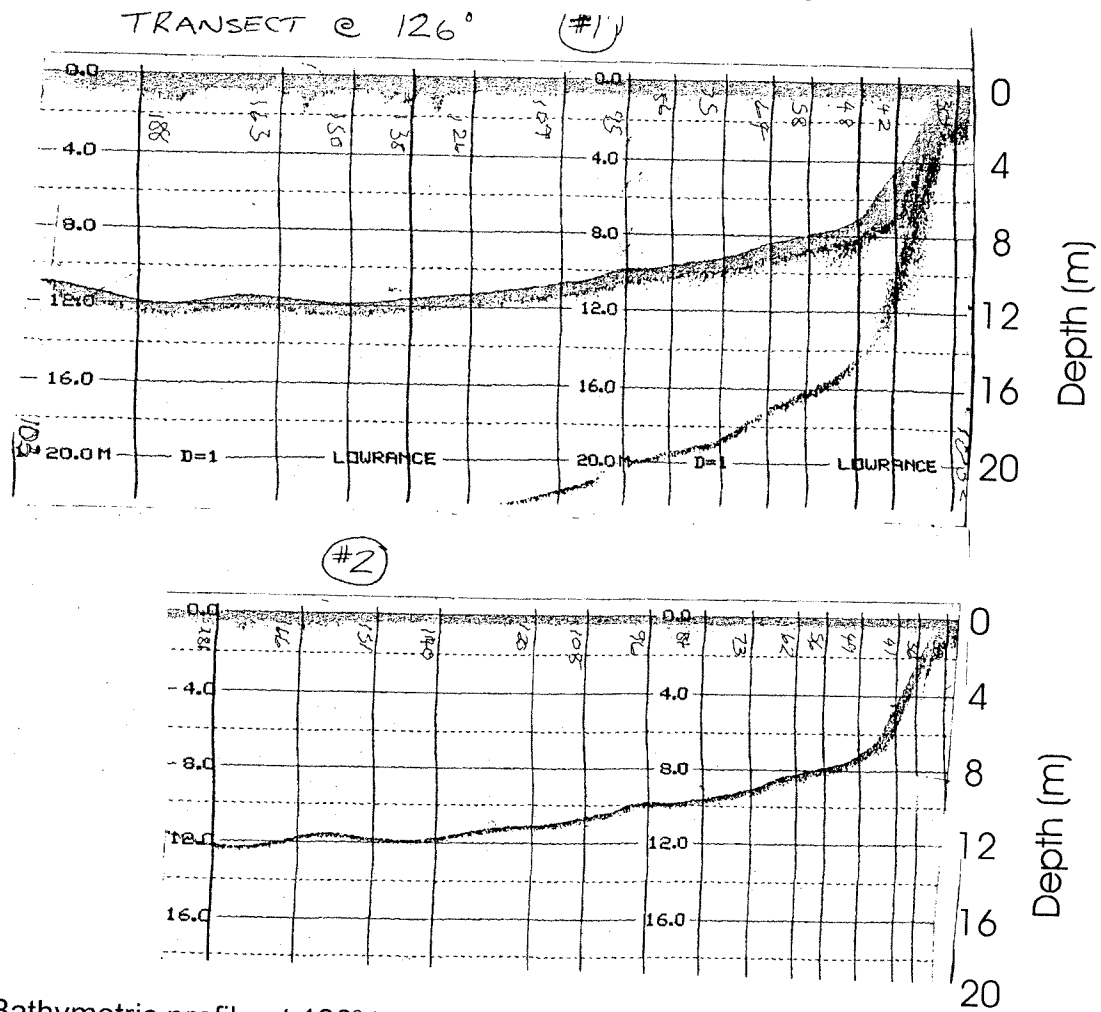


Figure B-2d Bathymetric profile at 126° true north. Two replicates shown, distance in yards.

## Appendix B-2e Bathymetry Profile 5

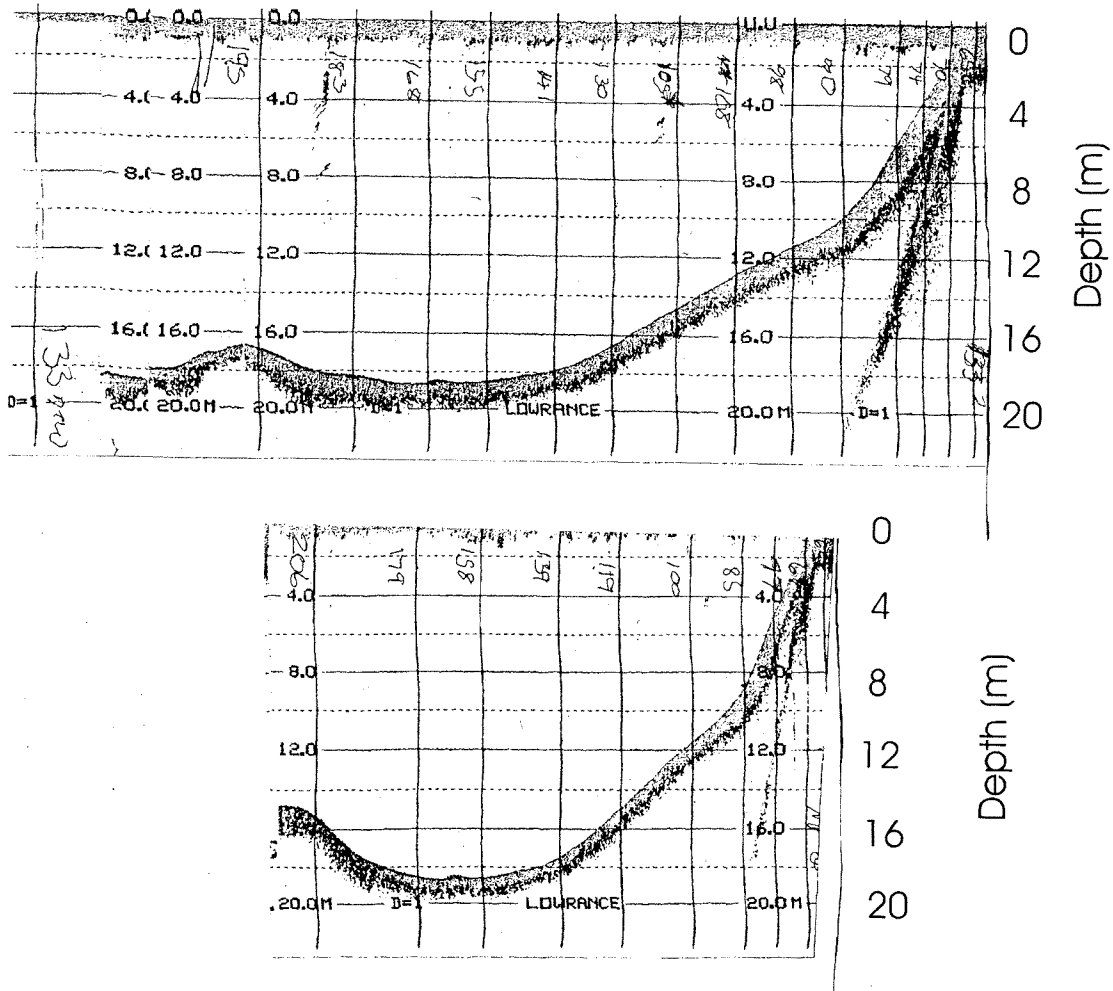


Figure B-2e Bathymetric profile at 141° true north. Two replicates shown, distance in yards.

## Appendix B-2f Bathymetry Profile 6

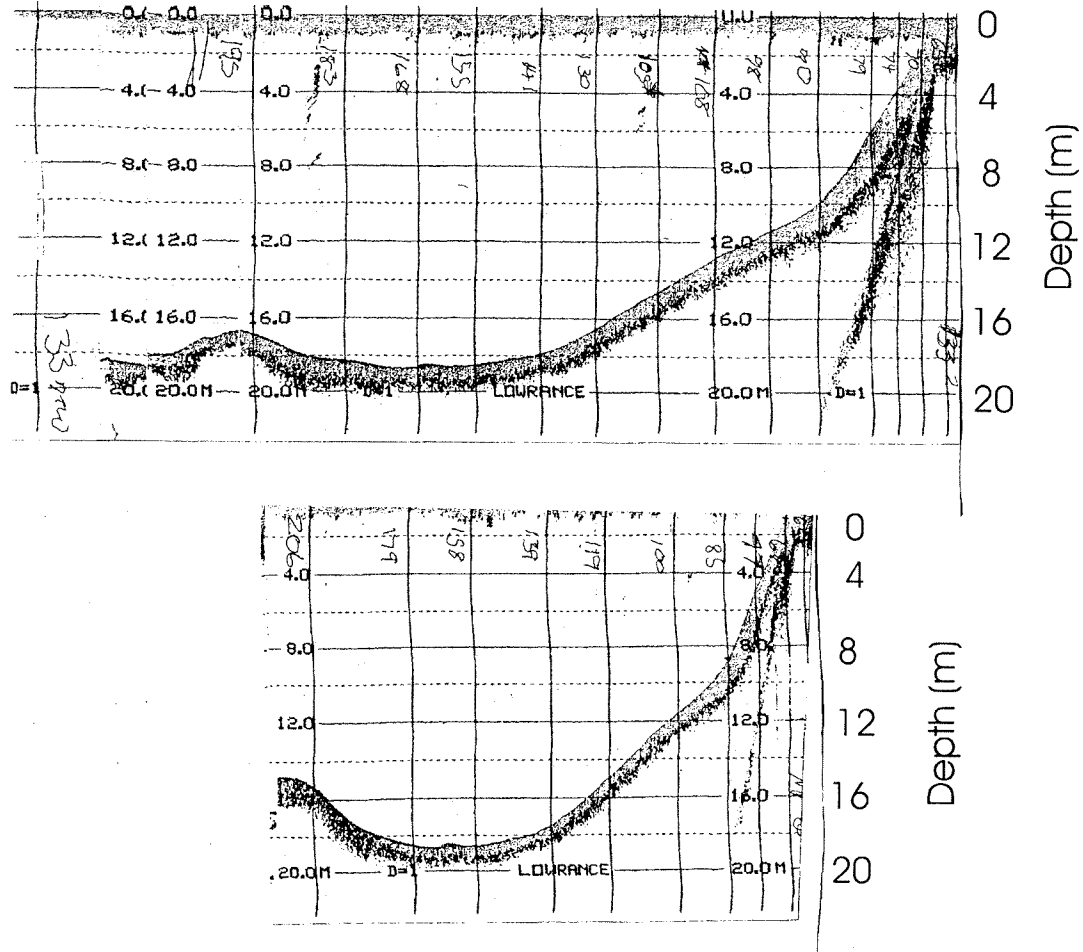


Figure B-2f Bathymetric profile at 156 °true north. Two replicates shown, distance in yards.



## Appendix B-2g Bathymetry Profile 7

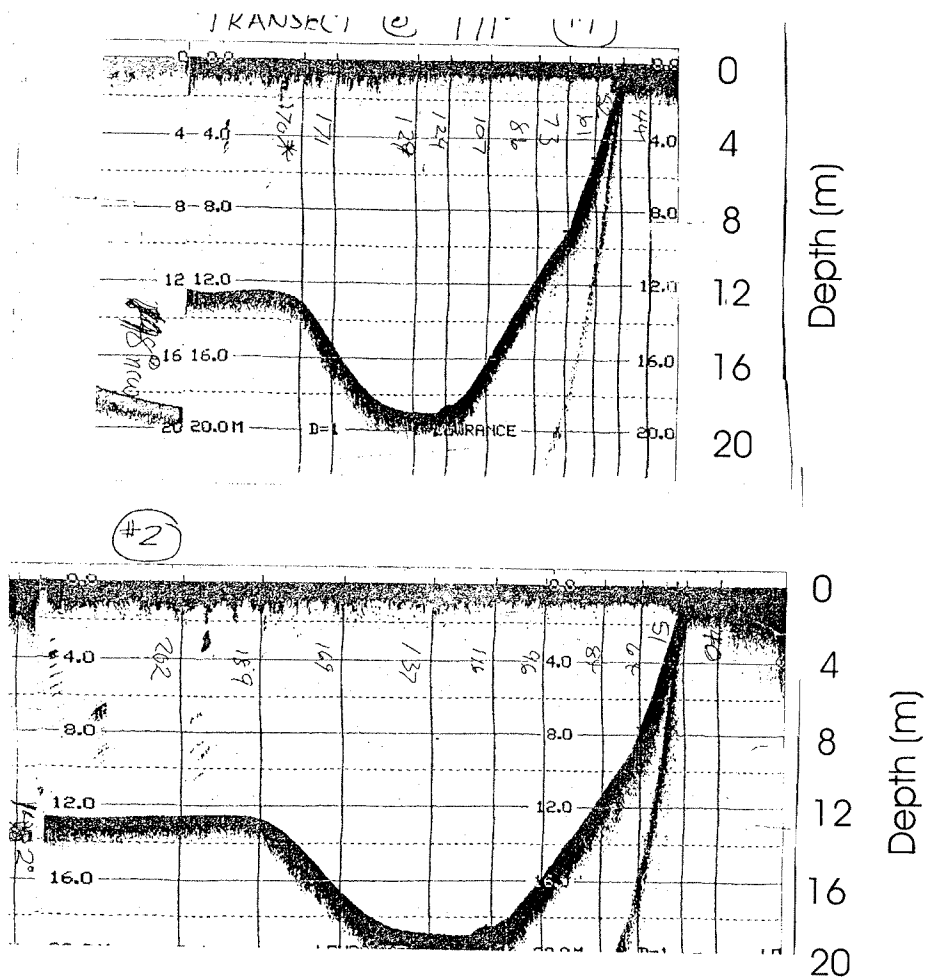


Figure B-2g Bathymetric profile at 171° true north. Two replicates shown, distance in yards.

## Appendix B-2h Bathymetry Profile 8

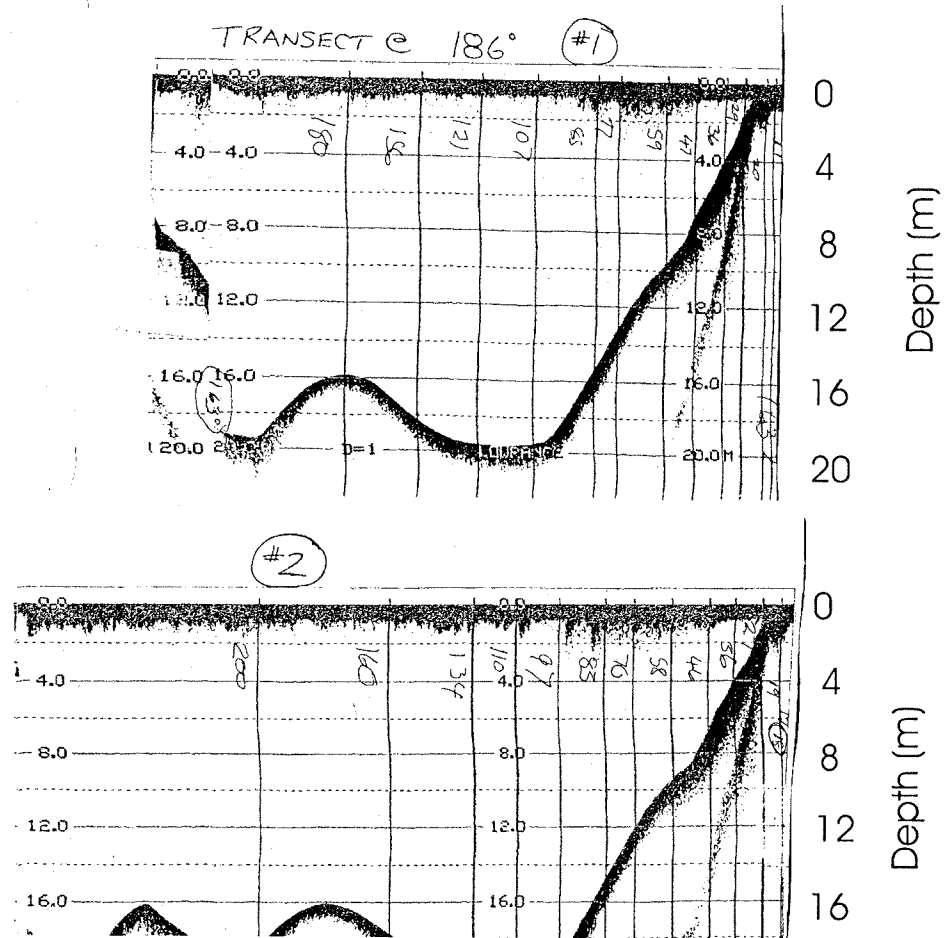


Figure B-2h Bathymetric profile at 186° true north. Two replicates shown, distance in yards.

## Appendix B-2i Bathymetry Profile 9

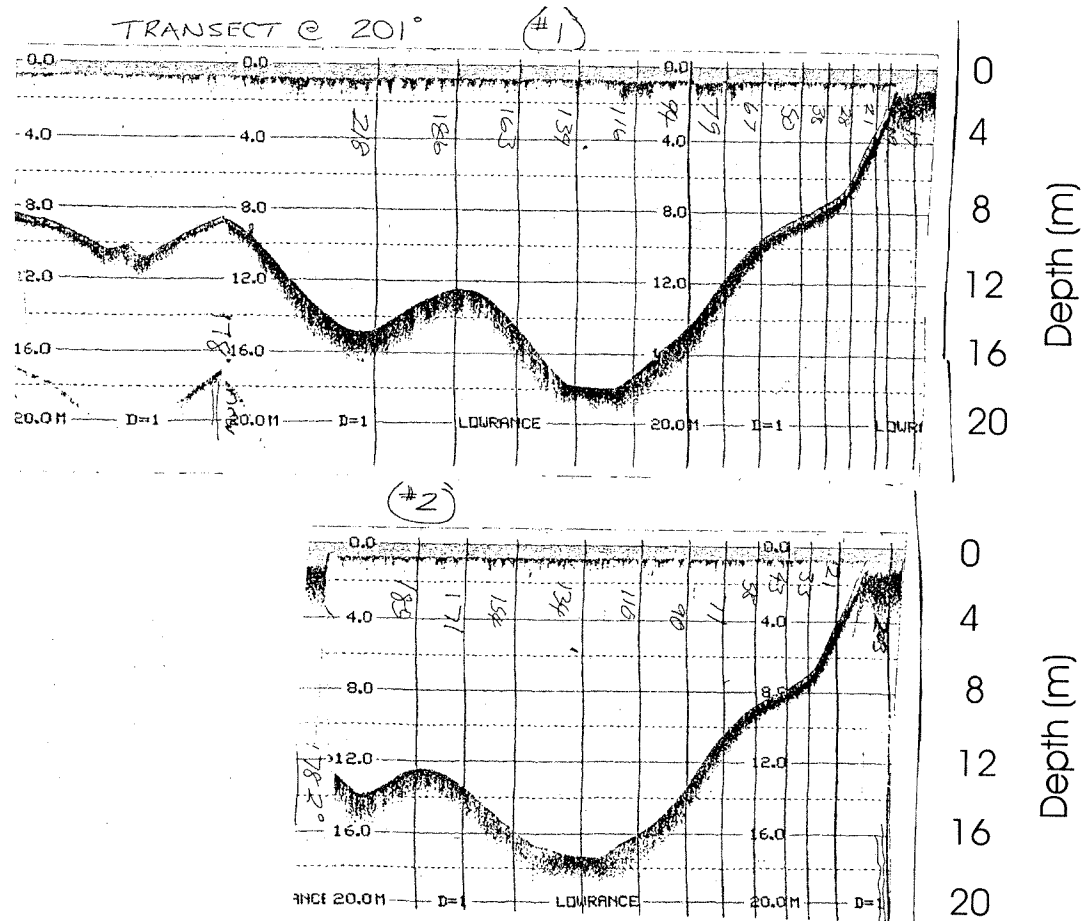
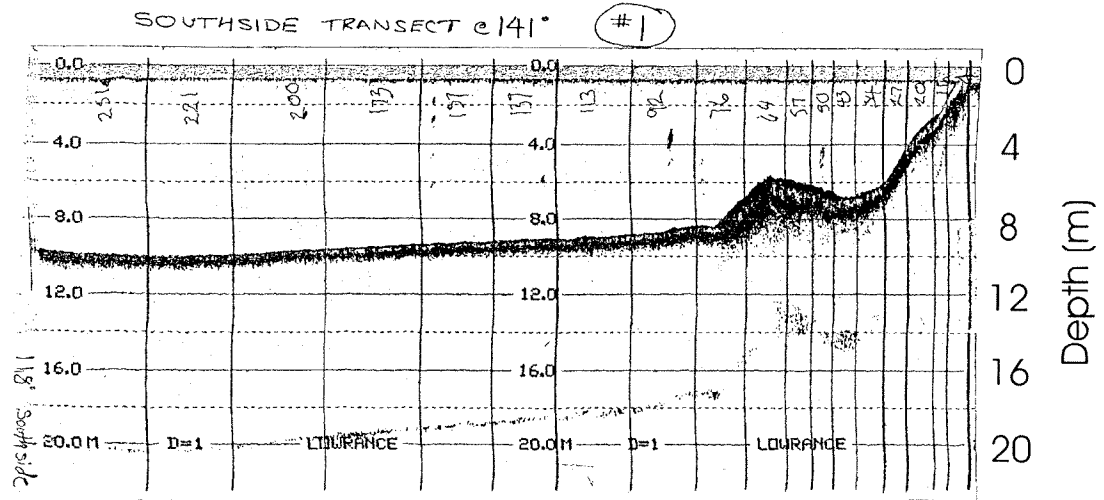


Figure B-2i Bathymetric profile at 201° true north. Two replicates shown, distance in yards.

# Appendix B-2j Bathymetry Profile 10

A (PAGE 1)



#2

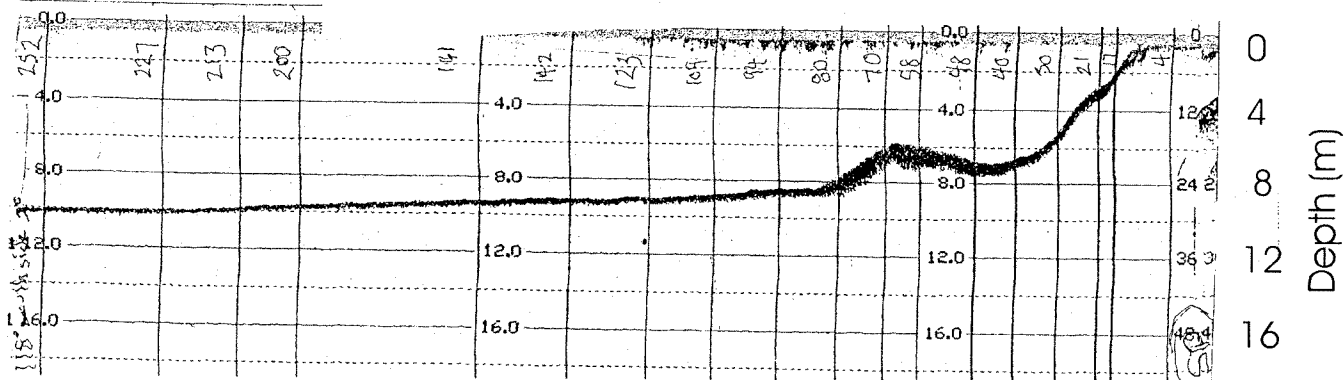


Figure B-2j Bathymetric profile at 141° true north. Two replicates shown, distance in yards.

## Appendix B-2k Bathymetry Profile 11

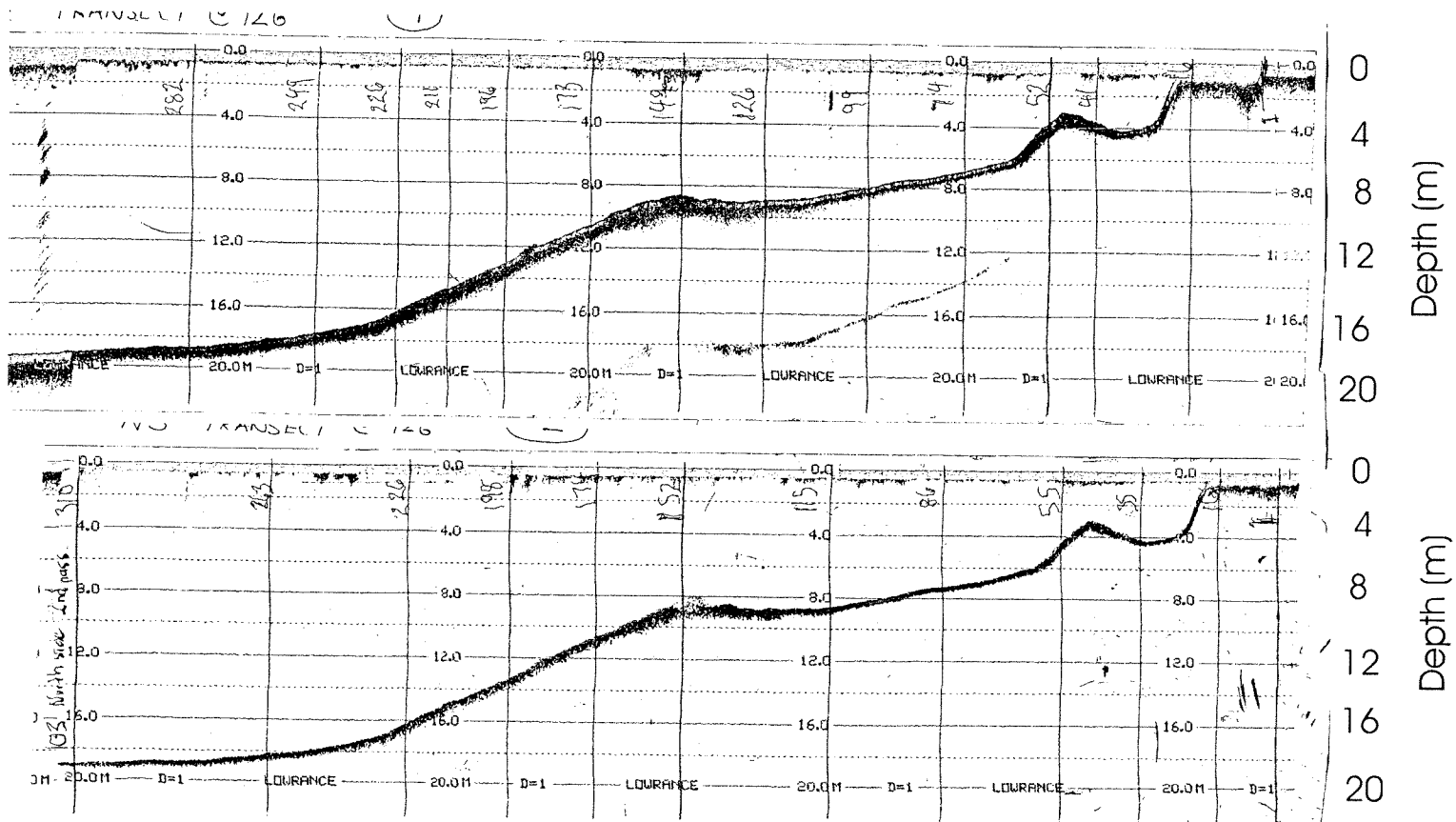
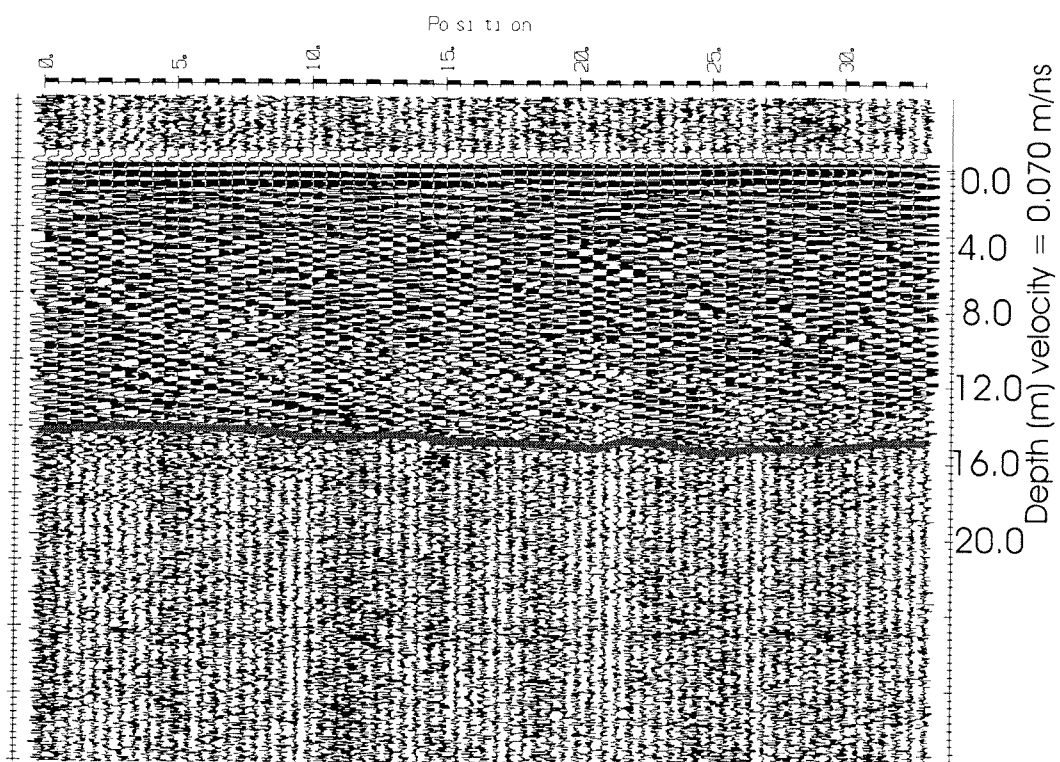


Figure B-2k Bathymetric profile at 126° true north. Two replicates shown, distance in yards.

### Appendix B-3a GPR Profile (FC1)



**Figure B-3a** FC1 GPR Profile. A preliminary GPR survey conducted with 100 Mhz antennae along the FC2 transect. Interpreted boundary layer is shown in bold.

## Appendix B-3b GPR Profile (FC6)

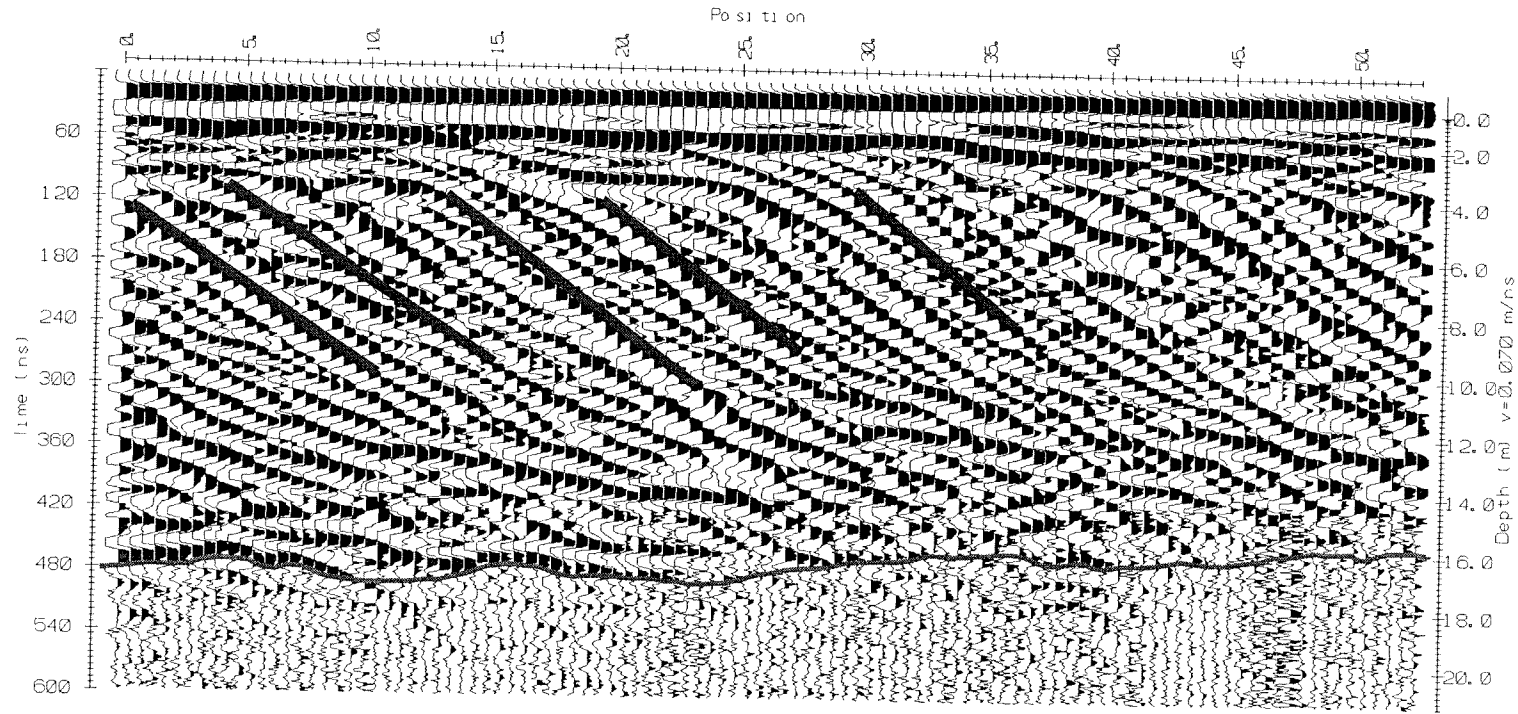


**Figure B-3b** FC6 GPR profile with the fan-delta - lake interface highlighted in bold and slope of foreset facies highlighted. Transect location is shown in Figure 3.2

### Appendix B-3c GPR Profile (FC7)

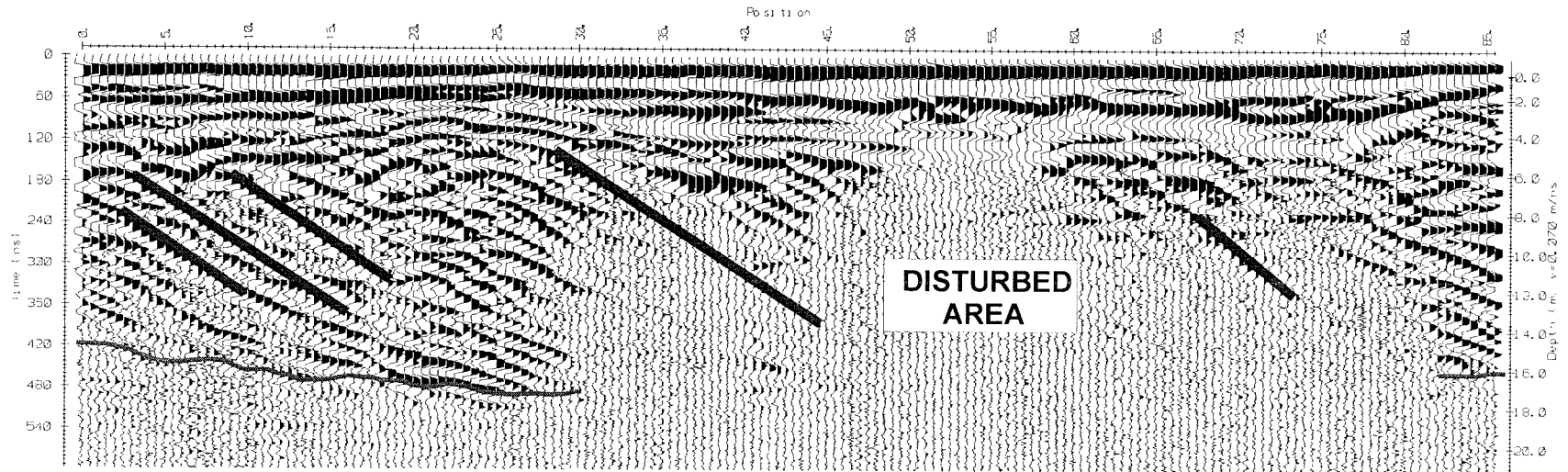


**Figure B-3c** FC7 GPR profile revealing the thickness of sediment in the fan-delta. Disturbed area is due to golf course development. Slope of foreset facies are also revealed.



## Appendix B-3d GPR Profile (FC9)

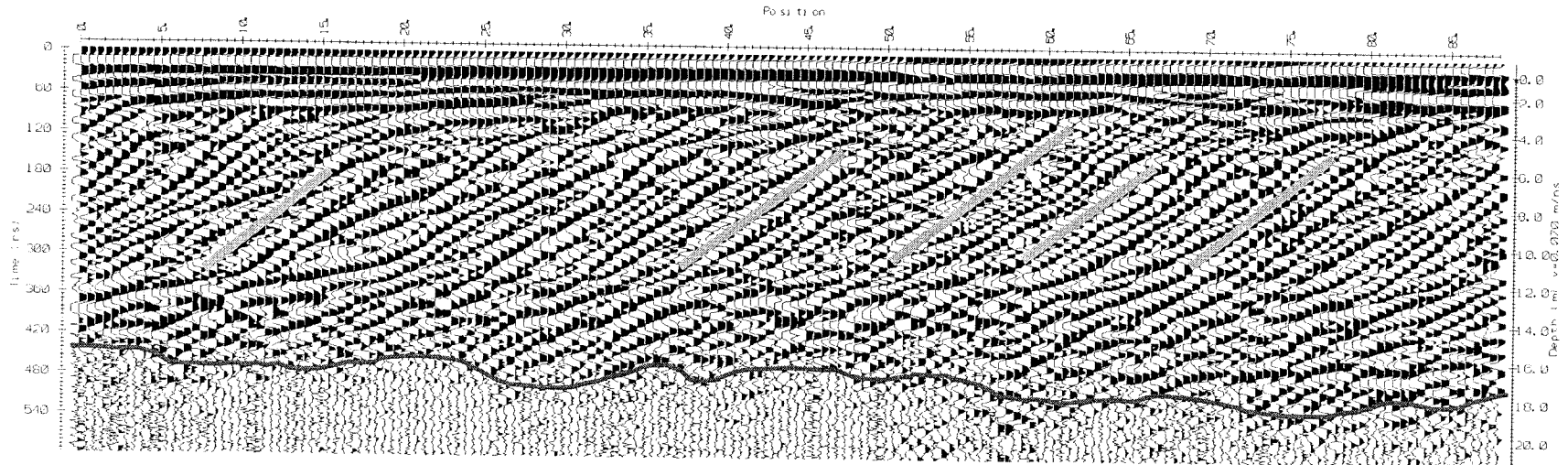


**Figure B-3d** FC9 GPR profile reveals the boundary layer and slope of the foreset facies. Profile location shown in Figure 3.2

### Appendix B-3e GPR Profile (FC11)

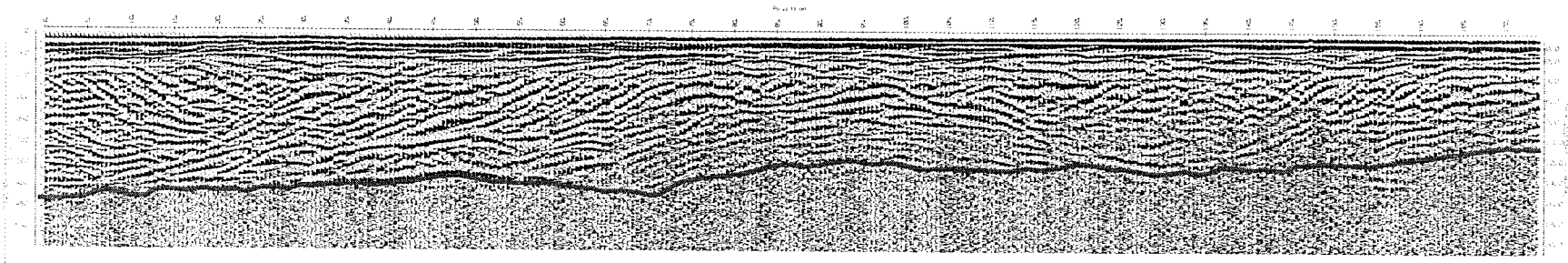


**Figure B-3e** Fc11 GPR profile showing the depth of sediment accumulated in the fan-delta along a transect shown in Figure 3.2. Interpreted boundary is highlighted in bold.

## Appendix B-3f GPR Profile (FC13)

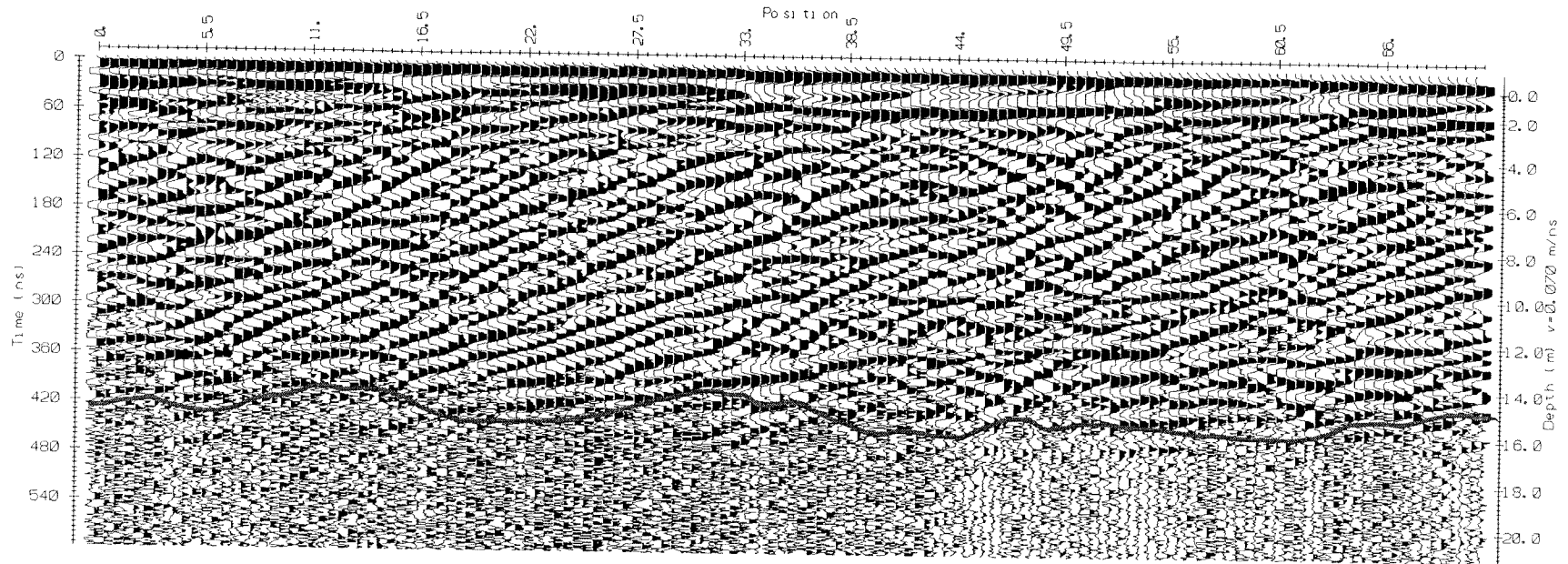


**Figure B-3f** FC13 GPR profile showing the depth of sediment in the fan-delta along the transect shown in Figure 3.2. Interpreted boundary is highlighted in bold.

### Appendix B-3g GPR Profile (FC14)

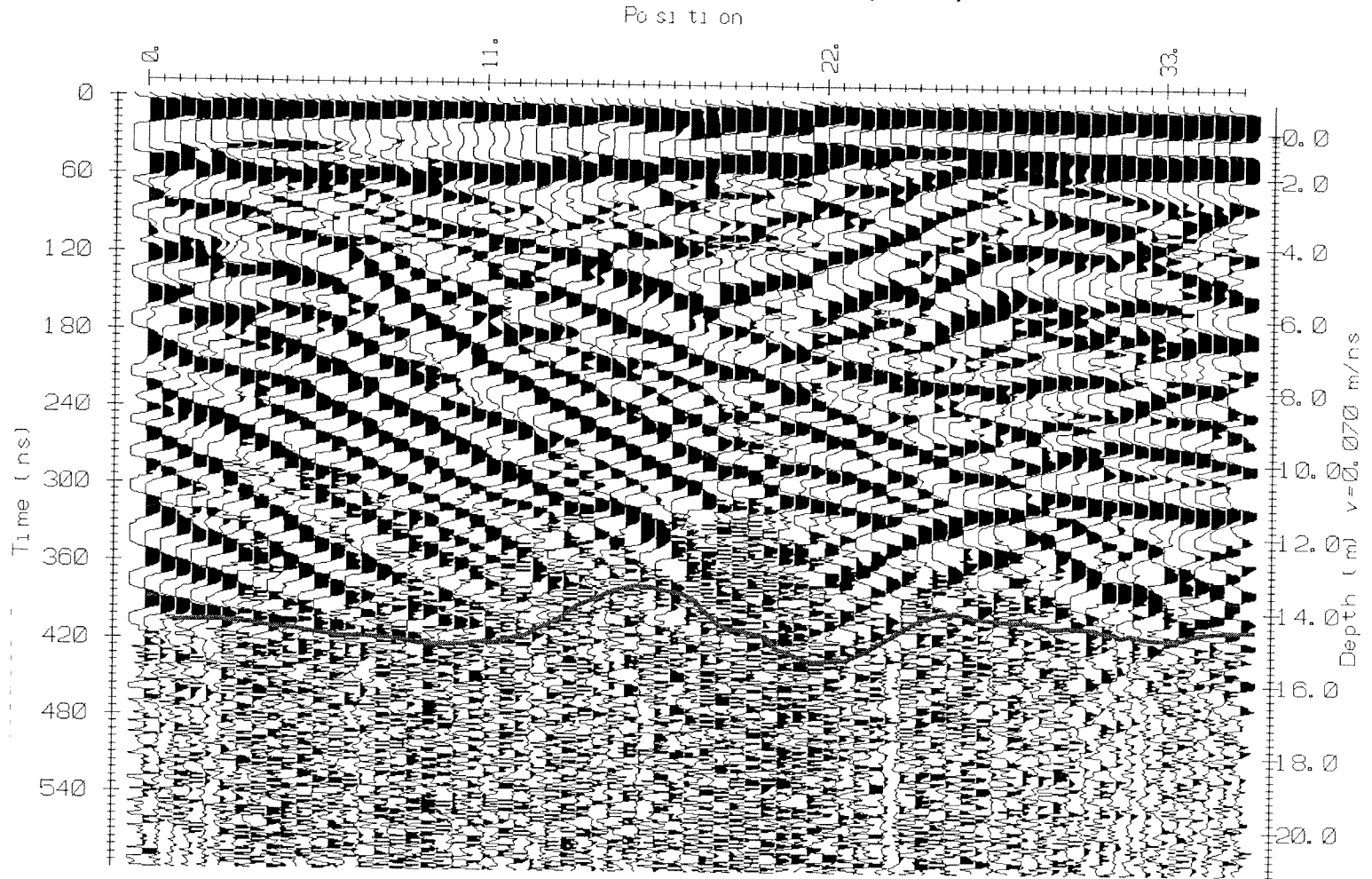


**Figure B-3g** FC14 GPR profile showing the interpreted boundary of the fan-delta and lake interface. This transect was not conducted in the apparent direction of dip as shown in Figure 3.2.

### Appendix B-3h GPR Profile (FC15)

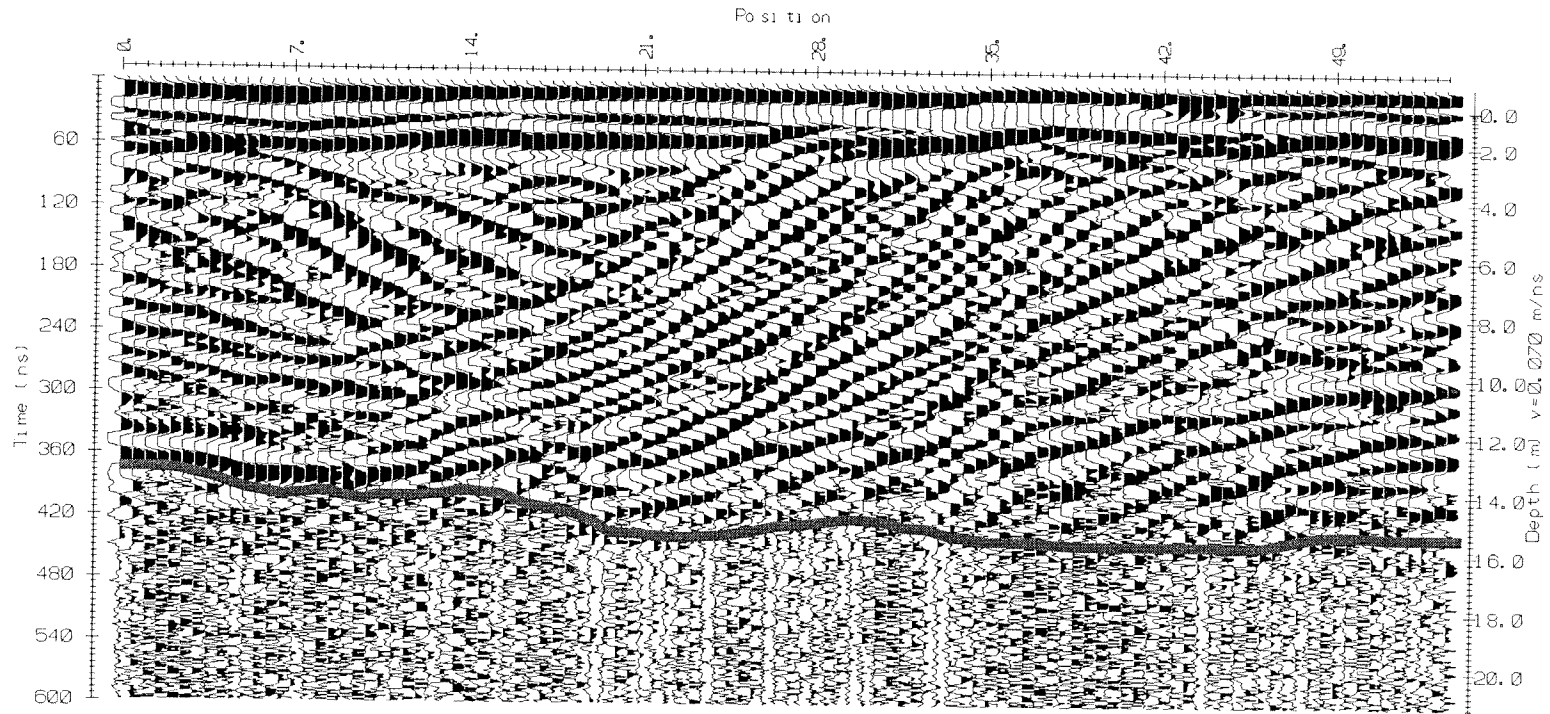


**Figure B-3h** FC15 GPR profile revealing the boundary between the fan-delta sediment and lake sediment. Transect location shown in Figure 3.2 and was not conducted on the apparent direction of dip.

### Appendix B-3i GPR Profile (FC16)

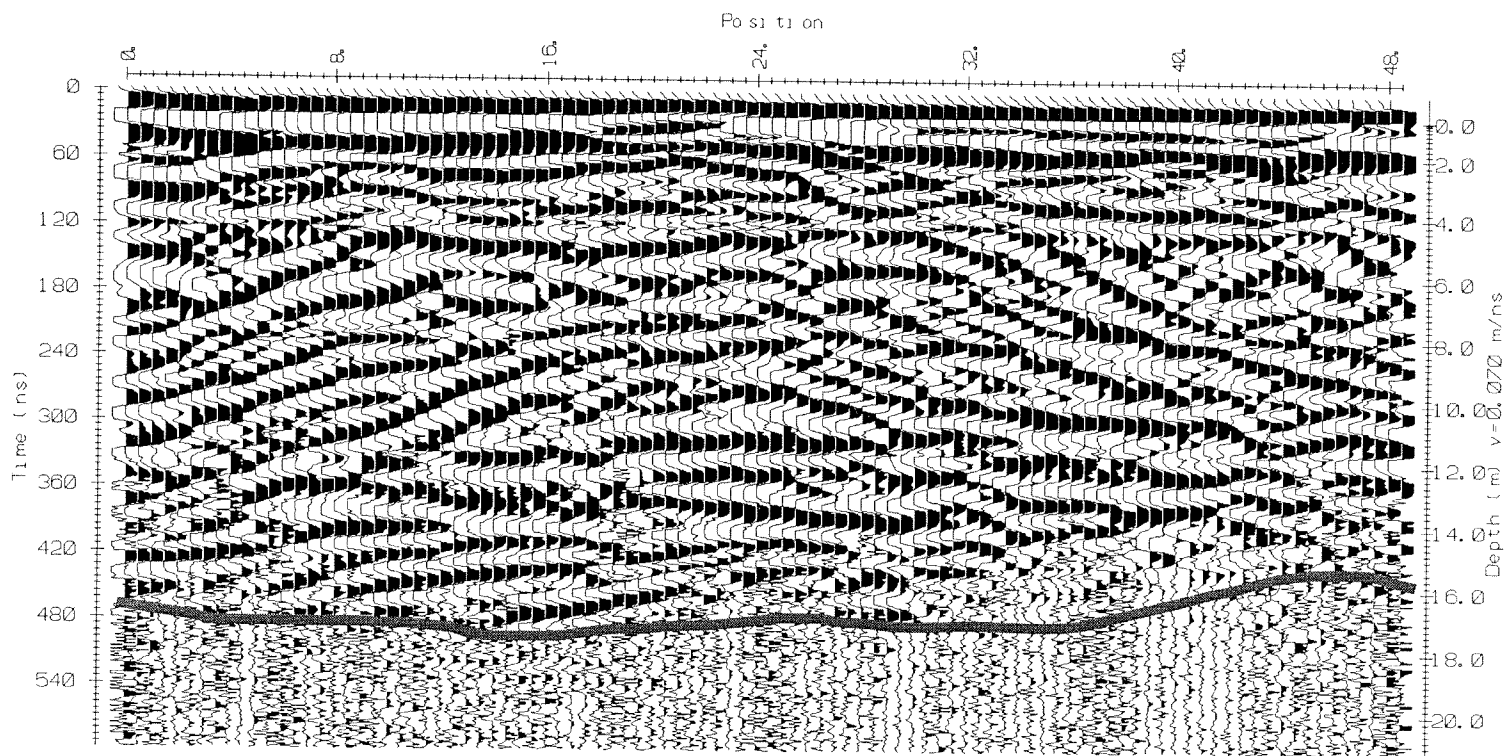


**Figure B-3i** FC16 GPR profile revealing the thickness of sediment in the fan-delta. Profile location is shown in Figure 3.2. Transect was not conducted in the apparent direction of dip.

## Appendix B-4 Sediment Core Composition Data

Table B-4 Summary and Percentage Composition of Sediment from Core Samples

Sample No.	Total Weight (+/- 2g)	Silt/Clay (+/- 0.01 g)	Sand (+/- 0.01g)	Gravel (+/- 0.01g)	% Silt/Clay	% Sand	% Gravel
1	3133	104.48	3025.88	2.83	3.33	96.58	0.09
2	3785	14.35	1162.92	2607.92	0.38	30.72	68.90
3	3951	7.90	869.26	3074.03	0.20	22.00	77.80
4	2879	132.47	2746.72	0.00	4.60	95.40	0.00
5	3751	5.22	1202.78	2543.19	0.14	32.06	67.80
6	3829	10.05	1407.95	2411.19	0.26	36.77	62.97
7	3811	7.72	1562.28	2241.19	0.20	40.99	58.81
8	3675	6.85	1755.15	1913.19	0.19	47.76	52.06
9	3539	8.12	2447.37	1083.70	0.23	69.15	30.62
10	3867	10.89	1911.11	1945.19	0.28	49.42	50.30
11	3359	9.14	2654.06	695.99	0.27	79.01	20.72
12	3507	13.25	2106.75	1387.19	0.38	60.07	39.55
13	4117	3.85	864.86	3248.48	0.09	21.01	78.90
14	3523	1.71	558.32	2963.16	0.05	15.85	84.10
15	3873	26.58	1721.42	2125.19	0.69	44.44	54.87
16	3933	6.84	1184.79	2741.56	0.17	30.12	69.70
17	3905	24.44	1285.56	2595.19	0.63	32.92	66.45
18	3183	62.89	2410.08	710.22	1.98	75.71	22.31
19	3407	202.19	1183.27	2021.73	5.93	34.73	59.34
20	3767	5.69	643.02	3118.48	0.15	17.07	82.78
21	3677	6.26	637.29	3033.64	0.17	17.33	82.50
22	3695	8.21	769.28	2917.70	0.22	20.82	78.96
23	3547	2.22	507.61	3037.36	0.06	14.31	85.63
24	3935	28.88	1969.12	1937.19	0.73	50.04	49.23
25	3369	2.41	1311.59	2055.19	0.07	38.93	61.00
30	3719	4.44	1110.50	2604.25	0.12	29.86	70.02
31	3563	7.74	1028.62	2526.83	0.22	28.87	70.91
32	3675	8.56	957.87	2708.76	0.23	26.06	73.70
33	3079	49.71	2901.94	127.54	1.61	94.24	4.14
34	3817	6.10	935.33	2875.76	0.16	24.50	75.34
35	3409	11.85	1820.15	1577.19	0.35	53.39	46.26
36	3917	23.21	1088.40	2805.58	0.59	27.79	71.62
37	4127	9.65	1114.30	3003.24	0.23	27.00	72.77
38	3661	18.00	920.27	2722.92	0.49	25.14	74.37
39	4035	11.94	811.03	3212.22	0.30	20.10	79.61
40	3683	19.97	1044.94	2618.28	0.54	28.37	71.09
41	3675	4.66	938.68	2731.85	0.13	25.54	74.33
42	3165	2.01	2616.20	546.98	0.06	82.66	17.28
43	3409	2.34	1923.66	1483.19	0.07	56.43	43.51
P1	3951	5.91	1286.09	2659.19	0.15	32.55	67.30
P2	3939	5.66	1428.34	2505.19	0.14	36.26	63.60

## LIST OF REFERENCES

- Ashmore, P. & Church, M. (1998) Sediment Transport and River Morphology: A Paradigm for Study. In: *Gravel-bed Rivers in the Environment* (Ed. by P. C. Klingeman, R. L. Beschta, P. D. Komar and J. B. Bradley), pp. 115-148. Water Resources Publications, LLC, Washington, USA.
- Beres, M., Huggenberger, P., Green, A. G. & Horstmeyer, H. (1999) Using two- and three-dimensional georadar methods to characterize glaciofluvial architecture. *Sedimentary Geology*, **129**, 1-24.
- Blair, T. C. & McPherson, J. G. (1994) Alluvial fans and their natural distinction from rivers based on morphology, hydraulic processes, sedimentary processes, and facies assemblages. *Journal of Sedimentary Research*, **A64**(3), 450-489.
- Bogen, J. (1992) Monitoring grain size of suspended sediment in rivers. In: *Erosion and sediment transport monitoring programmes in river basins, Vol. 210* (Ed. by J. Bogen, D. E. Walling and T. Day), pp. 183-190. International Association of Hydrological Sciences, Oslo.
- Boggs, S. J. (1995) *Principles of Sedimentology and Stratigraphy*. Prentice-Hall, Inc., New Jersey, 774 pp.
- Brown, A. (1993) The August 1991 Fitzsimmons Creek Flood. In: *Whistler and Water: Building a City in the Mountains* (Ed. by A. G. Chantler), pp. 115-128. BiTech Publishers Ltd., Whistler, BC.
- Chow, V. T. (1964) *Handbook of Applied Hydrology*. McGraw-Hill Book Company, Toronto, 17-I.
- Church, M., Ham, D., Hassan, M. & Slaymaker, O. (1999) Fluvial clastic sediment yield in Canada: scaled analysis. *Canadian Journal of Earth Sciences*, **36**, 1267-1280.
- Church, M. & Kellerhals, R. (1979) On hydrological data needs in Canada. In: *River basin management* (Ed. by D. Hay), pp. 651-670. Canadian Society for Civil Engineering, Vancouver.
- Church, M., Kellerhals, R. & Day, T. J. (1989) Regional clastic sediment yield in British Columbia. *Canadian Journal of Earth Sciences*, **26**, 31-45.
- Church, M., Kellerhals, R. & Ward, P. R. B. (1985) Sediment in the Pacific and Yukon Region: Review and Assessment, pp. 1-219. Kellerhals Engineering Services, Ltd., Vancouver.



- Church, M. & Slaymaker, O. (1989) Disequilibrium of Holocene sediment yield in glaciated British Columbia. *Nature*, **337**(6205), 452-454.
- Coates, G. (1984) *Practical Sedimentology*. Macmillan of Canada, Agincourt, Ontario.
- Cohn, T. A., L., D. L., Gilroy, E. J., Hirsch, R. M. & Wells, D. K. (1989) Estimating Constituent Loads. *Water Resources Research*, **25**(5), 937-942.
- Davis, J. L. & Annan, P. (1989) Ground-penetrating radar for high-resolution mapping of soil and rock stratigraphy. *Geophysical Prospecting*, **37**, 531-551.
- De Chant, L. J., Pease, P. P. & Tchakerian, V. P. (1999) Modelling Alluvial Fan Morphology. *Earth Surface Processes and Landforms*, **24**, 641-652.
- Environment Canada, (1981) Canadian Climatic Normals, Temperature and Precipitation, 1951-1980, British Columbia. Atmospheric Environment Service, Canadian Climate Program, Downsview, Ontario.
- Evans, M. & Church, M. (2000) A method for Error Analysis of Sediment Yields Derived From Estimates of Lacustrine Sediment Accumulation. *Earth Surface Processes and Landforms*, **25**, 1257-1267.
- Ferguson, R. I. (1986) River Loads underestimated by Rating Curves. *Water Resources Research*, **22**(1), 74-76.
- Flores, R. M. (1990) Transverse and longitudinal Gilbert-type deltas, Tertiary Coalmont Formation, North Park Basin, Colorado, USA. In: *Coarse-Grained Deltas* (Ed. by A. Colella and D. B. Prior), pp. 223-233. Blackwell Scientific Publications, London.
- Geological Survey of Canada, (1977) Geological Coverage - Pemberton Map Sheet, 1:250000, Geological Survey of Canada.
- Gilbert, G. K. (1890) Lake Bonneville, Monograph 1. United States Geological Survey.
- Gilbert, R. (1975) Sedimentation in Lillooet Lake, British Columbia. *Canadian Journal of Earth Sciences*, **12**(10), 1697-1711.
- Gomez, B. (1987) Bedload. In: *Glacio-Fluvial Sediment Transfer* (Ed. by A. M. Gurnell and M. J. Clark), pp. 355-376. John Wiley & Sons Ltd., Toronto.
- Gomez, B. & Church, M. (1989) An Assessment of Bed Load Sediment Transport Formulae for Gravel Bed Rivers. *Water Resources Research*, **25**(6), 1161-1186.
- Graf, W. H. (1971) *Hydraulics of Sediment Transport*. McGraw-Hill, New York, 513 pp.

- Gurnell, A. M. (1987) Fluvial Sediment Yield from Alpine, Glacierized Catchments. In: *Glacio-Fluvial Sediment Transfer* (Ed. by A. M. Gurnell and M. J. Clark), pp. 415-420. John Wiley & Sons Ltd., Toronto.
- Ham, D. G. & Church, M. (2000) Bed-material transport estimated from channel morphodynamics: Chilliwack River, British Columbia. *Earth Surface Processes*, **25**, 1123-1142.
- Heinemann, H. G. (1984) Reservoir trap efficiency. In: *Erosion and Sediment Yield: Some Methods of Measurement and Modelling* (Ed. by R. F. Hadley and D. E. Walling), pp. 218. Geo Books, Cambridge.
- Hickin, E. J. (1989) Contemporary Squamish River sediment flux to Howe Sound, British Columbia. *Canadian Journal of Earth Sciences*, **26**, 1953-1963.
- Holmes, A. (1965) *Principles of Physical Geology*. Thomas Nelson, London, 1288 pp.
- Huggenberger, P., Meier, E. & Beres, M. (1994) Three-dimensional geometry of fluvial gravel deposits from GPR reflection patterns; A comparison of results of three different antenna frequencies. In: *Fifth International Conference on Ground Penetrating Radar*, pp. 805-816, Guelph, Ontario.
- Jol, H. M. (1993) Ground Penetrating Radar (GPR): A new geophysical methodology used to investigate the internal structure of sedimentary deposits (field experiments on lacustrine deltas). Ph.D. Dissertation, University of Calgary.
- Jol, H. M. & Smith, D. G. (1991) Ground penetrating radar of northern lacustrine deltas. *Canadian Journal of Earth Sciences*, **28**, 1939-1947.
- Jol, H. M. & Smith, D. G. (1992) Geometry and Structure of Deltas in Large lakes: A Ground Penetrating Radar Overview. In: *Fourth International Conference on Ground Penetrating Radar, Vol. 16* (Ed. by P. Hanninen and S. Autio), pp. 159-168. Geological Survey of Finland, Rovaniemi, Finland.
- Knighton, D. (1998) *Fluvial Forms & Processes, A New Perspective*. John Wiley & Sons, Inc., New York, 383 pp.
- Lane, S. N. & Richards, K. S. (1997) Linking River Channel Form and Process: Time, Space and Causality Revisited. *Earth Surface Processes and Landforms*, **22**, 249-260.
- LeClerc, R. F. & Hickin, E. J. (1997) The internal structure of scrolled floodplain deposits based on ground-penetrating radar, North Thompson River, British Columbia. *Geomorphology*, **21**, 17-38.

- Leopold, L. B., Wolman, M. G. & Miller, J. P. (1964) *Fluvial Processes in Geomorphology*. Dover Publications, Inc., New York, 522 pp.
- Martin, Y. & Church, M. (1995) Bed-Material transport estimated from channel surveys: Vedder River, British Columbia. *Earth Surface Processes and Landforms*, **20**, 347-361.
- Martin, Y. & Church, M. (2000) Re-examination of Bagnold's empirical bedload formulae. *Earth Surface Processes and Landforms*, **25**, 1011-1024.
- McPherson, J. G., Shanmugam, G. & Moiola, R. (1988) Fan deltas and braid deltas: conceptual problems. In: *Fan Deltas: Sedimentology and Tectonic Settings* (Ed. by W. Nemeč and R. J. Steel), pp. 14-22. Blackie and Son Ltd., Glasgow.
- McPherson, J. G., Shanmugam, G. & Moiola, R. J. (1987) Fan-deltas and braid deltas: Varieties of coarse-grained deltas. *Geological Society of America Bulletin*, **99**, 331-340.
- Meade, R. H., Yuzyk, T. R. & Day, T. J. (1990) Movement and Storage of sediment in rivers of the United States and Canada. In: *Surface Water Hydrology, Vol. 0-1*, pp. 374. The Geological Society of America, Boulder, Colo.
- Menounos, Brian (2000) unpublished Green Lake Core Sample Location Map, Department of Geography, University of British Columbia, Vancouver.
- Mierzejewski, J. K. (1992) Preliminary Geotechnical Investigation and Stability Analysis Fitzsimmons Creek Slide, Whistler, B.C., pp. 1-28. Golder Associates Ltd., Vancouver.
- Milliman, J. D. & Syvitski, J. P. M. (1992) Geomorphic/Tectonic Control of Sediment Discharge to the Ocean: The Importance of Small Mountainous Rivers. *The Journal of Geology*, **100**, 525-544.
- Ministry of Environment, Lands and Parks (1999), original aerial photographs.
- Naegeli, M. W., Huguenberger, P. & Uehlinger, U. (1996) Ground penetrating radar for assessing sediment structures in the hyporheic zone of a prealpine river. *Journal of the American Benthologic Society*, **15**(3), 353-366.
- Nemeč, W. & Steel, R. J. (1988) What is a fan delta and how do we recognize it? In: *Fan Deltas: Sedimentology and Tectonic Settings* (Ed. by W. Nemeč and R. J. Steel), pp. 3-13. Blackie and Son Ltd., Glasgow.
- Owens, P. & Slaymaker, O. (1992) Late Holocene sediment yields in small alpine and subalpine drainage basins, British Columbia. In: *Erosion, Debris Flows and Environment in Mountain Regions*, I.A.H.S (209), pp. 147-154.

- Parker, G., Klingeman, P. C. & McLean, D. G. (1982) Bedload and size distribution in paved gravel-bed streams. *Journal of the Hydraulics Division, American Society of Civil Engineers*, **108**, 544-571.
- Patric, J., H., Evans, J. O. & Helvey, D. J. (1984) Summary of Sediment Yield Data From Forested Land in the United States. *Journal of Forestry*, **82**(2), 101-104.
- Pizzuto, J.E., Hession, W. & McBride, M. (2000) Comparing gravel-bed rivers in paired urban and rural catchments of southern Pennsylvania. *Geology*, **28**(1), 79-82.
- Postma, G. (1984) Slumps and their deposits in fan delta front and slope. *Geology*, **12**, 27-30.
- Postma, G. (1990) Depositional architecture and facies of river and fan deltas: a synthesis. In: *Coarse-Grained Deltas* (Ed. by A. Colella and D. B. Prior), pp. 13-27. Blackwell Scientific Publications, London.
- Reynolds, J. M. (1997) *An introduction to applied and environmental geophysics*. John Wiley & Sons Ltd., Rexdale, Ontario.
- Roberts, R. G. & Church, M. (1986) The sediment budget in severely disturbed watersheds, Queen Charlotte Ranges, British Columbia. *Canadian Journal of Forest Research*, **16**, 1092-1106.
- Rothlisberger, H. & Lang, H. (1987) Glacial Hydrology. In: *Glacio-Fluvial Sediment Transfer* (Ed. by A. M. Gurnell and M. J. Clark), pp. 207-284. John Wiley & Sons Ltd., Toronto.
- Ryan, S. E. & Troendle, C. A. (1997) Measuring bedload in coarse-grained mountain channels: procedures, problems, and recommendations. In: *Water Resources Education, Training, and Practice: Opportunities for the Next Century*, pp. 949-958. American Water Resources Association.
- Scheifer, E. (2000) unpublished Green Lake Bathymetry Map, Department of Geography, University of British Columbia, Vancouver.
- Schumm, S. A. (1995) Sediment yield from disturbed earth systems. *Geology*, **23**(5), 391-394.
- Sensors and Software, (1996) *pulseEKKO IV Run User's guide version 4.2, Technical Manual 20*. Sensors and Software, Ltd., Mississauga, Ontario, 59 pp.
- Slaymaker, O. H. (1972) Sediment yield and sediment control in the Canadian Cordillera. In: *BC Geographical Series*, pp. 235-245. Department of Geography, University of British Columbia, Vancouver, BC.

- Smith, D. G. (1991) Canadian Landform Examples 22 - Lacustrine Deltas. *The Canadian Geographer*, **35**(3), 311-316
- Smith, D. G. & Jol, H. M. (1997) Radar Structure of a Gilbert-type delta, Peyto Lake, Banff National Park, Canada. *Sedimentary Geology*, **113**, 195-209.
- Syvitski, J. P. M. & Daughney, S. (1992) Delta2: Delta progradation and basin infilling. *Computers and Geosciences*, **18**(7), 839-897.
- Trimble, S. W. (1997) Contribution of Stream Channel Erosion to Sediment Yield from an Urbanizing Watershed. *Science*, **278**(21), 1442-1444.
- Troendle, C. A., Nankervis, J. M. & Ryan, S. E. (1996) Sediment Transport from small, steep-gradient watersheds in Colorado and Wyoming. In: *Sixth Federal Interagency Sedimentation Conference, Vol. 2*, pp. 39-45. Subcommittee on Sedimentation Interagency Advisory Committee on Water Data, Las Vegas, Nevada.
- Vandenberghe, J. & van Overmeeren, R. A. (1999) Ground penetrating radar images of selected fluvial deposits in the Netherlands. *Sedimentary Geology*, **128**, 245-270.
- Water Survey of Canada, (1999) Daily discharge records for Fitzsimmons Creek BC 08MG026 and Lillooet River BC 08MG005, *Vol. 1999*. Water Survey of Canada.
- Wescott, W. & Ethridge, F. G. (1990) Fan Deltas - Alluvial Fans in Coastal Settings. In: *Alluvial Fans: A Field Approach* (Ed. by A. H. Rachocki and M. Church), pp. 195-211. John Wiley & Sons Ltd., Rexdale, Ontario.
- Wolman, G. M. (1954) A Method of Sampling Coarse River-Bed Material. *Transactions, American Geophysical Union*, **35**(6), 951-956.
- Wood, M. L. & Ethridge, F. G. (1988) Sedimentology and architecture of Gilbert-and mouth bar-type fan-deltas, Paradox basin, Colorado. In: *Fan Deltas: Sedimentology and Tectonic Settings* (Ed. by W. Nemecek and R. J. Steel), pp. 251-263. Blackie and Son Ltd., Glasgow.
- Woods, P. J. (1993) The Fitzsimmons Creek Setback Training Berm. In: *Whistler and Water: Building a City in the Mountains* (Ed. by A. G. Chantler), pp. 21-30. BiTech Publishers Ltd., Whistler, BC.
- Woodward, D. J. (1997) Calculating suspended sediment loads and yields using suspended sediment/discharge rating curves. In: *Physical Geography Now: Erosion and Sediment Transfer in River Catchments*, pp. 373-376, London.

